



THE HONG KONG  
POLYTECHNIC UNIVERSITY

香港理工大學

Pao Yue-kong Library

包玉剛圖書館

---

## Copyright Undertaking

This thesis is protected by copyright, with all rights reserved.

**By reading and using the thesis, the reader understands and agrees to the following terms:**

1. The reader will abide by the rules and legal ordinances governing copyright regarding the use of the thesis.
2. The reader will use the thesis for the purpose of research or private study only and not for distribution or further reproduction or any other purpose.
3. The reader agrees to indemnify and hold the University harmless from and against any loss, damage, cost, liability or expenses arising from copyright infringement or unauthorized usage.

### IMPORTANT

If you have reasons to believe that any materials in this thesis are deemed not suitable to be distributed in this form, or a copyright owner having difficulty with the material being included in our database, please contact [lbsys@polyu.edu.hk](mailto:lbsys@polyu.edu.hk) providing details. The Library will look into your claim and consider taking remedial action upon receipt of the written requests.

**MULTI-FUNCTIONAL THERMORESPONSIVE  
HYDROGEL AND APPLICATION ON TEXTILE  
FOR SKIN AND WOUND CARE**

**WANG XIAOWEN**

**Ph.D**

**The Hong Kong Polytechnic University**

**2017**

The Hong Kong Polytechnic University

Institute of Textiles and Clothing

**Multi-functional Thermoresponsive Hydrogel and  
Application on Textile for Skin and Wound Care**

**WANG Xiaowen**

A thesis submitted in partial fulfillment of the requirements for the  
degree of Doctor of Philosophy

June 2016

## **CERTIFICATE OF ORIGINALITY**

I hereby declare that this thesis is my own work and that, to the best of my knowledge and belief, it reproduces no material previously published or written, nor material that has been accepted for the award of any other degree or diploma, except where due acknowledgement has been made in the text.

— (Signed)

WANG Xiaowen (Name of student)

## Abstract

The thesis presented a general and effective route to the synthesis of thermoresponsive hydrogels based on poly(ethylene glycol)-poly( $\epsilon$ -caprolactone)-poly(ethylene glycol) (PEG-PCL-PEG), as well as the antibacterial modification of the PEG-PCL-PEG block copolymers through quaternization using quaternary ammonium salts (QAS). The study subsequently made use of the synthesized functional hydrogels for the fabrication of smart textile-based materials by a simple coating method, which can be used as a functional complex dressing for skin and wound care.

The study primarily includes three research systems:

(i) Design, synthesis and characterization of PEG-PCL-PEG hydrogel through coupling PEG and PCL with a chemical linker hexamethylene diisocyanate (HMDI)

The as-obtained amphiphilic block copolymers-based hydrogel had non-cytotoxicity and showed a thermosensitive sol-gel-sol transition behavior. The chemical structure of the synthesized block copolymers was confirmed by FTIR and  $^1\text{H-NMR}$  spectra. The surface morphology, the mechanism of the sol-gel transition behavior, and the in vitro drug release performance of the thermoresponsive hydrogel were investigated in detail through various characterization analyses.

(ii) Synthesis, characterization and evaluation of a PEG-PCL-QAS-PCL-PEG antibacterial hydrogel with QAS as an antibacterial modification agent

Biomaterials are readily infected with microorganisms, thus posing a serious threat to the human health care. The study was extended to the

antibacterial modification of PEG-PCL-PEG copolymer with an inexpensive and commercial quaternary ammonium salt, namely bis(2-hydroxyethyl) methylammonium chloride (DMA), as an antibacterial modification agent. The effective synthesis of the antibacterial copolymer PEG-PCL-DMA-PCL-PEG was well confirmed by FTIR and <sup>1</sup>H-NMR spectra. At an appropriate level, the modification of the copolymer PEG-PCL-DMA-PCL-PEG by DMA could render efficient antibacterial property to it without altering its fascinating intrinsic properties including the thermosensitivity (e.g. the skin temperature-induced sol-gel transition), non-cytotoxicity, and drug controlled release. A detailed study on the sol-gel-sol transition behavior of different extent modified copolymers showed that an appropriate extent of modification with DMA could lead to the formation of an optimized antibacterial hydrogel. The work presented here will open up an avenue towards synthesis of various antibacterial copolymers with different kinds of blocks other than PEG and PCL using DMA or its analogues as the functional building block.

(iii) Fabrication of a smart multi-functional textile-based material for topical skin applications by coating the as-prepared antibacterial thermoresponsive hydrogel onto a nonwoven fabric

A functional textile-based hydrogel system has been prepared by a coating method, which can be used as wound dressing for skin and wound care or as a facial mask. It is worth pointing out that the novel moisture & exudate management property was obtained after the effective combination of the prepared thermoresponsive hydrogel with flexible absorbent textile substrates. The sweat, blood and other body fluids can be effectively drained out of the skin in a unidirectional manner (from inside to outside), which shows great

significance in keeping the topical skin area clean, comfortable, and appropriate for building a good moist micro-environment. The as-fabricated complex dressing seems to be an ideal dressing material for skin care and wound treatment applications based on its fascinating properties such as biocompatibility, breathability, controlled drug release and moisture management. It will pave the way for development of various polymer-or textile-based functional materials that are applicable in large scale to various industries.

## List of Publications

### International journals:

1. Huawen Hu, Xiaowen Wang, Ka I Lee, Kaikai Ma, Hong Hu & John H. Xin. Graphene oxide-enhanced sol-gel transition sensitivity and drug release performance of an amphiphilic copolymer-based nanocomposite. Scientific Reports. Article number: 31815 (2016), doi:10.1038/srep31815.
2. Xiaowen Wang, Huawen Hu, Wenyi Wang, Ka I Lee, Chang Gao, Liang He, Yuanfeng Wang, Chuilin Lai, Bin Fei, John H. Xin. Antibacterial modification of an injectable, biodegradable, non-cytotoxic block copolymer-based physical gel with body temperature-stimulated sol-gel transition and controlled drug release. Colloids and Surfaces B: Biointerfaces. 2016,143,342-351.
3. Xiaowen Wang, Huawen Hu, Zongyue Yang, Yeeyee Kong, Bin Fei, John H. Xin. Visible light-active sub-5 nm anatase TiO<sub>2</sub> for photocatalytic organic pollutant degradation in water and air, and for bacterial disinfection. Catalysis Communications. 2015, 72, 81-85.
4. Xiaowen Wang, Huawen Hu, Zongyue Yang, Liang He, Yeeyee Kong, Bin Fei and John H. Xin. Smart hydrogel-functionalized textile system with moisture management property for skin application. Smart Mater. Struct. 2014, 23, 125027-125037.

**International conferences:**

1. John H. Xin, Wang Xiaowen, KongYeeyee, Yang Zongyue, Hu Huawen, He Liang. Smart Thermoresponsive Hydrogel Coated Textile Materials for Skin Application. Proceeding of AA Seminar Series 8, **2013**, 1-7.

## **Acknowledgements**

I would like express my sincerest gratitude to my chief supervisor Prof. Xin for providing the opportunity for this project to be taken. Without his expert advice, support and guidance, this project would not have been possible.

I would also like to thank Dr. Fei Bin for his enlightening suggestion, interesting discussion, and kind help in my research works.

My sincere thanks also go to my colleagues who gave suggestions to my project and helped me in various aspects throughout completion of this thesis. They include but not limited to Dr. HuaWen Hu, Dr. Haifeng Lu, Mr. Zongyue Yang, Dr. Liang He, Ms. Ka I Lee, Ms. Vicky Lai Lai So, Mr. Wenyi Wang, Mr. You Wu, Mr. Lin Tan, Ms. Chang Gao, Mr. Yang Liu, Dr. Yeeyee Kong, Mr. Yuanfeng Wang and Dr. Chuilin Lai. My thanks are also extended to the technical staffs in laboratories and workshops of Institute of Textiles and Clothing, for their assistance in experimental work.

Finally, I would gratefully acknowledge our department, Institute of Textiles and Clothing of The Hong Kong Polytechnic University and ITF funding (Tier3) of the Hong Kong SAR Government (project code: ITS/038/12).

## Table of Contents

<b>Abstract</b> .....	II
<b>List of Publications</b> .....	V
<b>Acknowledgements</b> .....	VII
<b>Table of Contents</b> .....	VIII
<b>List of Abbreviations</b> .....	XII
<b>Chapter 1 Introduction</b> .....	1
<b>1.1. Research background</b> .....	1
<b>1.2. Aims and objectives of study</b> .....	4
<b>1.3. Overall methodology</b> .....	6
<b>1.3.1. Synthesis of thermoresponsive hydrogel</b> .....	6
<b>1.3.2. Preparation of hydrogel-nonwoven complex dressing</b> .....	6
<b>1.3.3. Characterization and evaluation of prepared hydrogel and hydrogel-nonwoven multi-functional complex dressing</b> .....	6
<b>1.4. Significance of study</b> .....	8
<b>1.5. Outline of thesis</b> .....	9
<b>Chapter 2 Literature review</b> .....	13
<b>2.1. Hydrogel materials</b> .....	13
<b>2.1.1. Thermoresponsive hydrogel</b> .....	15
<b>2.1.2. Thermo-induced gelation mechanism</b> .....	17
<b>2.1.3. Materials used for the synthesis of amphiphilic block copolymers</b> .....	18
<b>2.1.4. Thermoresponsive hydrogels based on biodegradable copolymers</b> .....	20
<b>2.1.5. Development of thermoresponsive hydrogels based on amphiphilic block copolymers with sol-gel-sol transition behavior</b>	23
<b>2.1.6. Thermoresponsive hydrogels as drug delivery system</b> .....	31
<b>2.2. Antibacterial polymeric materials with quaternary ammonium salt</b>	33
<b>2.2.1. Antibacterial polymer with pendant quaternary ammonium salts</b>	36

2.2.2.	<b>Polymer with quaternary ammonium salts in the main chain</b>	43
2.2.3.	<b>Immobilization of QAS on material surfaces</b>	47
2.3.	<b>Wound dressing</b>	52
2.3.1.	<b>Nonwoven fabric dressings</b>	54
2.3.2.	<b>Hydrogel dressings</b>	56
<b>Chapter 3 Research methodology</b>		60
3.1.	<b>Experimental plan</b>	60
3.2.	<b>Materials selection</b>	62
3.2.1.	<b>Materials for thermoresponsive amphiphilic block copolymers</b>	62
3.2.2.	<b>Materials for modification of antibacterial hydrogel</b>	63
3.2.3.	<b>Textile substrate materials selection</b>	65
3.2.4.	<b>Model drug and nutrient selection</b>	66
3.2.5.	<b>Testing bacteria selection</b>	67
3.3.	<b>Experiment procedures</b>	67
3.3.1.	<b>Synthesis of PEG-PCL-PEG triblock copolymers</b>	67
3.3.2.	<b>Synthesis of PEG-PCL-DMA-PCL-PEG copolymers</b>	68
3.3.3.	<b>Preparation of functional dressing with prepared hydrogel</b>	70
3.4.	<b>Characterization and evaluation techniques</b>	71
3.4.1.	<b>Fourier transform infrared spectroscopy (FTIR)</b>	71
3.4.2.	<b>Differential scanning calorimetry (DSC)</b>	72
3.4.3.	<b>Nuclear magnetic resonance (NMR)</b>	73
3.4.4.	<b>Gel permeation chromatography (GPC)</b>	74
3.4.5.	<b>Freeze-drying</b>	75
3.4.6.	<b>Scanning electron microscopy (SEM)</b>	75
3.4.7.	<b>Ultraviolet-visible spectroscopy (UV-Vis)</b>	76
3.4.8.	<b>Sol-gel-sol transition behavior detection</b>	77
3.4.9.	<b>Cytotoxicity test</b>	78
3.4.10.	<b>In vitro skin toxicity test</b>	79

3.4.11.	<b>In vitro drug release behavior test</b> .....	80
3.4.12.	<b>Antibacterial test</b> .....	81
3.4.13.	<b>Transdermal drug delivery (TDD)</b> .....	82
3.4.14.	<b>Water vapor transmission rate (WVTR)</b> .....	83
3.4.15.	<b>Air permeability (AP)</b> .....	83
3.4.16.	<b>Moisture management test (MMT)</b> .....	84
<b>Chapter 4 Thermoresponsive hydrogel system based on amphiphilic block copolymers: synthesis, characterization and application</b> .....		85
4.1.	<b>Introduction</b> .....	85
4.2.	<b>Results and discussion</b> .....	86
4.2.1.	<b>Synthesis of PEG-PCL-PEG copolymers</b> .....	86
4.2.2.	<b>Structure analysis of PEG-PCL-PEG triblock copolymer</b>	89
4.2.3.	<b>Microscopic morphology of hydrogel by SEM observations</b>	91
4.2.4.	<b>Sol-gel phase transition behavior detection</b> .....	91
4.2.5.	<b>Cytotoxicity study</b> .....	94
4.2.6.	<b>In vitro drug release behavior study</b> .....	95
4.2.7.	<b>Transdermal drug delivery study</b> .....	97
<b>Chapter 5 Antibacterial modification of thermoresponsive hydrogel: synthesis, characterization and application</b> .....		99
5.1.	<b>Introduction</b> .....	99
5.2.	<b>Results and discussion</b> .....	102
5.2.1.	<b>Synthesis of antibacterial modified copolymer with QAS</b>	102
5.2.2.	<b>Characterization of antibacterial modified copolymer</b> ....	103
5.2.3.	<b>Study of the phase transition behavior of the modified hydrogel</b> .....	110
5.2.4.	<b>Study of in vitro skin toxicity</b> .....	114
5.2.5.	<b>Study on the antibacterial modified hydrogel</b> .....	116
<b>Chapter 6 Smart hydrogel coated textile materials for skin and wound care</b> .....		124
6.1.	<b>Introduction</b> .....	124
6.2.	<b>Results and discussion</b> .....	125
6.2.1.	<b>Morphology of hydrogel coated nonwoven fabric</b> .....	125

6.2.2. Unidirectional water transport test .....	126
6.2.3. Moisture management analysis.....	127
6.2.4. Water vapor transmission rate (WVTR) analysis.....	131
6.2.5. Air permeability (AP) analysis.....	132
<b>Chapter 7 Conclusion .....</b>	<b>134</b>
<b>Chapter 8 Future work and potential application .....</b>	<b>137</b>
8.1. Future work .....	138
8.2. Potential application of the research .....	140
References .....	141

## List of Abbreviations

AATCC	American Association of Textile Chemists and Colorists
AP	Air permeability
A.R.	Analytical reagent
CFU	Colony-forming units
CGC	Critical gelation concentration
D.I. water	Deionized water
DMA	Bis(2-hydroxyethyl) methylammonium chloride
DNA	Deoxyribonucleic acid
DSC	Differential scanning calorimetry
E. coli	Escherichia coli
FDA	Food and Drug administration
FWHM	Full width at half maximum
FTIR	Fourier transform infrared
GPC	Gel permeation chromatography

HMDI	Hexamethylene diisocyanate
IPDI	Isophorone diisocyanate
LCGT	Lower critical gelation temperature
LDH	Lactate dehydrogenase
MMT	Moisture management test
mPEG	Poly (ethylene glycol) methyl ether
$M_n$	Number-average molecular weight
$M_w$	Weight-average molecular weight
NMR	Nuclear magnetic resonance
PNiPAAm	N-isopropylacrylamide
PDI	Polydispersity
PEG	Poly (ethylene glycol)
PCL	Poly ( $\epsilon$ -caprolactone)
PEO	Poly(ethylene oxide)

PET	Polyethylene terephthalate
PLLA	Poly(L-lactide)
PDLLA	Poly-DL-lactide
PNIPA	Poly(N-isopropylacrylamide)
PLA	Poly(lactic acid)
PLGA	Poly(lactic-co-glycolic-acid)
PBS	Poly(butylene succinate)
PBT	Poly(butylene terephthalate)
PVA	Polyvinyl alcohol
PVP	Polyvinylpyrrolidone
SEM	Scanning electron microscope
SA	Staphylococcus aureus
SD	Standard deviation
SDS	Sodium dodecyl sulfonate
TDDA	Transdermal drug delivery amount

THF	Tetrahydrofuran
UCGT	Upper critical gelation temperature
UV/vis	Ultraviolet/visible
WVTR	Water vapor transmission rate
WAXS	Wide angle X-rays cattering
XRD	X-ray diffraction
3D	Three-dimensional

# Chapter 1 Introduction

This chapter firstly introduces the research background of the project. The current problems, research objectives and methodology are thereafter highlighted. Finally, the significance of the study and the framework of the thesis are outlined.

## 1.1. Research background

Skin is the biggest external defence system and the largest organ in the body. Generally, a defect or break in the skin as a result of physical or thermal damage is called wound[1]. From old times, people tried to care skin and heal wounds with crude drug extracts (mostly of plant origin), animal fat and honey[2]. With the improvement of living standards, textile-based skin and wound care products used in hygiene, medical, cosmetic, personal care and healthcare sectors become an important and rapidly growing usage of textiles especially in recent years.

The category of wound dressings can be differentiated by function or by form. Basic textile wound dressings such as gauze, lint, and wadding are of “traditional” form category, while the “advanced” form category comprises hydrocolloids, alginates, hydrogels, films, and other biomaterials. Basic functions of traditional wound dressing are to some extent of body liquid absorbency and wound protection, while advanced functions include moisture maintenance and bioactivity[3].

Modern wound dressings often integrate multiple non-textile functional components (gels, films, and biomaterials) together in order to provide advanced performance at a dramatically higher cost. Current modern wound dressings are designed to achieve specific properties and functions that satisfy certain personal

and clinical demands in self-care and professional usages. It is understood that a moist wound environment promotes skin care and wound healing [4]. Additionally, the functions that protecting healing tissue, offering a barrier to bacteria, and providing appropriate adherence/non-adherence to wound bed are highly important and desirable. In recent years various efforts have been made towards the research and development of this kind of functional artificial dressings which will meet the requirements necessary for skin care and wound treatment.

As always, most of research and development are mainly focused on achieving an ideal wound dressing, and the system based on hydrogels is one of remarkable research results, which is more suitable for biomedical and personal care applications. Due to significant moisture holding and drug release properties, hydrogel dressings have many advantages for skin care and wound treatment applications [5]. However, inherently weak mechanical strength of most biomedical hydrogels makes them difficult to handle and use. Moreover, this kind of hydrogel-based biomaterials is readily infected by microorganisms. Additionally, cytotoxicity and biocompatibility of biomaterials may cause alarming allergy and irritation to human skin. In these regards, combination of hydrogels with conventional textile dressings may bring complementary effects to enhance functionalities. Additionally, the problems related to hydrogel-based materials may be resolved by proper design and fabrication, including raw materials selection, adjustment of hydrogel synthesis conditions, integration of hydrogel with substrate (woven and nonwoven, etc.), and other optimization treatment.

To meet the growing social needs on low cost and high patient comfort in recent years, as well as to afford an efficient skin care treatment in the biomedical field, there is an increasing trend with respect to the simplification of the topical drug delivery process[6]. It is evident from the literature survey[7] that there is still much room remaining for improving the performance of skin and wound care using textile materials. On the basis of the literature review, the knowledge gaps and the problems are summarized as follows:

(1) Generally, high absorbency of textile materials causes wound to dry out which is not good for wound healing and regeneration. In addition, using traditional cost-effective textile wound dressings alone cannot provide ideal wound healing conditions in terms of drug control release, antibacterial activity and moist holding on wound bed, etc. Modern wound dressings often integrate multiple biomaterials with traditional textile dressings to offset the weakness and to achieve multi-functionalities.

(2) In recent years, most of studies have been carried out on synthesis, characterization and investigation of smart responsive behaviors of hydrogels. On one hand, hydrogel dressings have demonstrated high potential to revolutionize skin and wound care by providing enhanced moisture management and drug release properties. On the other hand, hydrogels possess inherently weak mechanical strength, making them difficult to handle. If a hydrogel is too soft and prone to break during handling, it would be difficult to carry out a treatment or post-treatment, e.g. difficult to completely remove it after usage. To broaden their potential applications, hydrogels should be reinforced so as to overcome the fragility through improving their

mechanical performance. One of the effective approaches is to reinforce hydrogels with matrix supporting.

(3) Currently hydrogels are extensively used in various biomedical fields. However, they are readily infected with microorganisms, thus posing a serious threat to the human health care. To address this problem, antibacterial modification of smart hydrogels is needed without impairing their inherent advantages.

(4) To date, most work has focused on the study of the property of polymer hydrogels. Few researchers have paid attentions to investigate the property and function of textile-based hydrogel systems. By combining the advantages of textile materials and smart hydrogels, some novel performances may be generated and are worth exploring.

## **1.2. Aims and objectives of study**

In view of above-described problems, this study is therefore focused on designing and developing a textile-based smart hydrogel system for skin and wound care applications. Specifically, this study aims to design, synthesize and characterize smart hydrogel materials and their functionalized textile-based composites for skin and wound care applications. Enhanced skin and wound care of the functionalized textile-based dressings are realized, ascribable to the combined advantages of the textile materials and smart hydrogels, as well as to the combined effect of both. This kind of smart textile-based dressing functionalized with biocompatible, drug control-release, antibacterial, thermosensitive hydrogel coating, in conjunction with the multi-layer bonded structures of nonwoven fabric, will have significant value in the biomedical field.

In this study, we aim to explore and develop thermoresponsive smart hydrogels, and to integrate them into textile-based gauze pad so as to design and fabricate a smart textile-based material which can be used as multi-functional dressings with enhanced drug control release, antibacterial activity, and moisture management capability for skin and wound care.

The specific objectives of this study are described as follows:

- (1) To design and synthesize an water-based, thermosensitive (body-temperature sensitive), biodegradable and biocompatible copolymer hydrogel system based on amphiphilic block copolymers comprising aliphatic polyesters, as the hydrophobic block, and poly(ethylene glycol) as the hydrophilic block with a linear triblock or multiblock architecture.
- (2) To modify the copolymers with bis(2-hydroxyethyl) methylammonium chloride (DMA), and consequently to obtain an antibacterial copolymer hydrogel system.
- (3) To characterize the as-prepared block copolymer hydrogel by FTIR, <sup>1</sup>H-NMR, DSC and GPC analysis.
- (4) To test and evaluate the structure and properties of the thermoresponsive hydrogels including sol-gel transition, microscopic morphologies, cytotoxicity, antibacterial performance, in vitro drug control release and transdermal drug delivery.
- (5) To apply smart hydrogels onto textile materials, and thus to design and fabricate multi-functional complex dressings.
- (6) To test the properties of complex dressing in terms of water vapor transmission rate (WVTR), air permeability (AP), and moisture management.

### **1.3. Overall methodology**

The general methodologies were presented below and the details such as materials, synthesis and characterization will be described in Chapter 3.

#### **1.3.1. Synthesis of thermoresponsive hydrogel**

The thermoresponsive hydrogel with sol-gel transition behavior are synthesized based on amphiphilic block copolymers comprising aliphatic polyesters, as the hydrophobic block, and poly(ethylene glycol) as the hydrophilic block with a linear triblock or multiblock architecture, and modified with double hydroxyl quaternary ammonium salt, bis(2-hydroxyethyl) methylammonium chloride (DMA).

#### **1.3.2. Preparation of hydrogel-nonwoven complex dressing**

Many kinds of methods can be applied to coat hydrogel onto the textile, for example spin-coating, dip-coating, slot-casting, spray-coating, doctor blade and so on. Here, we integrate the hydrogels onto the surface of nonwoven fabric by doctor blading method to fabricate a multi-functional complex dressing for skin and wound care.

#### **1.3.3. Characterization and evaluation of prepared hydrogel and hydrogel-nonwoven multi-functional complex dressing**

For the synthesized copolymers, the chemical structure was unraveled by FTIR and <sup>1</sup>H-NMR. The characteristic temperature transition, melting, and crystallization temperature, melting and crystallization behavior, specific heat capacity, and thermal stability of the hydrogel were studied through DSC. GPC

was used to determine the molecular weight and distribution of synthesized copolymers.

For the prepared hydrogels, the sol-gel transition was verified visually by a test tube inversion method. SEM was employed to investigate the microscopic morphologies of the as-formed hydrogel after freeze-drying in liquid nitrogen. The cytotoxicity of the prepared hydrogel was evaluated by investigating the skin keratinocytes inhibitory effect and MTT and LDH assays. Aloin and curcumin are selected as the hydrophilic and hydrophobic model drugs respectively for drug control release study. The in vitro cumulative drug release was monitored by a UV-vis spectrophotometer, and calculated by the calibration curve of aloin and curcumin. Because of the fluorescence of Rhodamine B and curcumin, they are selected as the hydrophilic and hydrophobic model drugs respectively for the study of transdermal drug delivery, which was investigated by qualitative observations using freshly excised pig skin simulating human skin. The antibacterial activity of hydrogels was tested qualitatively and quantitatively by inhibition zone and viable cell count methods respectively against two representative clinically relevant bacterial strains, namely *S. aureus* (Gram-positive) and *E. coli* (Gram-negative).

For the designed hydrogel-nonwoven complex dressing, the water vapor transmission rate (WVTR) across the hydrogel coated nonwoven fabric was determined as stipulated by ASTM standard E96-00. The air permeability was test according to ASTM D 737 at 100Pa. The capacities of unidirectional water transport and exudate management were evaluated by moisture management tester according to AATCC 195-2011 liquid moisture management properties of textile fabrics.

#### **1.4. Significance of study**

Over the past decade, numerous smart textiles in the biomedicine field have been well developed, along with making improvements in the performance and efficiency. However, there are still much room that remains for exploration and improvements, e.g., to lower the production cost, to prepare non-toxic and environmentally benign materials, to simplify the material synthesis/application procedures, and to enhance performance (including durability, mechanical strength, and hand feel, etc). In addition, some synthesis and formation mechanisms are still ambiguous, the side-effect to human skin or environment are not well tested/ evaluated, and innovative design, fabrication, and modification of bio-materials for public healthcare are much required. One of the primary methods for making smart textile is to apply the as-prepared smart materials onto the textile, but there is a big challenge of meet the end-use requirements of the smart textile to a satisfied extent, such as biocompatibility, no cytotoxicity and skin irritation, novel functions, comfort and suitable air permeability. To this end, selection of materials including textile fabrics and smart functional materials, design and combination of textile substrates with smart materials are required.

In this study, a thermoresponsive hydrogel system with a sol-gel transition behavior based on amphiphilic block copolymers, and then modified it with DMA to achieve antibacterial capability was prepared. A possible mechanism for the sol-gel-sol transition behaviors of the copolymers was also presented, and so is the effect of the quaternization on the thermoresponsive sol-gel-sol transition behavior. Following these, a functional hydrogel-nonwoven complex dressing by a surface coating method for skin and wound care was designed and developed.

This kind of complex dressing was equipped with biocompatible and thermoresponsive hydrogel coating and the multi-layer structure of nonwoven fabrics, and consequently possessed the following fascinating properties: (i) proper air permeability and WVTR for wound treatment, (ii) drug control-release function and (iii) moisture/ exudate management ability. This kind of smart hydrogel coated nonwoven dressing is useful and convenient for topical administration. It is therefore a promising biomedical textile material with high added value for skin and wound care.

## **1.5. Outline of thesis**

This thesis describes the design and fabrication of smart hydrogel biomaterials and their functionalized nonwoven fabric which can be used as a functional complex dressing for skin and wound care. In this study, thermoresponsive PEG-PCL-PEG hydrogels, antibacterial modified PEG-PCL-DMA-PCL-PEG hydrogels and hydrogel coated nonwoven complex dressings were designed and fabricated. The thermoresponsive sol-gel transition behavior, cytotoxicity, controlled drug release, antibacterial activity and moisture management performance of hydrogel-coated nonwoven complex dressings were investigated systematically.

This thesis consists of seven chapters to report the research and outputs of this study, and the structure of these chapters is shown in **Figure 1.1**.

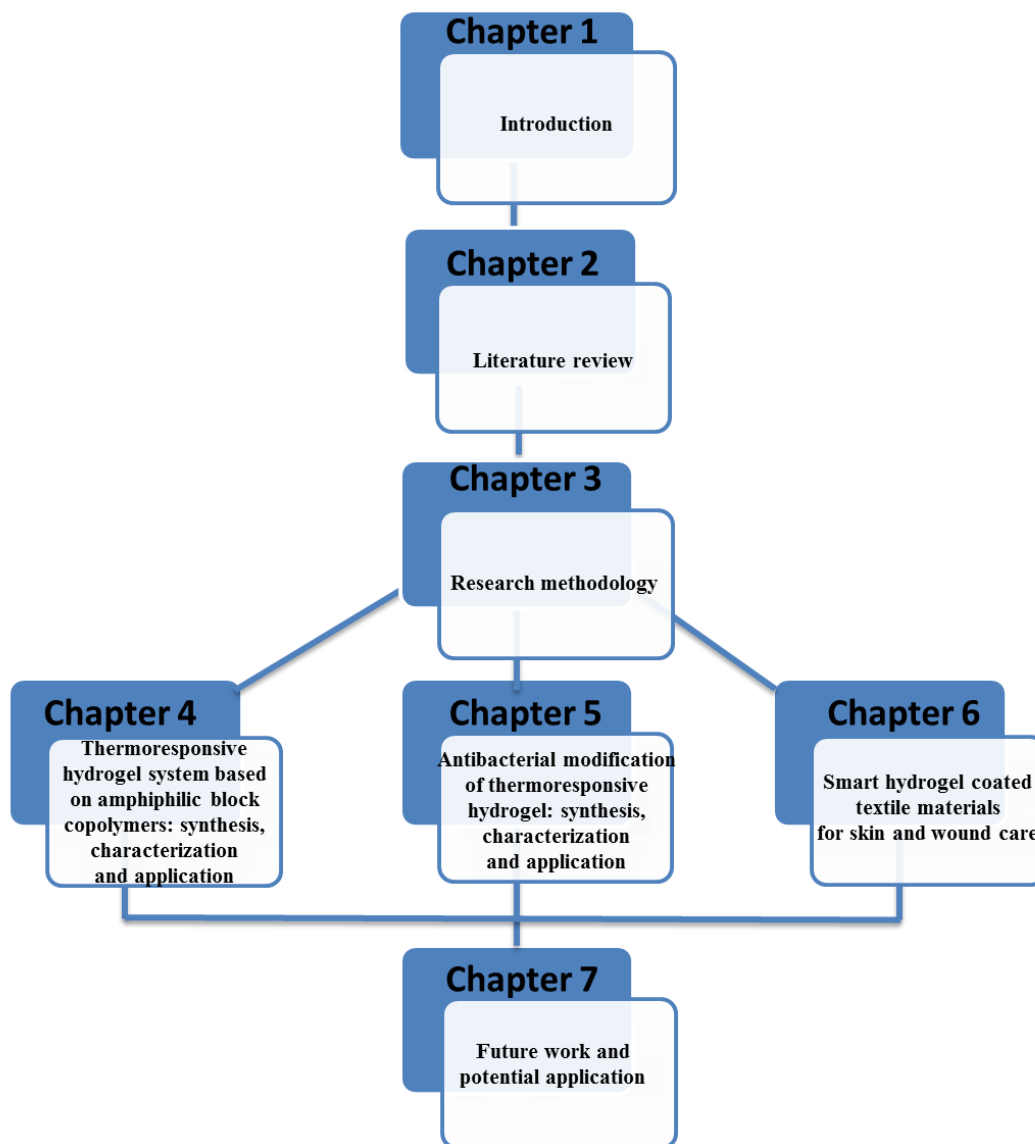


**Figure 1.1** Thesis structure and contents

In Chapter 1, the research background of investigation, existing problems, the objectives, methodology and significance of this study are introduced.

In Chapter 2, a literature review of the research and development of thermoresponsive hydrogel, antibacterial polymeric materials with quaternary ammonium salt and wound dressings is performed.

In Chapter 3, the research methodology is further divided into the following subordinate parts: experiment plan design, materials selection, experimental procedures, characterization and evaluation techniques. The characterization

methods are Fourier Transform Infrared Spectroscopy (FTIR), Nuclear Magnetic Resonance (NMR), Differential Scanning Calorimetry (DSC), Gel Permeation Chromatography (GPC), Scanning Electron Microscopy (SEM), UV-Visible Spectroscopy (UV-Vis). The evaluation and analysis of hydrogel include sol-gel transition behavior, cytotoxicity, MTT and LDH assays, in vitro drug control release, transdermal drug delivery, and antibacterial activity. The evaluation and analysis of hydrogel-nonwoven smart textile include water vapor transmission rate (WVTR), air permeability, unidirectional water transport and exudate management (MMT).

In Chapter 4, thermoresponsive hydrogel system PEG-PCL-PEG is successfully synthesized using HMDI as the coupling agent between PEG and PCL. The sol-gel transition is visually observed by the tube inverting method, which is mainly dependent on the hydrophilic/hydrophobic balance of the macromolecular structure under different temperature conditions. The structure and surface morphology of the thermoresponsive hydrogel, sol-gel transition behavior, in vitro drug release behavior, and the cytotoxicity are also investigated in detail.

In Chapter 5, a general route is presented to the antibacterial modification of previous PEG-PCL-PEG type block copolymer system with double hydroxyl quaternary ammonium salt, DMA. After the characterization and evaluation analysis, we also discuss a probable mechanism for the sol-gel-sol transition behaviors of the copolymers, and study the relationship between the quaternization with DMA and the sol-gel-sol transition behaviors. The work presented in this chapter will open up an avenue towards the synthesis of various

antibacterial copolymers with different kinds of blocks other than PEG and PCL using DMA or its analogue as a functional building block.

In Chapter 6, a smart textile - hydrogel coated nonwoven fabric is developed, which can be used as complex dressing for skin and wound care. This kind of smart hydrogel-nonwoven system is a combination of nonwoven fabric structure with the drug loaded thermoresponsive hydrogel coating. It can serve as both a drug control-release system and a moisture and exudate management system. The liquid like sweat, blood and body fluid out of skin can be transported unidirectionally from inside to outside. From the testing and evaluation, this complex dressing seems to be an excellent dressing material for skin care and wound treatment applications because of its special properties like biocompatibility, drug control-release, breathability and moisture management.

In Chapter 7, the whole work of the thesis, and some future work suggestions and potential applications are summarized.

# Chapter 2 Literature review

In this chapter, the literature related to the research and development of thermoresponsive hydrogels, its modified derivative, and hydrogel-coated textile-based wound dressing is reviewed and summarized.

## 2.1. Hydrogel materials

A glycolmethacrylate-based hydrophilic gel, featuring a three-dimensional (3-D) network structure, was firstly introduced by Wichterle and Lim in early 1960s [8], which is biocompatible, similar to the body tissue and capable of containing a high percentage of water. Since then, a significant amount of research efforts and studies have been devoted to advancing technology development and extending the attributes of hydrogels [9-11]. The ever-growing hydrogel technology and applications have led to the remarkable progresses and advances in biomedical and pharmaceutical fields [12-14]. To conclude, hydrogels are, generally, polymeric networks with 3-D configuration, being capable of containing high amounts of water or biological fluids.

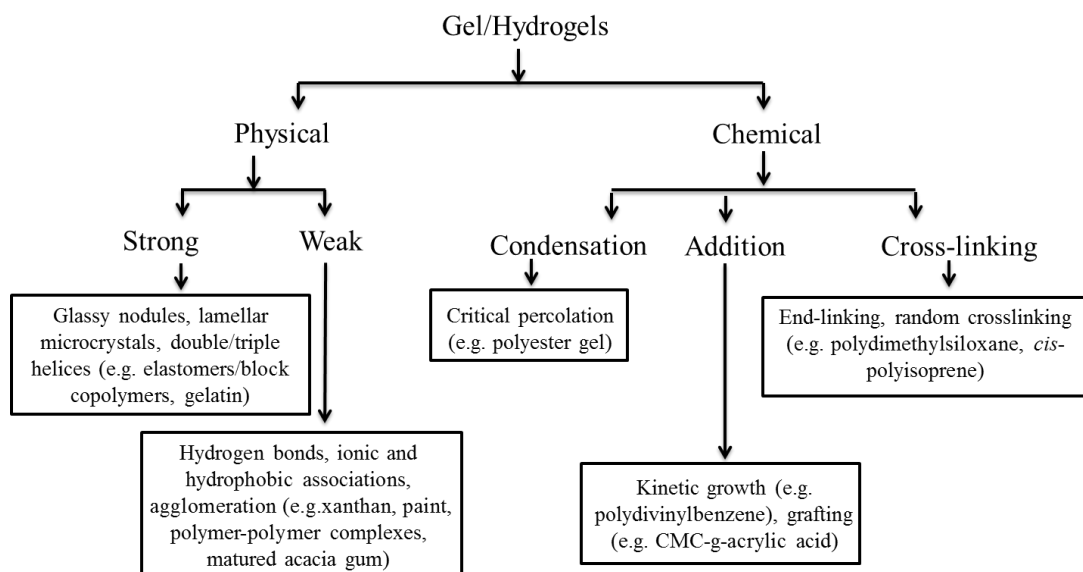


**Figure 2.1** The classification of gelation mechanism and relevant examples [15]

**Figure 2.1** presents the classification of gelation mechanisms and relevant examples. Gelation usually refers to the crosslinking of polymeric macromolecular chains in a chemical or physical fashion, which initially leads to progressively larger branched yet soluble polymers depending on the conformation and structure of the raw and processed materials. The mixture of such polydisperse soluble branched polymer is called 'sol'. Continuation of the linking process results in increasing the size of the branched polymer, and meanwhile, decreasing solubility. This 'infinite polymer' is called the 'gel' with network structure and is permeated with finite branched polymers. The sol-gel transition refers to a system with a finite branched polymer to infinite molecules and the critical point where gel firstly appears is called the 'gel point' [16].

Different types of gelation mechanism are summarized in **Figure 2.1**. Gelation can take place either by chemical linking (chemical gelation) or by physical linking (physical gelation). Chemical gelation can result in a strong gel due to covalent cross-linking bonding. Condensation, vulcanisation and addition polymerisations are three main chemical gelation processes. On another hand, physical gels can be categorised as strong physical gels and weak gels. Strong physical gel has strong physical bonds between polymer chains and is effectively permanent at a given set of experimental conditions. Hence, strong physical gels are analogous to chemical gels. The main strong physical bonds include glassy nodules, lamellar microcrystals or double and triple helices. Weak physical gels have reversible links formed from temporary associations between polymer chains. These associations have finite lifetimes, and are able to form, break and reform continuously. The main weak physical bonds include hydrogen bonds, aggregation interactions in block copolymer micelles, and ionic associations.

### **2.1.1. Thermoresponsive hydrogel**

Hydrogels can be divided into several groups based on their stimulus responsivity. Stimuli-responsive hydrogels can rapidly change their dimension, configuration or physical properties with small changes in the appropriate stimuli such as light [17], pH value [18], heat [19], electricity [20], magnetic field [21], water/moisture [22], and solvent [23].

Due to their unique composition, structure, and physicochemical properties, stimuli-responsive hydrogels are considered to be an important class of tailor-made functional materials. The properties such as swelling, sol-gel transition, tunable degradability and permeability, make hydrogels appropriate for a wide range of applications, especially in the biotechnology and biomedicine fields, e.g. microfluidics and biosensors [24], optoelectronic switches [25], delivery of drugs and soluble substances [26, 27]. While getting deeper insights into the chemistry and mechanisms that induce conformational changes in polymer structures, this kind of hydrogel-based smart materials is becoming increasingly prevalent. Based on this knowledge, more and more ways are developed so as to exploit, and modulate them. Considerable efforts and research have been made to immobilize or encapsulate cosmetically active ingredients in hydrogels in order to achieve the controlled drug release, and in the meantime to protect them from being oxidized [28].

To trigger the environmentally responsive polymers, temperature is one of the most useful and widely-used stimuli, because it can be easily controlled and universally applied [29-31]. In recent years, both chemical and physical crosslinks have been used for the preparation of hydrogels that can be triggered and applied under physiological conditions. One of important developments in

this area is the “in situ” formed hydrogel system. It is injectable fluids that can be introduced and applied into the body cavity, organ, or any tissue in a minimally invasive manner before gelation [32]. The gelation networks of thermoresponsive hydrogels are insoluble and start to form at body temperature, as a result of chemical crosslinks by covalent bonds, or physical crosslinks by hydrophobic interactions, ionic interactions, or hydrogen bonds [33, 34]. With such smart hydrogel-based systems featuring the body temperature-triggered sol-gel transition, there is no need for additional surgical procedures by virtue of the initially flowing nature of the smart material, which ensures proper shape adaptation as well as a good fit with surrounding tissues.

For reversible thermoresponsive hydrogels, if the physical crosslinks are disrupted by a temperature change, a sol (a flowing fluid) is formed. This sol to gel transition is fully reversible and can create opportunities to apply such temperature-responsive hydrogels into the body or on the skin or wound. In this way, drug and nutriment can be loaded into the hydrosol at room temperature, followed by a control release from the hydrogel at body temperature.

Compared to physically crosslinked hydrogels, chemically crosslinked hydrogels usually have better mechanical properties and are more resistant to degradation. This implies that physical gels, in most cases, possess a biodegradability superior to chemical gels, which is significant for practical applications. For example, despite the fact that Pluronic and N-isopropylacrylamide (PNiPAAm) copolymer are important and frequently-used thermoresponsive hydrogels, because they are flowing liquid at or below ambient temperature and form gels at physiological temperatures [35], their drug delivery applications are limited and problematic because they are

nonbiodegradable and likely to be accumulated in the body [36].

In recent years, a good deal of physical crosslinked thermosensitive hydrogels have been extensively researched and studied for biomedical applications due to their biocompatible and biodegradable properties. Notably, amphiphilic block copolymers have gained an increasing interest for drug delivery applications [34, 37, 38].

The design of biodegradable thermoresponsive hydrogels being available today are mainly based on amphiphilic block copolymers comprising aliphatic polyesters, as the hydrophobic block, and poly(ethylene glycol) (PEG) as the hydrophilic block with a linear triblock or multiblock architecture [39-41]. The temperature, at which the transition from a sol to a gel takes place, depends on several parameters like the composition of the copolymers, the copolymer concentration in water and the molecular weight.

In the following sections, physically crosslinked thermoresponsive hydrogels with a sol-gel transition behavior, as well as their gelation mechanisms will be mainly discussed. And the emphasis will be placed on biodegradable amphiphilic block copolymers with PEG as the hydrophilic block.

### **2.1.2. Thermo-induced gelation mechanism**

Hydrogen bonding, hydrophobic interactions, and physical entanglements are the main features that form the junction zones in thermo-responsive physically crosslinked hydrogels. Hydrogen bonding occurs primarily at low temperatures and is disrupted by heating. Hydrogen bonding is the root cause for the gelling upon cooling, and become soluble upon heating, such as the gels based on the natural polymer gelatin. Hydrogen bonding provides the stable helical structures in naturally occurring proteins and polysaccharides [33, 42].

The gelation mechanism of polysaccharides is showed in **Figure 2.2**. Random coils become helices, which subsequently aggregate to form the physical cross-linked gel.

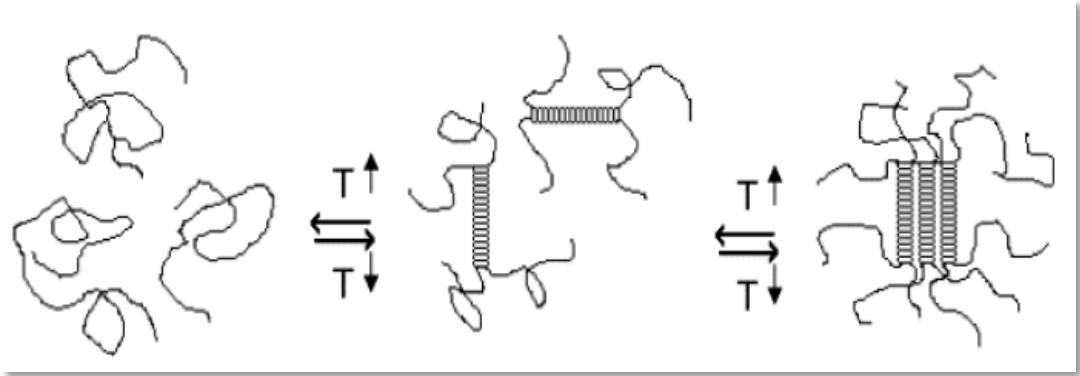


**Figure 2.2** Gelation mechanism of polysaccharides in water [42]

For sol to gel transition upon heating, the gelation mechanism of thermoresponsive hydrogels which becomes non-flowing gel by heating and turns into flowing sol by cooling, is proposed as a result of the enhanced hydrophobic interactions during temperature rising. Subsequently, the polymers self-assemble and form physical crosslinks.

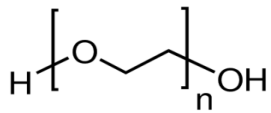
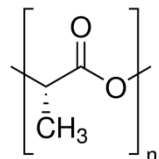
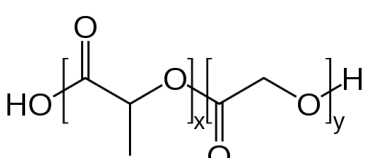
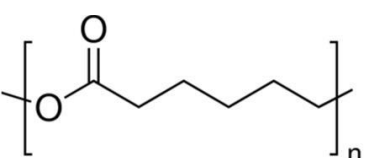
For sol to gel transition upon cooling, the physical entanglements are proposed as another reason for some hydrogels based on synthetic polymers, in addition to the cause involving hydrogen bonding.

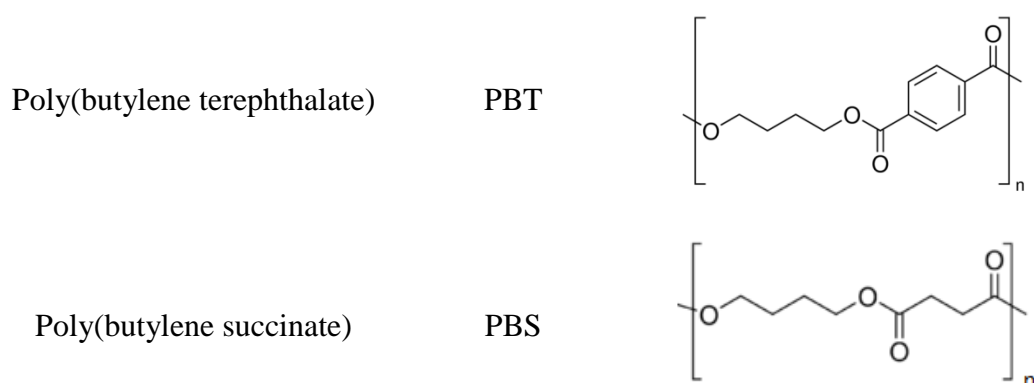
### **2.1.3. Materials used for the synthesis of amphiphilic block copolymers**

Materials with a broad range of properties can be obtained by varying the type, length or weight ratio of the building blocks. Amphiphilic block copolymers are classified into di-block copolymers (AB-type), tri-block copolymers (ABA-type), multiblock copolymers ((AB)<sub>n</sub>-type) and star block copolymers.

The polymers that constitute a hydrogel network may either be synthetically or naturally derived. Commonly-used natural polymers include proteins such as gelatin [43], fibrin [44] and collagen [45]. Polysaccharides such as alginate [46], dextran [47], chitosan [48] and hyaluronic acid [49, 50] have been applied as well. Naturally occurring polymers generally possess a less defined chemical structure compared to synthetic polymers, which may result in less controlled mechanical properties and degradability. Further, they may provoke a severe immunological response, accommodate viruses or microbes and their supply from one source may be limited [51]. The chemical structure of several important building blocks of amphiphilic block copolymers is shown in **Table 2.1**.

**Table 2.1** Building blocks frequently used in amphiphilic block copolymers [52]

Name	Abbreviation	Molecular formula
Poly(ethylene glycol)	PEG	
Poly(lactic acid)	PLA	
Poly(lactic-co-glycolic acid)	PLGA	
Poly(ε-caprolactone)	PCL	



As hydrophilic block, poly(ethylene glycol) (PEG), also referred to as poly(ethylene oxide) (PEO), is most frequently used as it is nontoxic, biocompatible and can be excreted by the kidney [53]. Indeed, PEG has been permitted by the US Food and Drug administration (FDA) for internal use in the human body [54]. Examples of frequently used hydrophobic blocks, as listed in **Table 2.1**, are polyesters like poly(butylene terephthalate) (PBT) [55-59], poly(butylene succinate) (PBS) [60], poly(lactic-co-glycolic-acid) (PLGA) [61, 62], poly(lactic acid) (PLA) [63-68], and poly( $\epsilon$ -caprolactone) (PCL) [36, 69-71].

#### **2.1.4. Thermoresponsive hydrogels based on biodegradable copolymers**

Thermoresponsive hydrogels based on biodegradable copolymers with PEG as a hydrophilic block can be divided into two classes: (1) materials that form a sol at low temperatures and turn into a gel with increasing temperatures. Further temperature increase leads to a sol phase again (**Figure 2.3 A**); and (2) materials that are in a gel state at low temperatures and turn into a sol state with increasing temperatures (**Figure 2.3 B**).

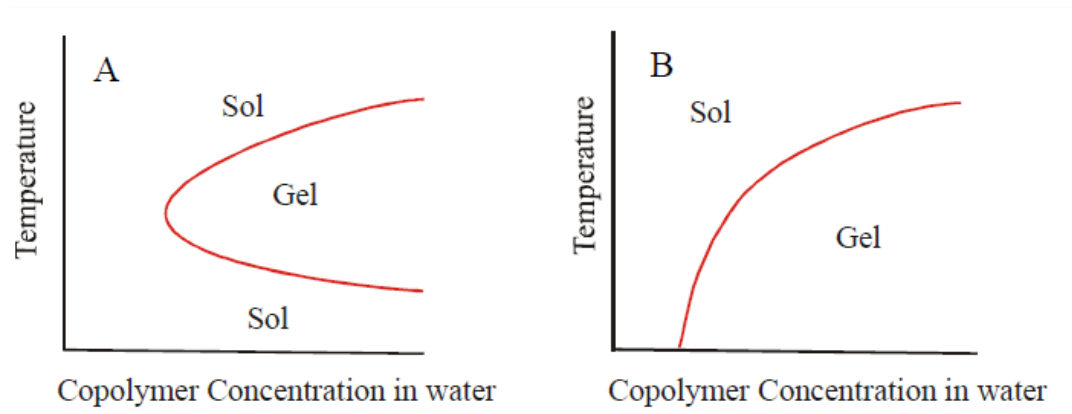


**Figure 2.3** Schematic representation of the transition diagrams of copolymers in water (A) sol-gel-sol transitions(class1) and (B) gel-sol transitions(class2) [72]

Whether a copolymer belongs to class 1 or 2 is dependent upon the total molecular weight of the copolymer and its hydrophobic/hydrophilic balance. In the case of the class 1 materials, the block length of the hydrophilic blocks of the copolymer is below the critical entanglement length [73] and the micelles are in a flowing state, and turn into a sol state, as shown in **Figure 2.4 A**. Upon increasing temperature, the hydrophobic interactions become stronger and the micelles start to aggregate.

The class 2 materials have hydrophilic block lengths above the critical entanglement molecular weight, and the micelles are connected to each other via these entanglements, resulting in a gel phase already at low temperatures, as shown in **Figure 2.4 B**. In both class 1 and class 2 cases, the upper transition from gel to sol is considered to be caused by dehydration of the PEG, which causes the micelles to shrink, resulting in weakened interactions between the different micelles. As a consequence, a sol phase is regenerated. If the dehydration is more severe, the formation of the sol phase is accompanied by precipitation of the copolymers out of the water, forming water-rich and copolymer-rich phases.

Hydrogels of class 1 is discussed in the following section in detail, with the emphasis on the relation of their thermo-responsive behavior to their structure and architecture. Following that, potential applications of these hydrogels as drug delivery systems are discussed.

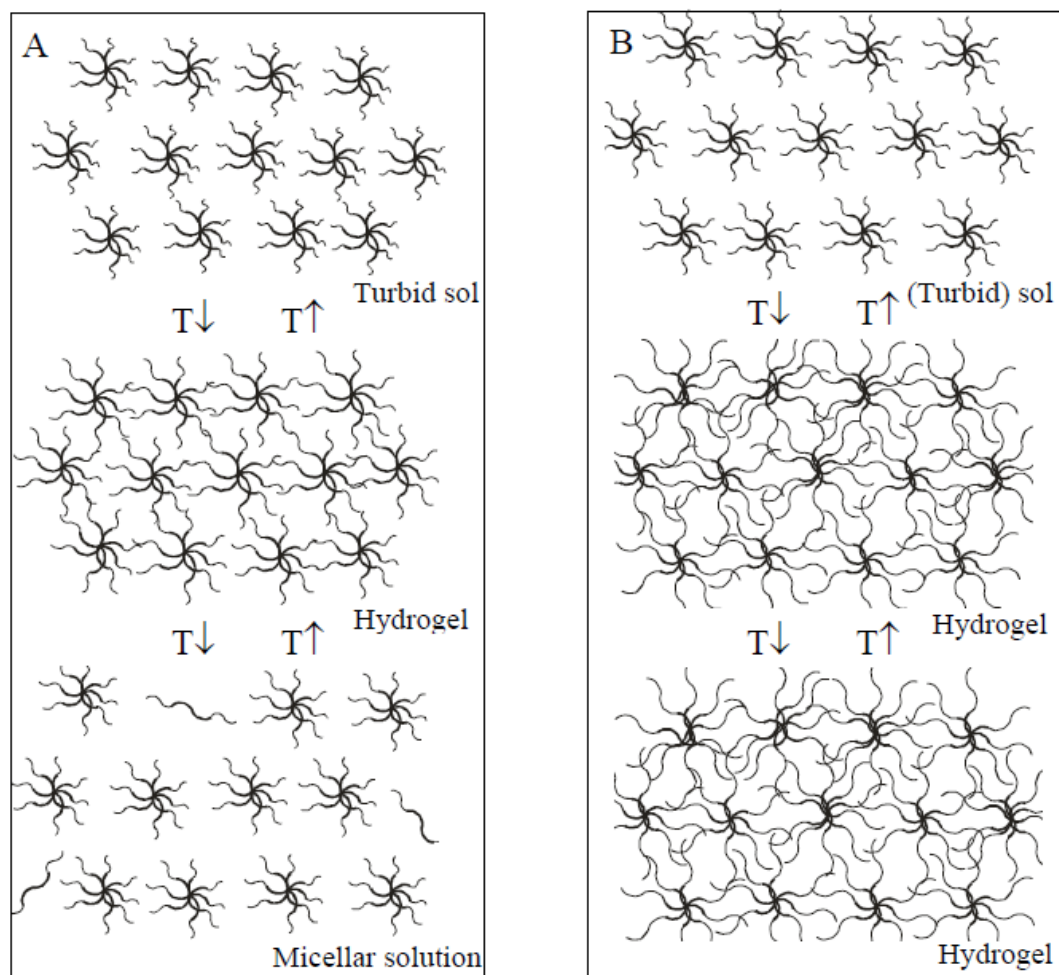


**Figure 2.4** Schematic representations of copolymeric micelles in water: (A) Class 1 copolymers sol-gel-sol transition upon increase in temperature and (B) Class 2 copolymers gel-sol transition upon increase in temperature [72]

### **2.1.5. Development of thermoresponsive hydrogels based on amphiphilic block copolymers with sol-gel-sol transition behavior**

Hydrogels prepared based on amphiphilic block copolymers with a sol-gel phase transition behavior have been reported since 1999 [74, 75]. During these almost 20 years, many efforts have been made to research and develop the reversible sol-gel thermoresponsive hydrogels based on PLA (poly(lactic acid)), PLGA (poly(lactic-co-glycolic acid)), or PCL (poly( $\epsilon$ -caprolactone)) as hydrophobic blocks and PEG (poly(ethylene glycol)) as a hydrophilic block.

PLA is comparatively more hydrophobic than poly(glycolic acid) (PGA) due to the presence of the additional methyl group. It is chiral in nature because of the structure of lactic acid, which commonly exists in three isomeric forms the D (-), L (+) and racemic (D, L) lactide. The crystalline nature of PLA depends upon the isomeric forms and molecular weight. Poly-L-lactide (PLLA) is hydrolyzed through normal metabolic pathway due to the presence of naturally occurring isomer (L-lactide). It has a melting point of 175 °C and glass transition temperature of 60-65 °C. It also possesses both high tensile strength and modulus with the values of 50-70 MPa and 4.8 GPa respectively. The degradation rate of PLLA is slower than PGA and usually takes around two to six years for the complete elimination from the body. On the other hand, poly-DL-lactide (PDLLA) is amorphous in nature due to the presence of a racemic mixture. It has the glass transition temperature of 55-60 °C and comparatively faster degradation rate compared with PLLA. The faster degradation kinetic renders PDLLA more suitable for drug delivery applications. All isomeric forms of PLA follow bulk erosion kinetics and can degenerate into lactic acid upon hydrolytic

cleavage [76].

Hydrogels based on alternating multiblock copolymers of PLA/PEG which undergo a sol-gel-sol transition as the temperature increases from 20 °C to 60 °C have also been reported. The polymers were synthesized by coupling hydroxyl of PEG and PLA using succinic anhydride [77, 78]. The synthesized PEG/PLLA multiblock copolymers system is a promising injectable biomaterial containing PEG and PLLA with molecular weights of 600 and 1100-1500 respectively. The prepared hydrogel exhibited a reversible thermal gelation behavior in the physiologically important temperature range, namely 30 °C - 45 °C. The gelation mechanism was considered to be micellar aggregation. The transition temperature and gel window could be adjusted by varying the molecular weight and composition of the PEG/PLLA multiblock copolymer. The in vivo and in vitro gel in situ forming abilities of this biodegradable injectable system was evaluated and demonstrated by subcutaneous injection into rats.

The influence of the architecture of stereo complexed PEG/PLA (PLLA or PDLA: A, PEG: B) block copolymers on the gelation properties has been investigated by Kimura's group [79, 80]. Mixed micellar solutions of enantiomeric ABA and BAB block copolymers exhibit very different gelation behaviors and crystal structures. Enantiomeric AB diblock and BAB triblock copolymers were synthesized by ring opening polymerization of L- or D- lactide initiated by mono- or di-hydroxyl PEG, whereas ABA triblock copolymers were prepared by coupling the AB diblock copolymers using hexamethylene diisocyanate (HMDI).

In the micellar solutions of the enantiomeric ABA triblock copolymers, the hydrophobic PLLA or PDLA segments aggregate to form a core region, while

the hydrophilic PEG segments expose outside in the form of a shell when the micelles are prepared separately. Consequently, the PLLA and PDLA segments can be isolated from each other when the micellar solutions of the enantiomeric block copolymers are mixed together. The mixed PLLA-PEG-PLLA and PDLA-PEG-PDLA systems exhibit an irreversible sol-gel transition behavior upon increasing temperature. Illustrated in **Figure 2.5 (a)** is a schematic of ABA system gelation, it showed that PLLA-PEG-PLLA and PDLA-PEG-PDLA micelles consist of a core region and a PEG shell. Under heating condition, the aggregation of the PLLA and PDLA segments at the core/shell interface of the micelles is weakened to allow the PLLA and PDLA polymer blocks to diffuse outside of the core, with interactions with each other. Consequently, stereo complexation promotes the crosslinking of micelles and a gel is consequently formed. Due to the high stability of the stereo complex crystals, the gel formation is irreversible and no gel-sol transition occurs upon cooling or heating.

The mixing system of BAB triblock copolymers exhibits a reversible gel-sol transition response to temperature, and corresponding gels can be formed hydrogels at high copolymer concentrations, as shown in **Figure 2.5(b)**. In aqueous solutions, the central PLLA and PDLA blocks are not easily exchanged among the micelles even when heated to high temperatures. It is suggested that the helical conformation of the PLLA and PDLA blocks is transmitted to the PEG chains and that aggregation of helical PEG chains with the opposite senses, leads to gelation at low temperatures. When the temperature is increased, the PEG domains collapse due to dehydration and the gel transforms into a sol. Upon cooling the inter micellar PEG crosslinks are able to re-form, leading the system to the gel state.

Mixed solutions of enantiomeric AB diblock copolymers exhibit a gel-sol transition upon increasing temperature. However, unlike previous ABA and BAB triblock systems, the transition is irreversible, as depicted in **Figure 2.5 (c)**. The authors suggested that the exchange of the core PLLA or PDLA blocks between micelles is much faster than in the BAB system, which was supported by wide angle X-rays cattering (WAXS) measurements showing that the stereo complex crystals grow with increasing temperature. Eventually most micelles comprise stereo complexed PDLA and PLLA blocks in their core at elevated temperatures. Inter micellar PEG interactions being responsible for the gelation of the system at lower temperatures, are weakened. The change in PEG interactions from inter-to intra-micellar is responsible for the irreversible gel-sol transition in the AB system.

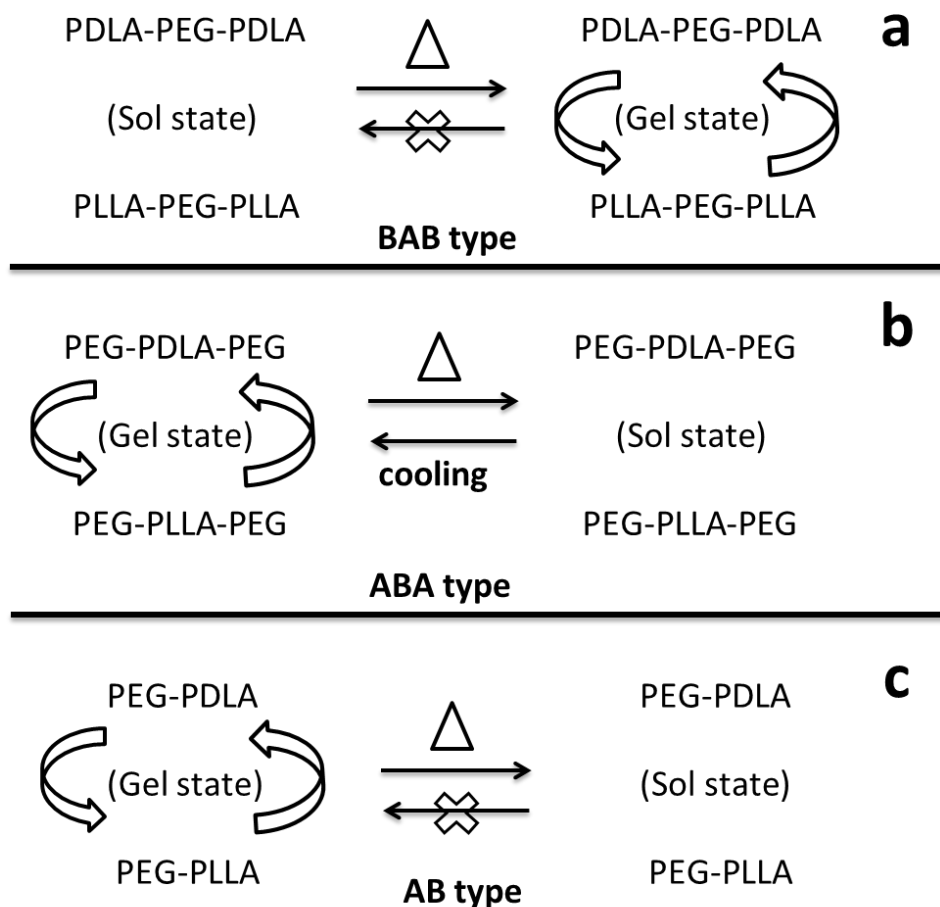


**Figure 2.5** Proposed gelation mechanisms of enantiomeric mixtures of ABA (a), BAB (b) or AB(c) type block copolymers, with B as the hydrophobic PLA block and A as hydrophilic the PEG block [81]

PLGA is approved by Food and Drug Administration using in therapeutic devices owing to its biocompatibility and biodegradability. Two different monomers of the lactic acid and cyclic dimers (1,4-dioxane-2,5-diones) of glycolic acid can be used to synthesize PLGA by random ring-opening co-polymerization method. PLGA is a kind of potential biomaterial. It can be broken up into the original monomers of glycolic acid and lactic acid after hydrolysis in the body. Because these two monomers are by-products of various metabolic pathways and can be completely dealt with in the body, there is minimal systemic toxicity to use PLGA as biomaterial and for drug delivery application. It is another advantage that the polymer degradation time can be tailored by adjusting the ratio and dosage of the monomers during the synthesis. This made PLGA a common choice in the production of a variety of biomedical devices, such as prosthetic devices, sutures, grafts, implants, micro and nanoparticles. ABA type of copolymer PLGA-PEG-PLGA was synthesized by ring opening polymerization of glycolide and lactide using a  $\alpha,\omega$ -dihydroxy PEG as the initiator. The inverse BAB triblock copolymer PEG-PLGA-PEG was prepared as follows. Firstly, synthesize diblock PEG-PLGA copolymers by ring opening polymerization of glycolide and lactide, using poly (ethylene glycol) methyl ether (mPEG) as the initiator. Subsequently, couple these diblock copolymers with hexamethylene diisocyanate as a coupling agent. The prepared triblock copolymer was water soluble hydrosol at low temperatures. It can be transformed into gel state by increasing temperatures. Overheating will lead to

phase separation, and this phase transition phenomenon is same as that of Pluronics. However, the proposed gelation mechanism differed from Pluronics since PLGA is more hydrophobic than poly(phenylene oxide) (PPO), and micelles are formed more readily. For these PEG-PLGA-PEG triblock copolymers the gelation mechanism is suggested to be a result of the increase in the size of the micelles, due to increased polymer-polymer attractions upon an increase in temperature. They can move relatively freely at low temperatures, and the sol-gel transition occurs at high temperature when the total volume fraction of micelles is over the maximum packing fraction (**Figure 2.6 A**). For the ABA type PLGA-PEG-PLGA copolymer hydrogels an additional mechanism is proposed. Micelles are formed from a core of PLGA loops and a PEG shell (**Figure 2.6 B**). Some copolymers form bridges between different micelles and form micellar groups. With increasing temperature, the number of bridging micelle groups increases abruptly, leading to gelation [82]. These bridges lead to a decrease in the critical gelation concentration (CGC), the concentration necessary to form a gel. For example, aqueous solutions of PLGA-PEG-PLGA of a molecular weight of  $3800 \text{ g mol}^{-1}$  and a PEG content of 34 wt% have a CGC of approximately 5 wt%, whereas aqueous solutions of a comparable PEG-PLGA-PEG copolymer have a CGC of approximately 25 wt%.

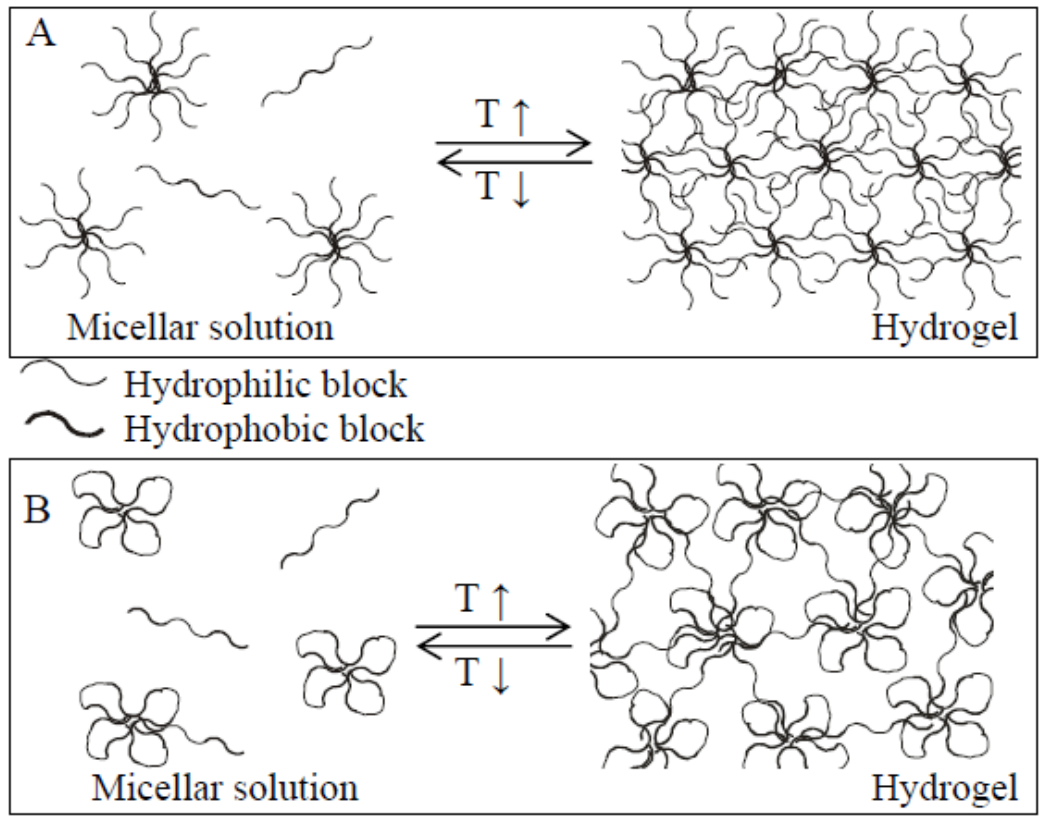


**Figure 2.6** Schematic representation of self-assembly of amphiphilic triblock copolymers (A) PEG-PLGA-PEG and (B) PLGA-PEG-PLGA in water upon a temperature change [92]

PCL is another kind of biomaterial that has been approved by FDA in terms of applications in medical devices and drug delivery systems [83, 84], because it is biodegradable and biocompatible. In an amphiphilic block copolymer system, i.e. PEG-PCL-PEG, PCL serves as the hydrophobic block. This kind of hydrogel is flowing sol at room temperature, in this case around 25 °C, and becomes a transparent non-flowing gel at body temperature, namely around 37 °C. This sol-gel transition is reversible and rapid, which allows PCL based thermoresponsive hydrogel system to be a noticeable and useful biomaterial for drug delivery [85]. PCL is a semi crystalline polymer that can be synthesized by ring opening polymerization of  $\epsilon$ -caprolactone. The glass transition temperature and melting

temperature are around -60 °C and 59 - 64 °C respectively. PCL was investigated for long-term delivery purpose due to the higher permeability to many drugs, unique thermoreversible properties, excellent biocompatibility and extremely slow hydrolytic cleavage of polyester backbone. The PCL-based Capronor® implant was developed for the controlled delivery of levonorgestrel. Numerous investigations were attempted to modulate the slower degradation of PCL which generally shows a degradation of two to three years. Copolymers consisting of  $\epsilon$ -caprolactone with D,L lactide or glycolide exhibit a remarkably better degradation profile. Yenice et al. evaluated the ocular bioavailability of cyclosporine A loaded with PCL nanoparticles alone and coated with hyaluronic acid. They observed significantly higher cyclosporine A levels in the corneal tissue of a rabbit. In PCL alone, they observed cyclosporine of a concentration of 5.9-15.5 ng/mg tissues and 11.4-23.0 ng/mg tissue in hyaluronic acid-coated PCL nanoparticles. These levels were found to be higher than the conventional eye drops and showed promising approach for the treatment of immune mediated corneal diseases [86].

The applications of PCL-based hydrogel system in drug deliver and sustained control-release formulations have been explored extensively in previous studies [36, 87-90]. However, earlier studies mainly focused on synthesis of PCL based amphiphilic block copolymers and release of hydrophilic and hydrophobic model drugs from the prepared hydrogel systems [91]. An aqueous solution of PCL-PEG-PCL at a 15 wt% concentration showed a sol-gel transition at 25 °C, whereas a PEG-PCL-PEG copolymer solution at the same concentration showed a sol-gel transition at 33 °C (**Figure 2.7**). The upper gel-sol transition temperature was 5 °C higher for this PCL-PEG-PCL hydrogel than that

for the PEG-PCL-PEG hydrogel. The effect of hydrophobicity of the A-block on the gelation behavior was investigated by changing A-block. As far as we know, PCL is more hydrophobic than PLGA. A PEG-PCL-PEG triblock copolymer showed a CGC, 10 wt% lower than the CGC of a PEG-PLGA-PEG triblock copolymer of comparable molecular weight and PEG content (**Figure 2.7**).

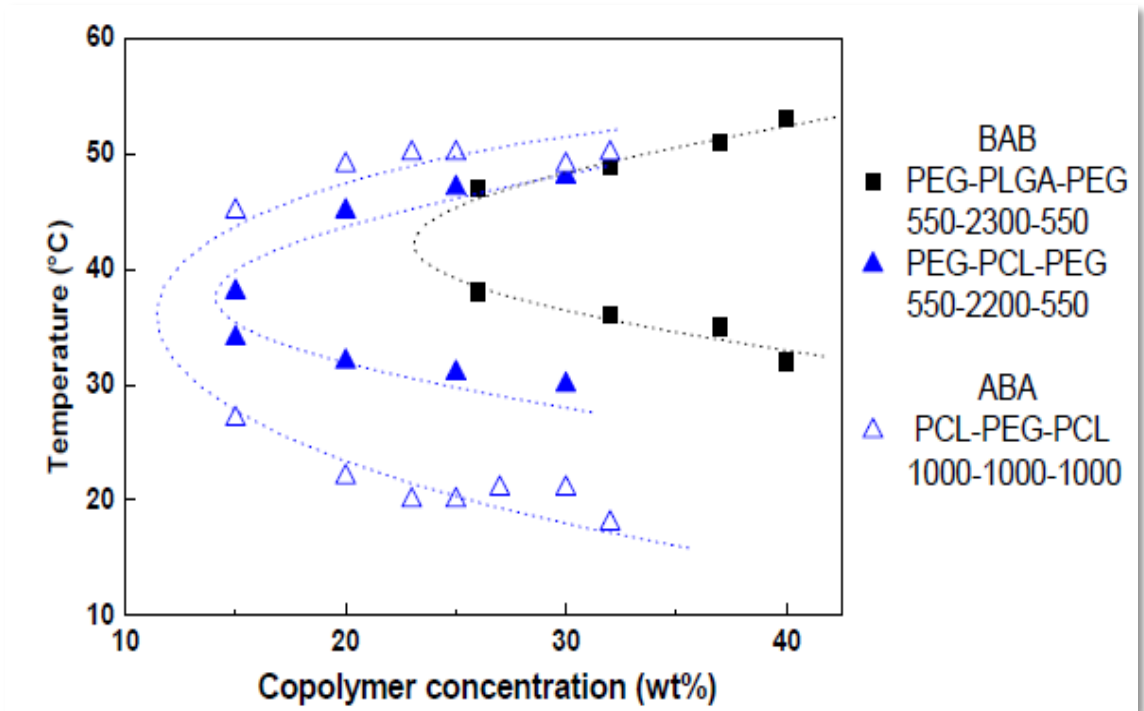


**Figure 2.7** ABA type and BAB type copolymers with PLGA (squares) or PCL (triangles) as the A blocks and PEG as the B blocks [40, 85, 92]

### 2.1.6. Thermoresponsive hydrogels as drug delivery system

The use of thermoresponsive hydrogels with a sol-gel transition behavior allows to prepare injectable delivery systems and to incorporate of bioactive agents by simple solution mixing. The advantages include easier applications compared to implants, and localized delivery for a site-specific action [93]. Diffusion is a kind of movement of drug that gradually releases out of polymer carriers. The diffusion through a polymer carrier can be described by Fick's law

[94, 95].

$$J = -D \cdot dC/dx$$

This law expresses the molar flux of a solute ( $J$ ) as a function of the concentration gradient ( $dC$ ) over a distance ( $dx$ ) between the solute-rich interior and the solute deficient surroundings of the matrix.  $D$  is the diffusion coefficient of the solute in the polymer matrix.

Formulations consisting of hydrophilic matrices, and from which the drug release is controlled by the inward flux of water from the outside environment, and consequent swelling of the matrix, are referred to as swelling-controlled release systems. An example is the release of dispersed water-soluble agent out of a dehydrated hydrogel in an aqueous environment. Initially, the diffusion is slow, but speeds up significantly when the gel is swollen by the absorption of water. The agent release involves the uptake of water from the surrounding media, and simultaneously, the diffusion of the active agent into the surroundings. The complication of the release behavior is that the diffusion coefficient is dependent on the water uptake as well, which makes it more difficult to predict the release rate.

The release of drugs from thermo-responsive hydrogels in vitro and in vivo was mainly investigated for PLGA/PEG copolymers. Having relatively low molecular weight ( $< 5000 \text{ g mol}^{-1}$ ), both ABA and BAB triblock copolymers, with PLGA and PEG as the A and PEG blocks respectively, have been claimed by Macromed as thermosensitive drug carrier systems with gelation properties [96]. In a previous study, PEG-PLGA-PEG triblock copolymer-based hydrosols were injected subcutaneously in rats and the gel depots were found to last for more than one month. It has also been demonstrated that there is no tissue

irritation at the injection site [97]. Furthermore, the release of hydrophobic and hydrophilic model drugs, that is, spironolactone and ketoprofen, respectively, from PEG-PLGA-PEG hydrogels was investigated in vitro [98].

Subcutaneously injected PLGA-PEG-PLGA hydrogels became smaller gradually over a period of two weeks, consequently forming a mixture of a gel in a viscous liquid [99]. A 23 wt% PLGA-PEG-PLGA solution in PBS buffer has been commercialized under the name ReGel® (Macromed). A formulation containing paclitaxel at a concentration of 6 mg g<sup>-1</sup> is called Onco Gel [99], and is designed to release paclitaxel into the tumor at a sustained rate over 4-6 weeks in order to achieve a higher concentration of paclitaxel in the tumor compared to intravenously administered drug. A similar type of PLGA-PEG-PLGA copolymers was also investigated for the in vitro release of 5-fluorouracil, lysozyme [100] and indomethacin [101], as well as for the in vivo drug delivery in rabbits for the potential treatment of superficial corneal burns [102].

Beeley et al. also designed a triamcinolone acetonide loaded polycaprolactone implant for the treatment of retinal diseases. PCL implant was well compatible with living tissues in the sub-retinal space of rabbit eyes, and the sustained release of TA could last for a period of four weeks [103].

## **2.2. Antibacterial polymeric materials with quaternary ammonium salt**

Microorganisms exist ubiquitously and can be ready to spread through various media including air, water and food. Pathogenic bacteria, fungi, and viruses have long been considered as a threat to public healthcare. Bacterial infection is, therefore, a typically concerned issue in many areas, especially those involving the use of biomaterials.

World Health Organization (WHO) statistics shows that over 1.4 million people worldwide suffer from infectious complications, which occurs most often in hospital [104-107].

Numerous kinds of antibacterial agents such as disinfectants, antiseptics, and antibiotics are substantially developed for controlling and preventing bacterial infections. However, the widespread and injudicious uses of these agents lead to the emergence of unprecedented antibacterial-resistant microorganisms, revealing the undoubtedly big challenges in the antibacterial tasks [108-111]. Recently, the continual emergence of new strains of global infectious pathogens, such as extensively antibiotic-resistant tuberculosis [112], avian influenza A (H5N1) and ebola [113] alerts us that there is an urgent demand for exploring novel antibacterial agents with broad-spectrum, long-lasting and efficient properties.

Molecular weight is one of the major factors to be considered when tailoring a novel antibacterial agent. Conventional antibacterial compounds in low-molecular-weight tend to cause environmental contamination and human poisoning due to biocidal diffusion [114, 115]. On the contrary, antibacterial materials in polymeric form is agreed as a worth-considering approach to address these problems by promoting antibacterial efficacy and lessening residual toxicity [116, 117]. In addition, chemical stability and non-volatility are the beneficial properties of antibacterial polymers to afford long-term activity [118]. Different from the polymeric antibacterial substances which are applied by physically entrapping or coating organic and/or inorganic active agents to the substrates during or after processing, antibacterial moieties, covalently substituted or linked to the polymer chain dramatically reduce the risk of the

permeation of low-molecular-weight biocides from the polymer matrices. Such antibacterial polymers promise satisfactory durability in an environmentally-friendly way [119, 120]. Polymeric antibacterial agents consisting of quaternary ammonium salts (QAS) are probably the most widely utilized and well-studied among all polymeric ones. Benzalkonium chlorides has been discovered to exert an antibacterial function by Domagk in 1935 [121]. QAS with various structures have further been designed and synthesized as disinfectants. A survey on approximately five hundred US EPA (Environmental Protection Agency) registered disinfectant products for households indicated that QAS, accounts for 57.8% of the total reagents used to prepare disinfectant products, thus indicating that it is the most popular reagent introduced to prepare the formulations of disinfectant products [122]. The global consumption of QAS was reported as 0.5 million tons in 2004, and was expected to be over 0.7 million tons by the year 2006 [123]. Versatile antibacterial activities can be obtained using polymeric QAS, which can be synthesized through either direct polymerization of monomers containing QAS groups or covalently incorporating QAS moieties within ordinary synthetic or natural polymers [124, 125]. Meanwhile, polymeric QAS can also function-as a potential driver for overcoming the antibiotic-resistance [126-129].

Certain literature [130-132] illustrated that polymers with QAS groups linked by covalent bonding exhibit strong antibacterial activities. Thus, it is a judicious to incorporate ammonium groups into the backbone of block copolymer to realize the antibacterial modification of the thermoresponsive hydrogels.

### **2.2.1. Antibacterial polymer with pendant quaternary ammonium salts**

One method of synthesizing polymers with pendant QAS is to prepare polymerizable QAS monomers which are subsequently polymerized or copolymerized with other monomers. Another method is the quaternization of polymers containing either tertiary ammonium groups or alkyl halides. In the direct polymerization process, the stability of the monomers may be a limiting factor. In comparison, post-quaternization overcomes the potential disadvantage of monomeric stability, while the impacts of neighboring groups and steric hindrance tend to lower the degree of quaternization [133]. Since it is difficult to obtain complete functionalization by post-quaternization of polymeric tertiary ammonium salts, the properties of the as-prepared polymers may vary due to the difference in the quaternization degree. To examine the antibacterial efficiency of water-soluble QAS polymers, assessments of the minimum inhibitory concentration and minimum bactericidal concentration of the polymeric agents are commonly adopted. The shaking flask test and inhibition zone measurement are two general and effective approaches for evaluating the antibacterial performance of water-insoluble polymers; moreover, the inhibition zone measurement, normally, can also quantify the diffusion of biocides.

To study the structure-activity relationship of quaternary pyridinium polymers, T.Eren et al. [134] synthesized a series of amphiphilic polynorbornenes with various quaternary alkyl pyridinium side chains (**Figure 2.8**). The pyridinium-functionalized- polynorbornene with an ethyl pendant group was prepared by employing two different methods, i.e., direct-polymerization and post-quaternization. Polynorbornenes with 100% and

85% of quaternization degrees were collected respectively. Their antibacterial activities against *Escherichia coli* (*E. coli*) and *Bacillus subtilis* were the same with the MICs of 200 µg/mL. On the other hand, the latter polynorbornenes demonstrated as twice hemolytic activity against fresh human red blood cells of demonstrated as the former one. This result implied their biological activity is influenced by the synthetic route of polymeric QAS, because the quaternization degree has a significant effect on the balance of hydrophobicity and hydrophilicity of the polymers.

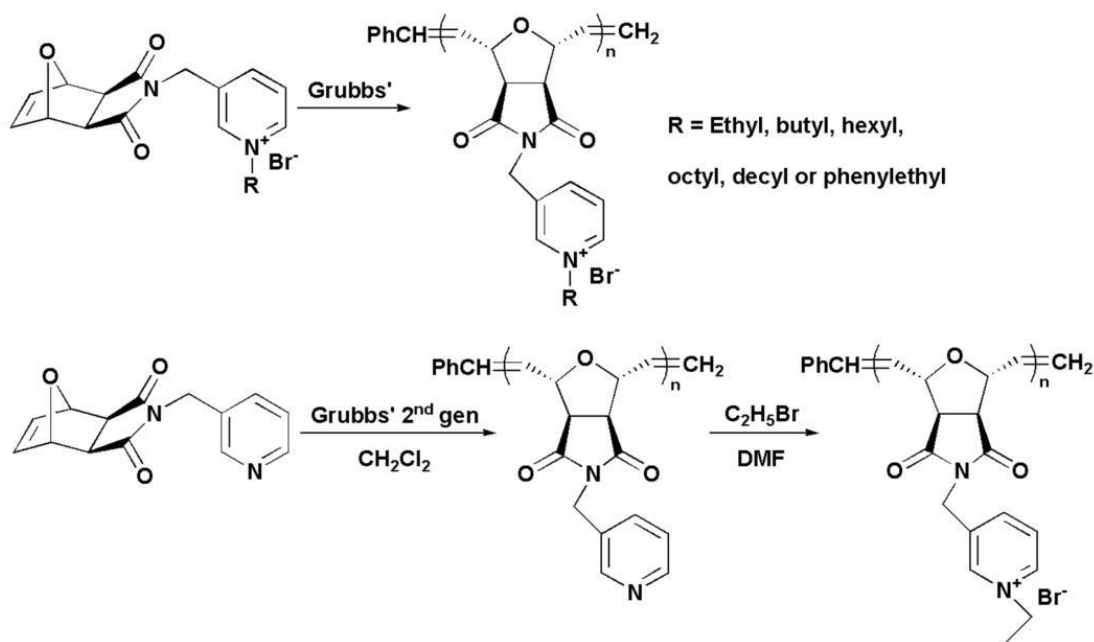


**Figure 2.8** Two synthesis methods based on oxanorbornene derivatives [134]

It was proven that a long alkyl chain substituent, i.e., at least eight carbons, renders QAS highly antibacterial [135]. On the basis of this finding, Dizman et al. [136] synthesized a methacrylate monomer containing pendant QAS based on 1,4-di-azabicyclo-[2.2.2]-octane, which contained either one butyl or a hexyl group (**Figure 2.9**). Although these monomers were incapable of contributing to any antibacterial functions, their corresponding homopolymers were effectively bactericidal against *S. aureus* and *E. coli*. In addition, it is found that their

counter-bacterial activity was dependent on the length of the hydrophobic segment; consequently, the polymer with hexyl groups was more potent than the one with butyl groups.

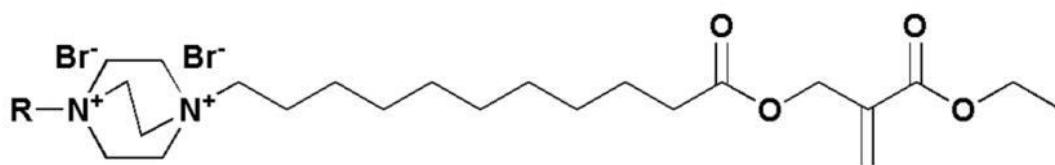


**Figure 2.9** Bis-quaternary ammonium methacrylate monomer based on 1,4-di-azabicyclo-[2.2.2]-octane [135]

To investigate the antibacterial performance of biodegradable cationic polycarbonates with quaternized nitrogen-containing heterocycles, Yang et al. [137][37] tailored a series of polycarbonates with propyl and hexyl side chains followed by quaternization with different N-heterocycles (**Figure 2.10**). All the synthesized N-heterocycle quaternized polycarbonates had higher antibacterial efficiency against bacteria and fungus when compared to their trimethylamine quaternized analogues. Hence, the amphiphilicity of the polymers was considered as an important factor affecting the antibacterial performance and hemolytic activity.

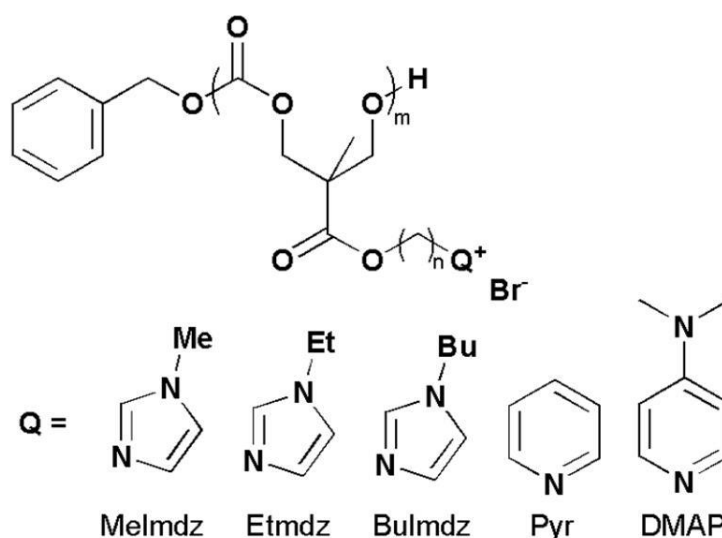


**Figure 2.10** Antibacterial polycarbonates with quaternized nitrogen-containing heterocycles [137]

Lenoir et al. [138] synthesized an antibacterial surfactant via quaternization of the amino groups of poly(ethylene-co-butylene)-b-poly[2-(dimethylamino)ethyl-methacrylate] copolymer with octyl bromide. The block copolymers were prepared by bromide-capped poly(ethylene-co-butylene) initiated atom transfer radical polymerization of 2-(Dimethylamino)ethyl methacrylate (**Figure 2.11**). In the shaking flask test against E. coli, such prepared surfactant carried comparable antibacterial activity to benzalkonium chloride, which is known as a commonly-used disinfectant.

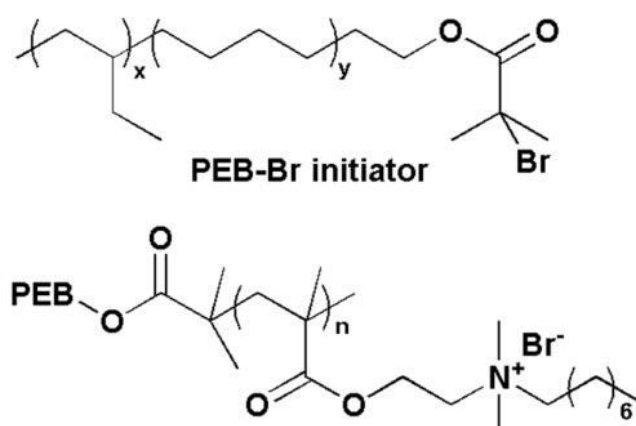


**Figure 2.11**

Poly(ethylene-co-butylene)-b-poly[2-(dimethylamino)ethyl-methacrylate]  
quaternized by 1-Bromooctane [138]

Biodegradable poly( $\epsilon$ -caprolactone) for antibacterial purpose [139] was generated by grafting alkyne-containing QAS onto the pre-synthesized azide-containing poly( $\epsilon$ -caprolactone) (**Figure 2.12**). In addition to biodegradability, a biocidal effect of the QAS-modified poly( $\epsilon$ -caprolactone) was observed via the analysis of the shaking flask test against E. coli.

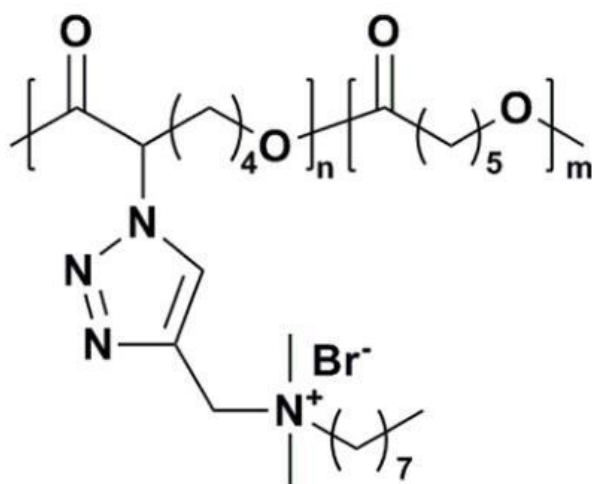


**Figure 2.12** Antibacterial poly( $\epsilon$ -caprolactone) [139]

To improve the hydrophilicity and biocompatibility of quaternized poly(vinylpyridine), high hydrophilic and biocompatible monomers hydroxyethylmethacrylate and polyethylene glycol methyl ether methacrylate were incorporated via copolymerization with 4-vinyl pyridine, respectively [140]. The pyridine groups were quaternized with hexylbromide, resulting in the formation of cationic copolymers with different compositions (**Figure 2.13**). By recording the photoluminescence attenuation induced by *E. coli* cells in contact with the polymer coated glass slides, optimally formulated copolymers were found to be over 20 times more active than the quaternized homo-poly(vinylpyridine). Combined with the results of the contact angle test, it was concluded that the enhancement of hydrophilicity could significantly improve both the antibacterial property and biocompatibility of polymeric materials.

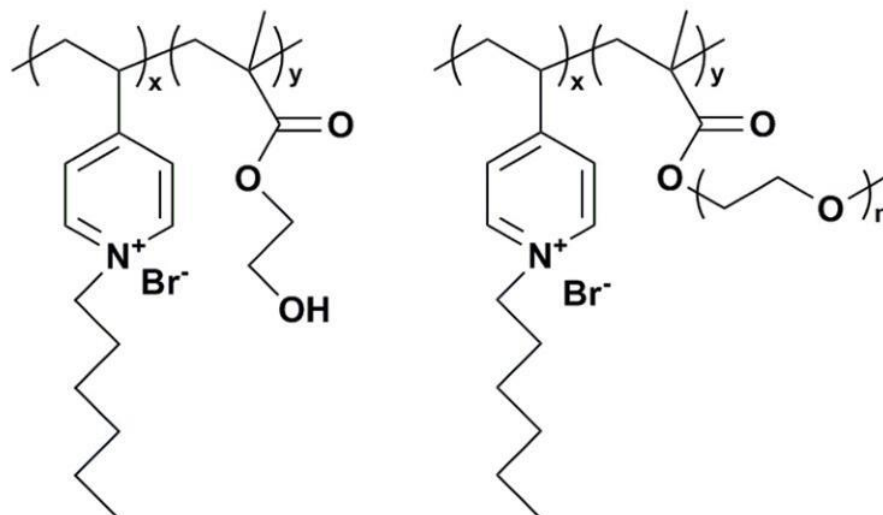


**Figure 2.13** Quaternized poly(vinylpyridine-co-hydroxyethylmethacrylate) and poly(vinylpyridine -co- polyethylene glycol methyl ether methacrylate) [140]

Two types of ionic dimethacrylate monomers containing QAS (**Figure 2.14**) were developed for novel antibacterial dental materials via a Menshutkin reaction, where one of them was incorporated into a bisphenol, glycerolate dimethacrylate, and triethylene glycol dimethacrylate (1:1) resin by photopolymerization [141]. The antibacterial assessment and macrophage viability assay revealed that the incorporation of the cationic monomer at a concentration of as low as 10% provides the resin with valid antibacterial performance and high biocompatibility.

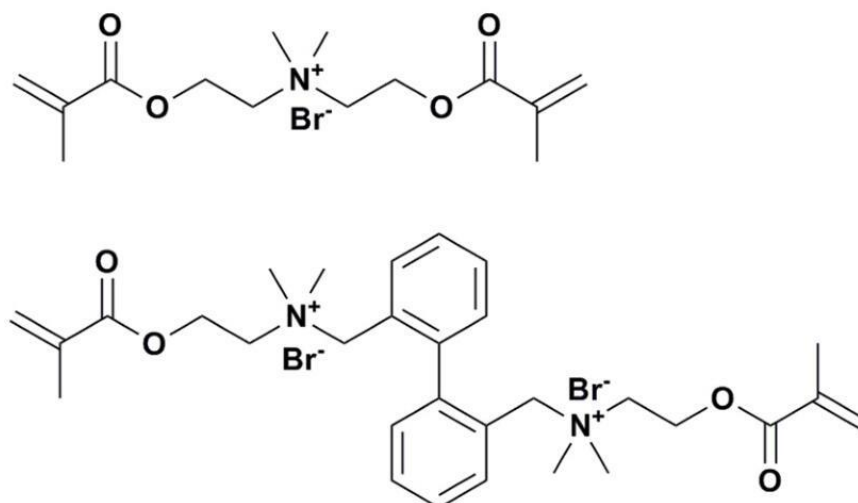


**Figure 2.14** Two types of ionic dimethacrylate monomers containing QAS [141]

Marini et al. [142] prepared antibacterial hybrid coatings involving a novel trialkoxysilane QAS (**Figure 2.15**) which is covalently bonded to the organic-inorganic network using a sol-gel technique. The antibacterial capability of polyethylene films with the QAS-containing coatings was evaluated against *E. coli* and *S. aureus* at different contact times. The film still maintained excellent antibacterial properties after repeated washings. Around 99% of biocidal efficiency was reported after 96 hours.

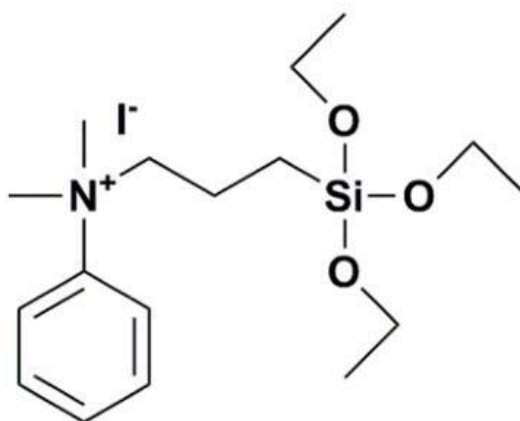


**Figure 2.15** QAS terminated with triethoxysilane [142]

The cellular membranes bacteria, which are mostly negatively charged, have been proven to belong to the target site of cationic biocides [143, 144]. The mechanism of biocidal QAS, a class of membrane-active cationic biocides, has been proposed to be the following steps: (i) penetration into the cell wall, (ii) destructive interactions with the cytoplasmic membrane, and (iii) the leakage of intracellular components and consequent cell death [145, 146]. Compared to low-molecular-weight QAS, polymeric QAS have a considerably higher positive charge density which promotes the initial adsorption onto the negatively charged

bacterial surfaces and consequent disruption of cellular membranes; therefore, the resulting antibacterial activity is extensively raised [147, 148].

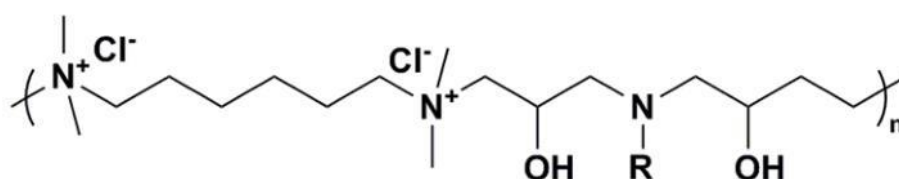
Benefiting from the rapid development of characterization technologies, various advanced techniques, including AFM [149, 150], fluorescence correlation spectroscopy [151, 152], and/or tracking the leakage of cellular constituents [153], have been applied to the comprehensive investigation on the action mode of antibacterial materials. These studies provide intuitive and persuasive evidence for supporting the hypothesis on the antibacterial mechanism of cationic biocides. At the molecular level, a model lipid bilayer membrane was employed to mimic the permeability barrier of cellular membrane for understanding the interaction between cationic biocides and bacterial membrane [154, 155]. The electrostatic interactions between the cationic polymers and the lipid head groups lead to the formation of interfacial complexes within the outer leaflet. The interactions also induce flip-flop of anionic lipid molecules from the inside to the outside leaflet, followed by remarkable distortions and phase separation of the phospholipid bilayer [156, 157].

### **2.2.2. Polymer with quaternary ammonium salts in the main chain**

As cationic polymers, ionene polymers include positive nitrogens due to the biocidal QAS within their main chain, so these are another kind of polymeric antibacterial agents [158, 159]. Ionene polymers are typically prepared either by step-growth polymerization of suitable monomers (e.g., the Menshutkin reaction between alkyl dihalides and nucleophilic ditertiary amines, self-polyaddition of aminoalkylhalides) or cationic functionalization of precursor polymers [160-162].

Through facile condensation polymerization of benzyl amine and epichlorhydrin, polyelectrolytes with QAS in the main chain were synthesized [163]. This agent showed substantial inhibition against bacteria, yeast and fungi in an agar well diffusion test, and it was also found that the antibacterial and anti-yeast activities of the polymer depended on the chain length.

A series of comb-like ionenes (**Figure 2.16**) were synthesized for rendering polyethylene materials antibacterial and antistatic [164, 165]. The comb-like ionenes with long aliphatic side chains imparted higher and faster biocidal effect against *E. coli*. than linear ionenes, apart from additional antimold properties against *Aspergillus niger* and *Chaetomium globosum*. By simply blending the prepared ionenes and low-density polyethylenes, functionalized PE sheets can be produced.



**R = ethyl, butyl, hexyl, dodecyl, octadecyl**

**Figure 2.16** Comb-like ionenes with aliphatic side chains [164]

Beyth and coworkers [166, 167] prepared the alkylated polyethyleneimine-based nanoparticles containing QAS antibacterial groups (**Figure 2.17**). The cationic nanoparticles were obtained from first crosslinking of polyethyleneimine, quaternisation with bromooctane, and finally methylation with methyl iodide. By incorporating 1% of the nanoparticles into commercial dental resin composites during polymerization, dental composites with a strong and enduring antibacterial activity against *Streptococcus mutans* were attained. It was verified that its activity could be almost retained without leaching of

nanoparticles and loss of mechanical properties in spite of lasting for over one month. Besides, it was also confirmed by 2,3-bis(2-methoxy-4-nitro-5-sulfophenyl)-5-[(phenylamino)carbonyl]-2H-tetrazolium hydroxide) assay and cytokine analysis and shown that, the modified resin composites did not affect either the viability or activity of the macrophage in human cells as compared to the native composites. As a result, such high biocompatibility becomes advantageous for the potential in vivo applications of these antibacterial dental resin composites [168].

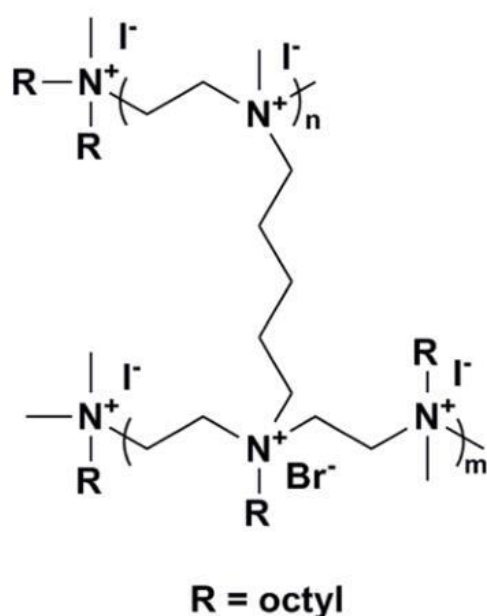


**Figure 2.17** Polyethyleneimine-based ionenes for preparation of dental composites[166]

The biocidal activity of the ionene polymers and the polymers with pendant QAS is dependent on the cationic moieties. Rembaum's [169, 170] reported that the bactericidal mode of ionenes resulted from complexes with heparin and DNA with respect to destruction of bacterial cells by adhesion, aggregation and lysis. Ikeda et al. [171] researched into the interaction between ionene polymers and phospholipid bilayer membranes. Owing to the rigid spacers, the ionenes had

stronger interactions with phospholipid bilayers to trigger phase separation of bilayer membranes. However, the hydrophilic moieties in the spacers tended to retard the initiation of phase separation. The effect of charge density and hydrophobicity of ionene polymers on yeast protoplast disruption was studied by Narita and coworkers [172, 173]. The results revealed that the ionenes contained separated longer hydrophobic segments but had lower charge densities giving more effectively biocidal ability than those with higher charge densities. It is thereby implied that the hydrophobicity is the dominant factor for cell disruption.

Mattheis et al. [174] synthesized a series of alkyloxyethylammonium ionenes with different alkyl chain substituents on the nitrogens and aliphatic spacers (**Figure 2.18**) via the step polymerization of alkyl dibromides with bis(2-N,N-dialkylamino)ethyl ethers. The relationship between the antibacterial performance and the structure including counter ion, alkyl spacer, and length of the pendant alkyl chains of the ionenes was assessed systematically via a broth dilution method. Ionenes with considerable antibacterial activities were generally endowed by appropriate pendant substituents (i.e., short methyl or relatively long octyl groups) and long backbone alkyl spacer; while the counter anions, among the investigated ionenes containing bromide, hydroxide and phosphate, contributed scantily to their antibacterial performance.

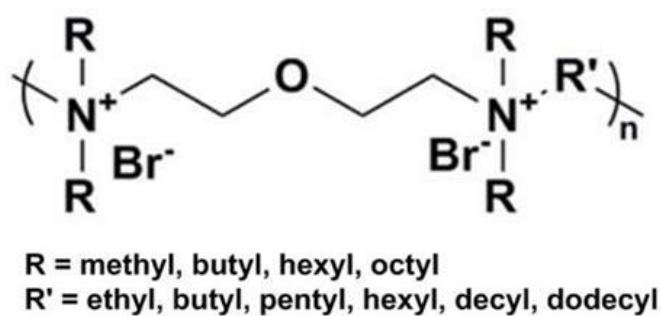


**Figure 2.18** Alkyloxyethylammonium ionenes [174]

### **2.2.3. Immobilization of QAS on material surfaces**

Functionalizing material surfaces with antibacterial substances is an alternative approach of preventing the formation of highly resistant biofilms, and can be realized by a variety of methods [175-181].

The finishing durability of disposable products is less important, and thus such surface coatings can be prepared by many methods, including spin-coating, dip-coating, slot-casting, spray-coating, doctor blade and so on. For permanent antibacterial surfaces, three main elaborate techniques have been developed, namely a surface grafting method, plasma polymerization, and layer-by-layer deposition [182-185].

For example, poly(4-vinyl-N-alkylpyridium bromide) with various alkyl chain lengths, i.e., from propyl to hexadecyl, was covalently grafted onto amino-modified glass slides [186]. It was found that the glass slide immobilized with hexyl- poly(vinylpyridine) was most effective in minimizing the bacterial cell counts, whereas neither the decyl- poly(vinylpyridine) nor non-alkylated poly(vinylpyridine)modified glass slides exhibited antibacterial effects.

Textile materials are commonly-used substrates for supporting/grafting the antibacterial coatings. For instance, a considerable amount of polymeric QAS-modified woven textiles have been developed by covalently bonding alkylated polyetherimide onto the textile surfaces [187]. The immobilization of polymeric QAS endowed wool, cotton, nylon and polyester with not only effectively antibacterial performance but also antifungal ability.

Waschinski et al. [188] developed a novel acrylate-based material with a contact-active antibacterial property via UV-induced radical copolymerization of antibacterial macromers with hydroxythylmethacrylate and

1,3-glyceroldimethacrylate on methacrylate modified glass slides. This antibacterial macromers were constituted of QAS terminal groups, a poly(2-methyl-1,3-oxazoline) chain with various spacer lengths and methacrylamide polymerizable groups (**Figure 2.19**).

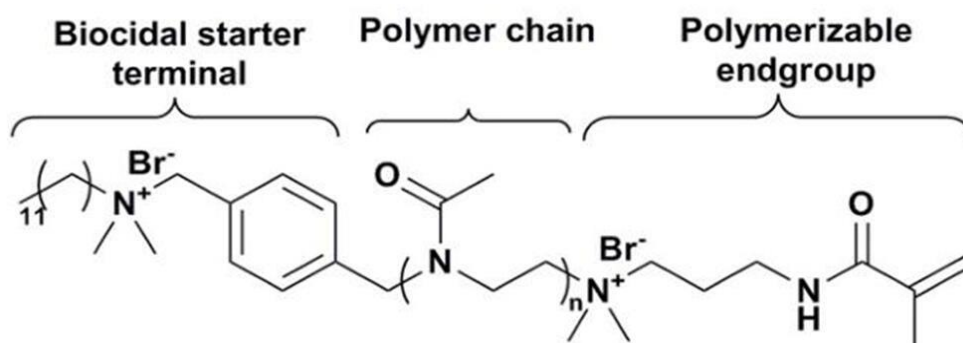


**Figure 2.19** Antibacterial macromer with one QAS and polymerizable end group[188]

Apart from glass sides and textile, other kinds of substrate materials have also been exploited. For instance, Cen et al. [189] applied antibacterial QAS onto the surfaces of polyethylene terephthalate (PET) films and filter papers by grafting copolymerization of 4-vinylpyridine and subsequent quaternization of the grafted pyridine groups with hexyl bromide (**Figure 2.20**). Both the surface-modified substrates were examined by both the waterborne and airborne assays against *E. coli* and proved to have promising bactericidal properties.

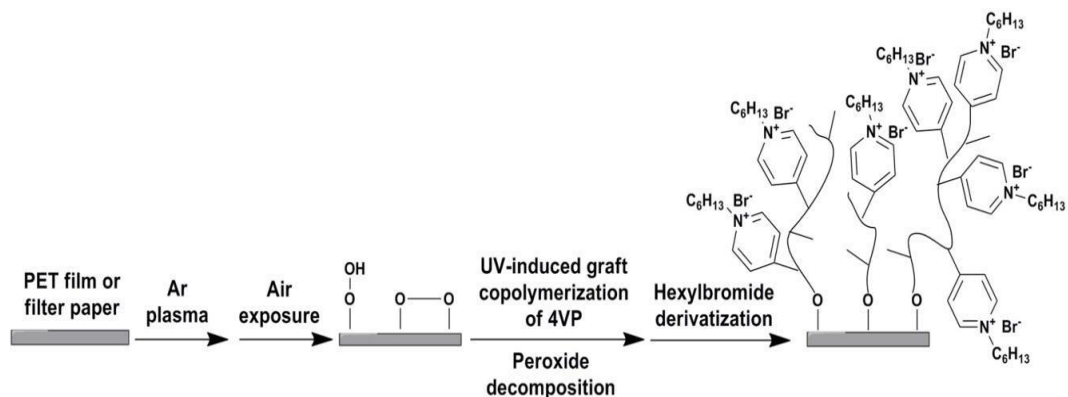


**Figure 2.20** Antibacterial modification for polymeric and cellulosic

surfaces [189]

Jamapala et al. [190] had tried to achieve the antibacterial surfaces by a novel bottom-up synthetic process. Initially, the surface of stainless steel was pretreated by O<sub>2</sub> and hexamethyldisiloxane plasma, and then the cellulose-based filter paper was functionalized with secondary amines via ethylene diamine plasma treatment. Afterwards, the plasma-deposited amines reacted with hexyl bromide and then with tertiary amines being quaternized with methyl iodide to finally form QAS-immobilized surfaces. The modified surfaces were evaluated against *S. aureus* and *Klebsiella pneumoniae*. The results confirmed the bactericidal properties of both stainless steel and filter paper surfaces which were endowed by the immobilized QAS as a non-leaching of biocidal.

Recently, a new and simple dip-coating technique utilizing catechols as the anchoring reagents was developed for preparing permanently antibacterial surfaces [191]. Tripolymers consisting of different molar ratios of catechol moieties, methoxyethyl groups and QAS with long alkyl chains were synthesized (**Figure 2.21**) and coated onto glass slides without surface pretreatment. This system comprising antibacterial QAS and the hydrophilic comonomers, which could improve the interaction between polymers and bacterial cells by adjusting the amphipathic balance, exerted extraordinary bactericidal properties on the coatings against both Gram-positive and Gram-negative bacteria. On the contrary, the coatings containing catechols prevented the development of biofilms for up to 96 h, and did not show leaching of the biocidal when compared to the control coatings without catechol groups. It was believed that the catechol groups could create hydrogen bonds, covalent bonds, and/or strong physical interactions, thus

enhancing the immobilization of polymers onto surfaces to a large extent [192-194].

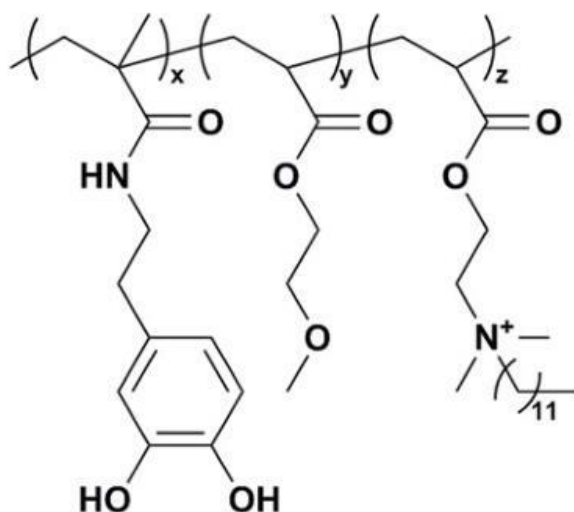


**Figure 2.21** Antibacterial amphiphilic polycations with catechol functional group[191]

Material surface with dual-functionalized antibacterial properties have been developed by incorporating covalently bonded QAS with releasable nanoparticles [195], metal ions and/or clays [196]. By employing a layer by layer method, Grunlan [197] and Li [198] both engineered antibacterial multilayer films containing both QAS and silver ions. The polyelectrolyte multilayer films prepared by Grunlan et al. were achieved via an alternative dipping process of poly(ethylene terephthalate) substrate into the solutions of biocidal agents (i.e. cetyltrimethylammonium bromide and/or silver), polyetherimide and poly(acrylic acid) (**Figure 2.22**). Inhibition zone measurement against *S. aureus* and *E. coli* indicated that the films manufactured with cetyltrimethylammonium bromide possessed higher antibacterial activity than the films containing either silver alone or cetyltrimethylammonium bromide/silver combination. On the other hand, the antibacterial thin film coatings tailored by Li et al. were

composed of a couple of distinct functional layers, that is, (i) a reservoir for loading and releasing of silver ions, (ii) and a nanoparticle surface cap immobilized with [3-(trimethoxysilyl)propyl] octadecyl-dimethylammonium chloride. Such dual-functional coatings thereby possessed both leaching and barrier properties that led to convincing initial bactericidal efficacy together with simultaneous retention of antibacterial activity even when the silvers were depleted.

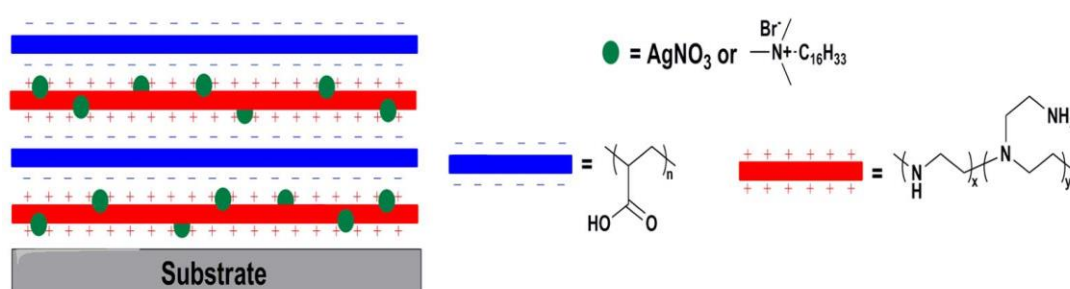


**Figure 2.22** Polyelectrolyte multilayer films containing silver and cetrinide [196]

Modification by polymeric QAS makes the material surface antibacterial against either airborne or waterborne bacteria on contact [199-201]. One hypothetical mechanism has been established to explain their antibacterial actions. Similar to their action mode in solution, the polycations fixed on material surfaces are capable of penetrating and interrupting the bacterial membrane/wall via electrostatic interactions with the negatively-charged phospholipids of the cell membrane [202-205]. During the bactericidal process, ion exchange between the mobile cations within the bacterial membrane and the positively-charged material surfaces may also be responsible for the bactericidal activities [206, 207].

### 2.3. Wound dressing

Skin is the largest organ and the biggest external defence system in the body. Skin temperature varies from 30 to 40 °C, depending on the environmental conditions [208]. It covers all our internal organs and protects them. Skin is sensitive and easy to damage. A defected or broken skin caused by thermal or physical damage is called as wound. From old times, people tried to use plant extracts, crude drug and animal fat to put on skin and wound for wound healing.

The wound care materials are used to absorb blood and exudates, and hence to protect against infection, and accelerate healing [209]. There are various skin and wound care materials in the market, from simple cotton gauzes and lint to sophisticated multifunctional systems made from natural or synthetic materials. There are two wound care dressing, namely traditional and advanced dressing. The functionalities of traditional and advanced dressings are given in **Table 2.2**.

**Table 2.2** The functionality of traditional and advanced dressing

<b>Traditional dressing</b>	<b>Advanced dressing</b>
Haemostatic	Remove exudates and necrotic tissue
Antisepsis	Keep temperature constant
Drying of the wound	Keep a moist environment
Protection from infection	Non-traumatic at the dressing change
Wound covering	Protection from infection
As secondary dressing	Easy to handle

More complex and functional wound dressings are designed and developed using composite materials consisting of an absorbent layer placed between a flexible base material and a wound contact layer. The wound contact

layer is non-adherent to a wound bed and easy remove without disturbing the tissue growth. The function of absorbent layer is to absorb blood or other exudate liquids, thus providing a cushioning effect to protect a wound. Basic complex dressings are always used as inexpensive secondary dressings to hold advanced wound care products in place. Nonwoven complex dressings are quite common and comfortable in use.

As far as we know, the healing conditions are critical for a successful healing process. The moist wound healing philosophy was scientifically explained in the top journal of Nature in 1960's by George Winter. On the basis of this theory, a new wound care treatment method was developed, promoting and respecting the physiological healing process.

The properties and characteristics of ideal wound dressings are list in the following **Table 2.3**.

**Table 2.3** The properties and characteristics of ideal wound dressing

<b>Properties and characteristics</b>	
<input checked="" type="checkbox"/> Non-toxic, non-irritant or non-allergic	<input checked="" type="checkbox"/> Biocompatible, biodegradable and bioresorbable [210]
<input checked="" type="checkbox"/> Creating a protective mechanical barrier and thermal isolation	<input checked="" type="checkbox"/> Enhance cellular interaction and tissue development
<input checked="" type="checkbox"/> Protecting against secondary infections	<input checked="" type="checkbox"/> Cost-effectiveness [211]
<input checked="" type="checkbox"/> Providing and keeping a moist environment	<input checked="" type="checkbox"/> Absorbing the exudate and anti-bacteria

Decreasing or removing trauma in the  
defected area

Providing simple gas  
exchange

---

### 2.3.1. Nonwoven fabric dressings

Nonwoven fabrics are one of the most common used textile materials. According to different situations and purposes, various types of nonwoven fabrics are prepared to provide specific properties such as absorbency, flame retardancy, liquid repellence, thermal insulation, softness, acoustic insulation, high mechanical strength, resilience, cushioning, anti-bacteria and so on for different applications. Due to the versatile nonwoven formation techniques, nonwoven fabrics can be developed into different types of structures with bonded multi-layer and various properties for medical and hygienic uses [212]. In the market, disposable medical absorbent spunlaced nonwoven gauze is odorless and soft, and has high absorbency & air permeability, thus being widely used as the basis for advanced skin and wound care products. It is usually made of 100% cotton, or 100% viscose, or 70% viscose+30%polyester. In order to integrate more properties and performances into nonwoven fabrics for making ideal wound dressings, e.g. protecting against infections, keeping moist environment, absorbing body liquid and exudate, providing gas exchange, creating a protective barrier and avoiding the secondary trauma. Surface modification with functional polymer is an indispensable process for production of traditional nonwoven dressings without sacrificing original properties. The following are the examples of commercially available wound dressing composites based on nonwoven fabric, as shown in **Figure 2.23**. Medicomp® is a nonwoven swab used as an alternative to the traditional gauze in the ward and

in outpatient treatment. It is made of 70% viscose and 30% polyester. It has an open gauze-like structure. It is very absorbent, soft and permeable to air. The nonwoven fabric is bonded mechanically and does not contain binding agents or optical brighteners. It is used for the general treatment of wounds. Fil-Zellin® is also a non-irritant common dressing consisting of a biocompatible nonwoven layer and several bleached cellulose layers as the absorbent layer. It has good absorption capacity and can be applied directly to wounds or as carrier for moist and ointment. Zetuvit® was specially designed for the highly exudative wounds treatment. The surface contacted with the skin is made of hydrophobic polyamide fibres. Because this hydrophobic layer cannot absorb body liquids, it protects from sticking to the wound, on the other hand, wound exudates can be quickly adsorbed by the inner surface of the nonwoven material consisting of hydrophilic cellulose fibres through the hydrophobic layer. Cosmopor steril® is a self-adhesive wound dressing. The characteristic is a water-repellent contact layer. This superhydrophobic layer allows exudate to pass quickly into the absorbent pad behind it while keeping itself absolutely dry. This layer makes the dressing non-stick to the wound. The dressing can be removed and changed painlessly due to the non-adherent property. The permeability of air and water vapour of nonwoven substrate ensures that Cosmopor steril® does not affect the skin's natural functions.



**Figure 2.23** The examples of commercially available nonwoven based wound dressing

### 2.3.2. Hydrogel dressings

Wound dressings can be classified into various ways such as based on physical form (ointment, film and gel), types of materials (hydrocolloid, collagen), functions (absorbent, antibacterial), traditional and advanced dressings. Some dressings belong to several classifications because they fit into the criteria in different groups, e.g. hydrogel dressings. As a suitable wound dressing material, hydrogels should fit into the following criteria showed in **Table 2.4**.

**Table 2.4** The criteria of hydrogel dressing

---

#### The criteria of hydrogel dressing

---

<input checked="" type="checkbox"/> Non-toxic, non-irritant or non-allergic	<input checked="" type="checkbox"/> Helpful to rehydration of dead tissues and the healing of debridement
<input checked="" type="checkbox"/> Providing and keeping a moist environment to promote healing	<input checked="" type="checkbox"/> Suitable for cleaning of dry, sloughy or necrotic wounds
<input checked="" type="checkbox"/> Stable without biological reacts	<input checked="" type="checkbox"/> Non-adherent and cool the surface of the wound

---

Hydrogels are recognized as an efficient and essential biomaterial for skin and wound care. This is attributed to the ability of moisture holding on the surface of the skin. Hydrogel dressings are usually applied for low level of exudate or dry wounds. Because the cooling sense of the hydrogels can relief pain to patients [213]. Hydrogels can be placed and removed with minimal pain and trauma from wound. However, due to their high water content (70-90%), hydrogels are not able to absorb more body liquids and exudates. Accumulation of fluid in hydrogels provides a suitable environment for bacterial growth, and afterward infected odor will be produced. To avoid this, hydrogels should be changed frequently. Low mechanical strength [214] is another disadvantage of hydrogels.

The most common types of hydrogel dressings are sheets, filler, amorphous gels and gauze types of materials. The followings are some examples of commercially available hydrogel wound dressings, as shown in **Figure 2.24**. Hydrosorb® is made of polyurethane polymers with 3-D gel structure contenting 60% of water. On the outer surface, covering with a semi-permeable polyurethane film which can prevent penetration of microorganisms and water.

Thus, it provides a moist environment for the wound bed and is suitable for chronic wounds treatment. The moist environment is very helpful in the formation of new tissues. It is non-sticky to wound, and, therefore, the dressing can be changed without causing a secondary damage to the wound. As Hydrosorb® is transparent, the wound may be inspected at any time without the need to remove the dressing. This thus reduces considerably the frequency of dressing changes. Hydrosorb® Gel is a viscous and clear gel with the properties of (i) promoting removal of devitalized tissue, (ii) softening and hydrating dry necrotic tissues and (iii) absorbing slight exudates. It can be washed away with a sterile rinsing solution.

Hydrocoll® is a kind of self-adherent and flexible absorbent hydrocolloid dressings for the moist wound treatment. Hydrocoll® forms a soft gel when in contact with body liquids, creating a moist wound environment suitable for autolytic debridement and hence protection of granulating tissues. It absorbs and retains exudates, and, in the meanwhile, maintains an adequate moisture balance to promote the wound healing.



**Figure 2.24** The examples of commercially available hydrogel dressings

Generally, in the wound dressing market, for disposable products, the durability is not that important, so many surface coating methods can be applied,

including spin-coating, dip-coating, slot-casting, spray-coating, doctor blade and so on.

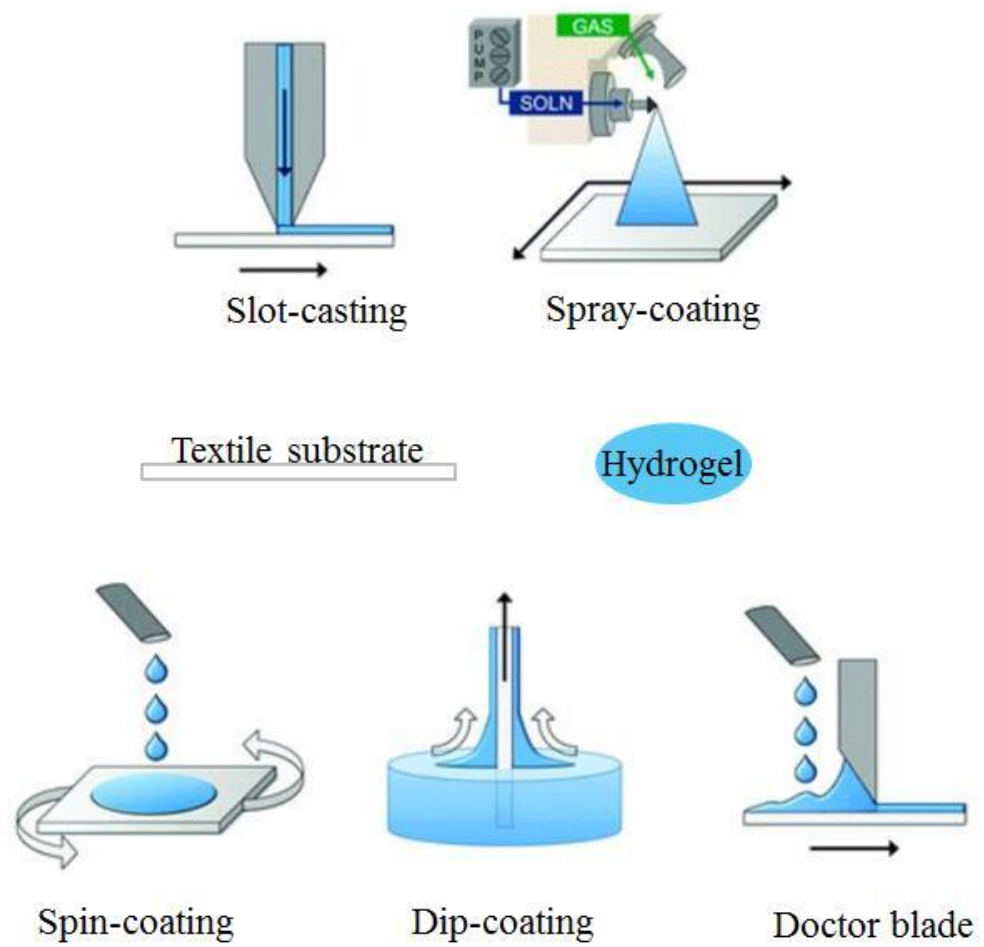


**Figure 2.25** Hydrogel coating application methods

# Chapter 3 Research methodology

The research methodology presented in this chapter is mainly divided into the four parts, that is, experimental plan, materials selection, experiment procedures, characterization and evaluation techniques, which will be introduced in sequence. These characterization techniques include fourier transform infrared spectroscopy (FTIR), differential scanning calorimetry (DSC), scanning electron microscopy (SEM), UV-visible Spectroscopy, gel permeation chromatography (GPC), and nuclear magnetic resonance (NMR). The properties of prepared hydrogels, such as the sol-gel-sol transition behaviors, cytotoxicity, in vitro skin toxicity, in vitro drug control-release behaviors, antibacterial activity, and the functions of hydrogel-coated textiles, such as the transdermal drug delivery, moisture management, water vapor transmission rate (WVTR), air permeability (AP) were also measured and evaluated by various methods according to corresponding standards.

## 3.1. Experimental plan

This study aims to study the smart textile materials functionalized with stimuli-responsive hydrogels for skin and wound care. Directing toward this target, the overall investigation plan is shown by **Figure 3.1**.

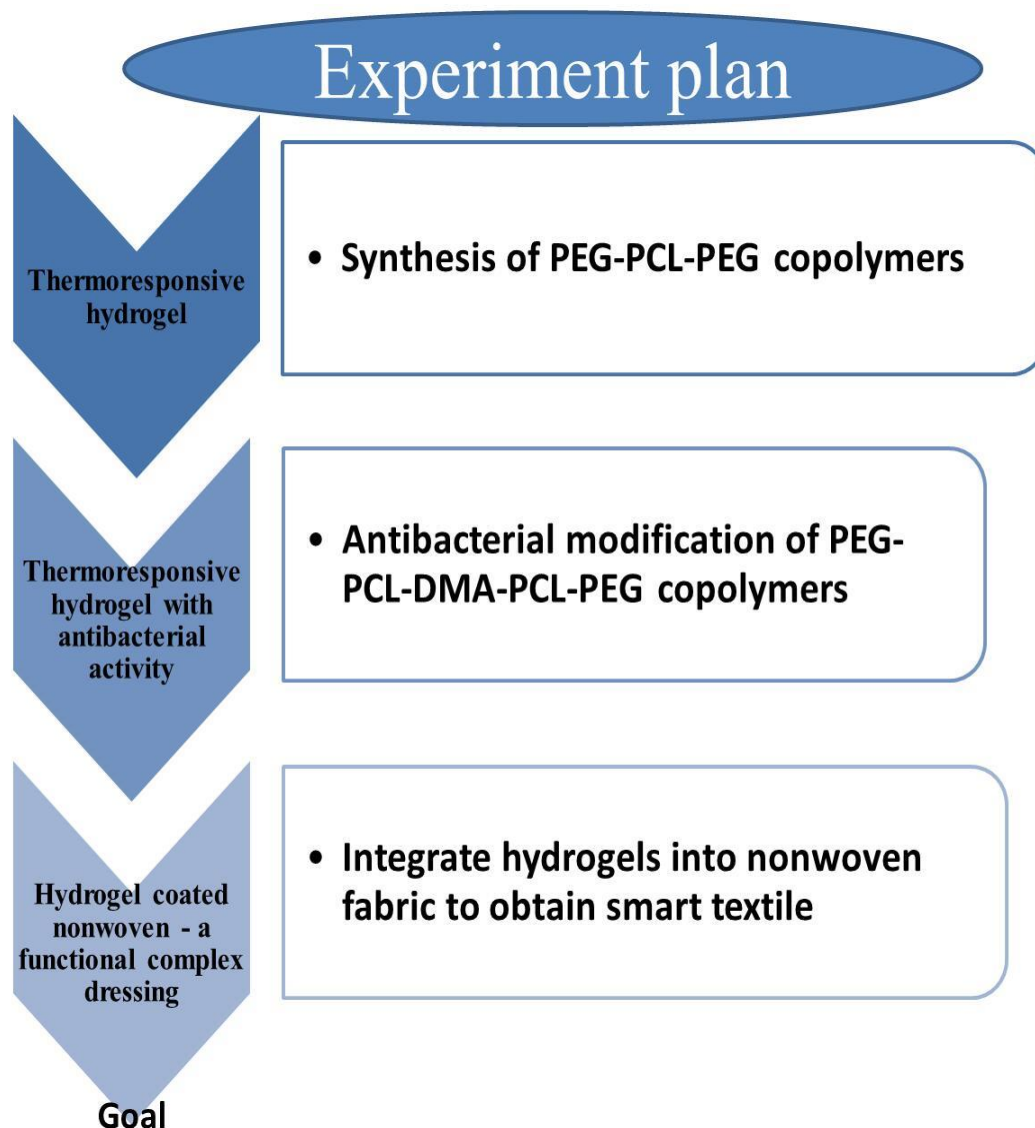


**Figure 3.1** Framework of the whole research

The injectable, biodegradable and biocompatible hydrogel based on amphiphilic block copolymers comprising aliphatic polyesters as the hydrophobic block, and poly(ethylene glycol) as the hydrophilic block with a linear triblock architecture was researched and developed in this study. In order to prepare the gelation of the hydrogels at human skin temperature, the PEG-PCL-PEG copolymer hydrogel is attempted to synthesize firstly.

The antibacterial property of the hydrogel is one of the necessary features in the medical and cosmetic fields. In order to explore a simple and inexpensive

way for achieving the antibacterial modification of the block copolymer, without sacrificing its fascinating intrinsic properties including the thermogelling ability, non-toxicity, and controlled drug release performance, inexpensive commercial bis(2-hydroxyethyl) methylammonium chloride (DMA) was selected as an antibacterial component to modified the PEG-PCL-PEG hydrogel.

Although the sol-gel transition behavior of hydrogel is conducive for drug loading and consequent control-release, the application of this hydrogel in the target field is restricted by its weak mechanical strength. In order to satisfy the proposed requirements, it is a promising method for integration of the hydrogels into textile materials so as to obtain smart functionalized textiles, as well as to combine the advantages of textile materials. The nonwoven fabrics have widespread-applications in the medical field due to their comfortable hand-feeling, excellent bulky property, easily made techniques and low cost. Considering these merits, the nonwoven fabric will be chosen to support the prepared copolymer hydrogel.

The experimental plan was made based on all these considerations described above. The following sections will discuss the experimental parts and characterization technologies.

## **3.2. Materials selection**

### **3.2.1. Materials for thermoresponsive amphiphilic block copolymers**

Materials with a broad range of properties can be obtained by varying the type, length or weight ratio of the building blocks. In this study, we focus on triblock copolymers (ABA) type of amphiphilic block copolymers. As

hydrophilic block, poly(ethylene glycol) (PEG), is most frequently used as it is nontoxic and biocompatible. Besides, PEG has been approved by the US Food and Drug administration (FDA) for internal use in the human body. Examples of frequently used hydrophobic blocks are polyesters like poly(lactic acid) (PLA), poly(lactic-co-glycolic-acid) (PLGA), poly( $\epsilon$ -caprolactone) (PCL), poly(butylene terephthalate) (PBT) and poly(butylene succinate) (PBS). PCL is more hydrophobic than PLA and PLGA. PCL is also a biodegradable and biocompatible polymer approved by FDA for applications in drug delivery systems and medical devices. Thereby, various molecular weights of PEG and PCL were selected as the hydrophilic and hydrophobic block respectively to synthesize the triblock copolymer.

Poly (ethylene glycol) methyl ether (mPEG) (average Mn 550,750), CAS Number 9004-74-4, Linear Formula  $\text{CH}_3(\text{OCH}_2\text{CH}_2)_n\text{OH}$ , Liquid;  $\epsilon$ -caprolactone, CAS Number 502-44-3, Empirical Formula  $\text{C}_6\text{H}_{10}\text{O}_2$ , Molecular Weight 114.14; Polycaprolactone diol (PCL) (average Mn 530, 1250, 2000), CAS Number: 36890-68-3; hexamethylene diisocyanate (HMDI), CAS Number 822-06-0, Linear Formula  $\text{OCN}(\text{CH}_2)_6\text{NCO}$ , Molecular Weight 168.19; stannous octoate ( $\text{Sn}(\text{Oct})_2$ ), CAS Number 301-10-0, Linear Formula  $[\text{CH}_3(\text{CH}_2)_3\text{CH}(\text{C}_2\text{H}_5)\text{CO}_2]_2\text{Sn}$ , Molecular Weight 405.12; methylene chloride, CAS Number 75-09-2 Empirical Formula  $\text{CH}_2\text{Cl}_2$ , Molecular Weight 84.93; petroleum ether, CAS Number 101316-46-5, boiling point 60-80 °C were purchased from Sigma-Aldrich USA and used without further purification.

### **3.2.2. Materials for modification of antibacterial hydrogel**

In ancient times, people managed to use crude drug extracts and herbs to care skin and heal wounds. It has been proved that some of these herbs and

extracts indeed have antioxidant and antibacterial effects. Most of biocompatible and biodegradable materials including hydrogels and others can be easily infected with microorganisms such as bacteria. Therefore it is highly desirable and significant to explore and develop a general route to the antibacterial modification of vulnerable biomaterials, which will enable better biomedical applications.

To satisfy the requirements for the medical and health care products, antibacterial properties are an essential aspect. The biocompatibility and nontoxicity should be considered as well. Quaternary ammonium salts (QAS) are recognized as the most commonly used antibacterial and antiseptic agents due to their excellent antibacterial properties, good environmental stability, excellent cell membrane penetration properties, low toxicity and slight skin irritation. The antibacterial activity of QAS is strongly dependent on the length of their alkyl chain and their overall molecular structure [215-219]. For bearing antibacterial activity, at least one of the alkyl groups must possess a chain length in the range of C<sub>8</sub>-C<sub>18</sub>. Bis(2-hydroxyethyl) methylammonium chloride (DMA) was used as an antibacterial unit. It could be easily grafted onto the mPEG-PCL-mPEG polymer chains to produce an intelligent thermogel with antibacterial performance.

MPEG (average M<sub>n</sub> 550), ε-caprolactone (ε-CL), hexamethylene diisocyanate (HMDI), stannous octoate (Sn(Oct)<sub>2</sub>), and aloin were purchased from Sigma-Aldrich and used without further purification. DMA was obtained from Xiamen Pioneer Technology Co., China. All other reagents were used as obtained until otherwise stated.

### 3.2.3. Textile substrate materials selection

Nonwoven fabric is one of the most commonly used textile materials for medical dressings. The versatility of nonwoven formation techniques enable the nonwoven fabrics to be developed into different types of multi-layer structures, with various desired properties for hygienic and medical uses. In the market, medical disposable absorbent spunlaced nonwoven gauze is odorless, soft, and has high absorbency & air permeability, thus being widely used as the basis for advanced skin and wound care products. It is usually made of cotton, viscose, or polyester. To create more additional value of nonwoven fabrics for ideal wound dressings, such as protecting against secondary infections, providing a protective barrier and thermal isolation, absorbing the exudates, keeping the wound environment moist and enhancing air permeability, surface modification with a suitable polymer is indispensable for treating nonwoven dressings without a loss of its original properties.

Textile materials, used as substrates in this study, are a nonwoven gauze pad (US SECURE CO.,LTD.) as detailed in **Table 3.1**. This kind of nonwoven gauze pad is absorbent, as liquid can be easily absorbed into it.

**Table 3.1** Ultrasoft Sterile Gauze Pad

<b>Brand:</b>	Ultra Ready
<b>Package:</b>	5pcs x 30 pack
<b>Size:</b>	3" x 3" 8 ply
<b>Description:</b>	Made of 30g/m <sup>2</sup> rayon and polyester nonwoven

fabric. It is absorbent and lint-free. Packed in peel-down pouches for aseptic handling.

**Application:** Suitable for general wound care management

**Product Code:** 4163

---

### **3.2.4. Model drug and nutrient selection**

There are two key factors that must be taken into account when the model drug and nutrient selecting. One factor is the widespread applications and typicality, and another one is the testing feasibility. The aloin (aloe extract) contains active compounds that alleviate pain and inflammation, and stimulate skin growth and repair. Curcumin (tumeric extract) is a powerful antioxidant and has anti-inflammatory properties. Apart from having several health benefits, curcumin is also a medicine for solving certain skin problems, such as acne, ageing, removal of dead cells etc. These two drugs were selected as the hydrophilic and hydrophobic model drugs for the study of controlled drug release.

Rhodamine B is a kind of fluorescence tracer dye and normally used to determine the transport, direction of flow and the flowing velocity in water. Rhodamine dye has been widely applied in biotechnology applications such as flow cytometry, fluorescence microscopy, and fluorescence correlation spectroscopy. Because of their fluorescences, curcumin and Rhodamine B are selected as the hydrophobic and hydrophilic model drugs respectively for the study of transdermal drug delivery.

Alcin, curcumin and rhodamine B were purchased from Sigma-Aldrich USA and used without further purification.

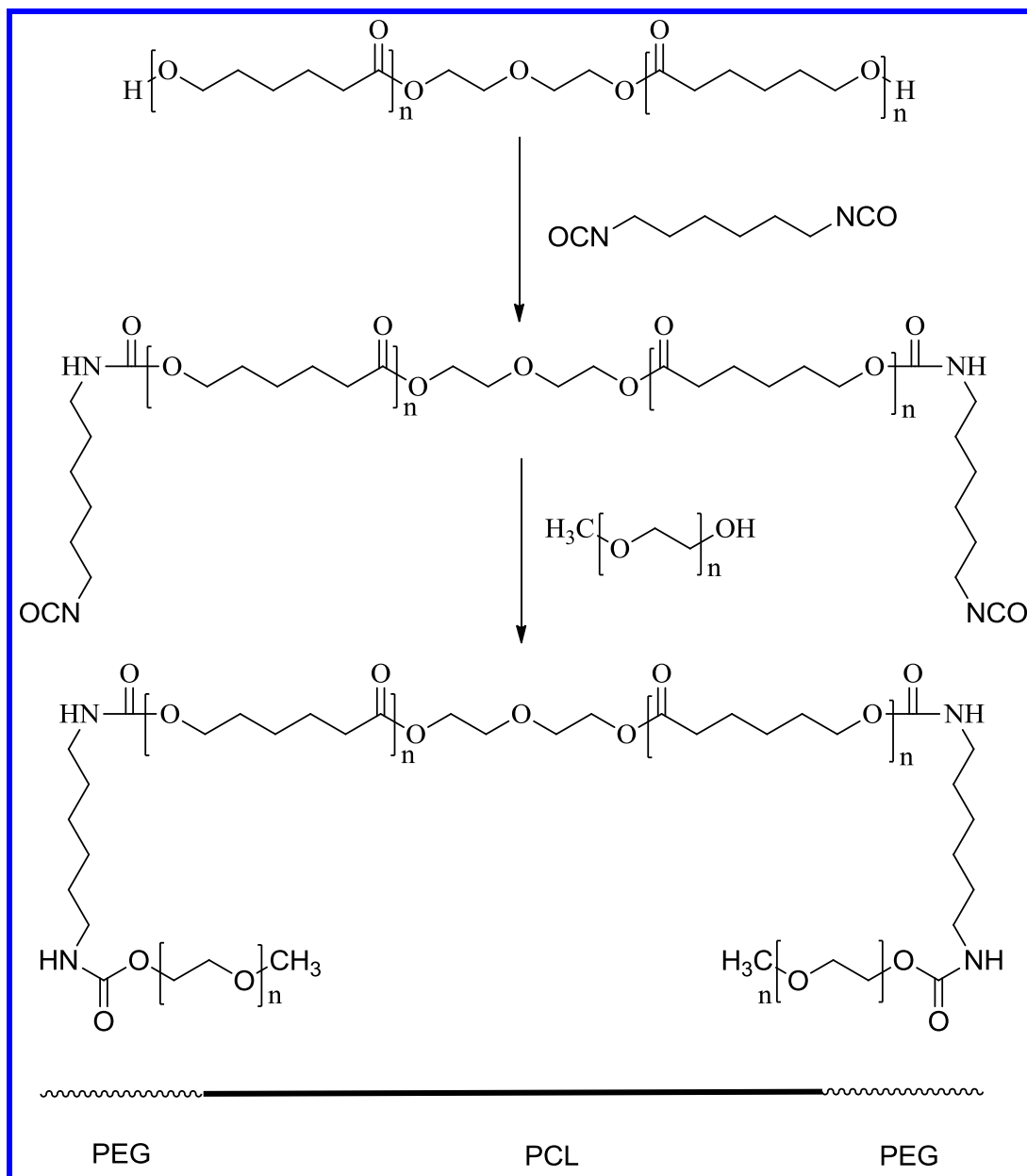
### **3.2.5. Testing bacteria selection**

In this study, two kinds of bacteria were selected to evaluate the antibacterial efficiency of the samples. One is Escherichia Coli (E. coli, ATCC8739, Gram-negative organism), and the other is Staphylococcus aureus (S. aureus, ATCC6538, Gram-positive organism).

## **3.3. Experiment procedures**

### **3.3.1. Synthesis of PEG-PCL-PEG triblock copolymers**

The triblock poly (ethylene glycol)-polycaprolactone-poly(ethylene glycol) (PEG-PCL-PEG) copolymers were synthesized by coupling mPEG and PCL with HMDI as a chemical linker, as schematically illustrated in **Scheme 3.1**. Typically, PEG-PCL-PEG copolymer was prepared as follows: 0.01mol of PCL and 0.02 mol of HMDI were mixed together in the reaction vessel, then 0.5 wt.% of total reactants Sn(Oct)<sub>2</sub> were added into the mixture and the reaction system was kept at 85 °C for 5h. Afterwards, 0.02mol of mPEG was charged into the reaction mixture, followed by stirring at 85 °C for 5h, which yielded the copolymer product. Finally, the resulting copolymer was purified by dissolving into methylene chloride, reprecipitated from the filtrate using excess cold petroleum ether, and filtered and vacuum dried to constant weight at room temperature.

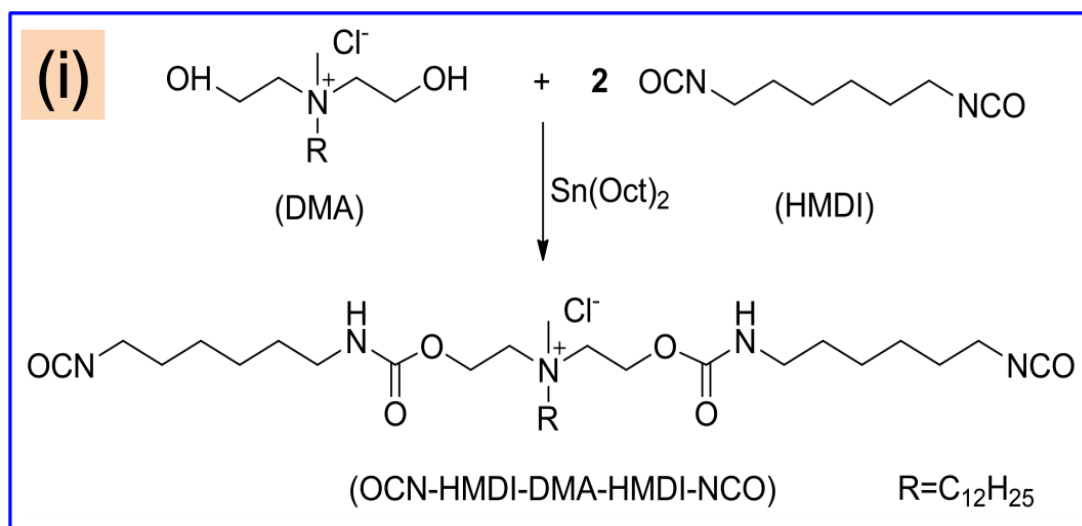


**Scheme 3.1** Synthesis scheme for PEG-PCL-PEG copolymers

### 3.3.2. Synthesis of PEG-PCL-DMA-PCL-PEG copolymers

As shown in the **Scheme 3.2**, OCN-HMDI-DMA-HMDI-NCO as part i was first prepared as follows: 0.005 mol of DMA, 0.01 mol of HMDI and 0.2 wt.% of Sn(Oct)<sub>2</sub> were added into a reaction vessel, and the reaction mixture was kept at 80°C for 3h. Separately, a diblock copolymer mPEG-PCL-OH as part ii (see **Scheme 3.2**) was synthesized as follows: 0.1 mol of ε-CL, 0.01 mol of mPEG,

and 0.3 wt.% of Sn(Oct)<sub>2</sub> were added into a reaction vessel under dry nitrogen atmosphere, and the reaction system was kept at 130 °C for 12h and then cooled to 80 °C. Finally, a given amount of part i and HMDI were added to part ii, and the resulting mixture was stirred at 80 °C for 3h, followed by degassing under vacuum for 1h and then cooling the resultant copolymer to room temperature. To form an antibacterial thermoresponsive hydrogel, the prepared mPEG-PCL-DMA-PCL-mPEG block copolymers were dissolved into D.I. water at a certain concentration to first form a polymer sol, and then have a sol-gel transition around the human skin temperature.





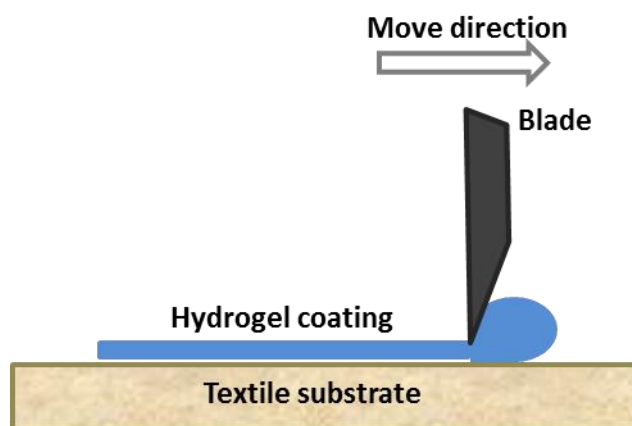


**Figure 3.2** Hydrogel coating by physical doctor blade method

### **3.4. Characterization and evaluation techniques**

#### **3.4.1. Fourier transform infrared spectroscopy (FTIR)**

FTIR spectroscopy is a highly diverse molecular spectroscopy technique and chemical analysis method. In the testing process, infrared ray is irradiated on the sample. Some of the infrared radiation is absorbed by the sample, this is absorption A%. And some of infrared radiation passes through the sample, this is transmission T%. The resulting absorption and transmission are displayed with real-time curve in spectrogram. This infrared spectrum of absorption and transmission is the molecular structures fingerprint of the sample. In this study, monomer for polymer and copolymer hydrogels were grounded with solid potassium bromide (KBr) powder and compressed into the disk for FTIR examination in transmission mode. The disk thickness was about 1.5mm. The FTIR spectra were recorded on a Perkin Elmer paragon 1000 infrared spectroscope (Waltham, Massachusetts, USA) by a compressed KBr disk technique at room temperature with the scanning range of 4000-630  $\text{cm}^{-1}$ .

### 3.4.2. Differential scanning calorimetry (DSC)

DSC is used to monitor the difference in heat flow between the sample and a reference as a function of temperature and time, while the sample is subjected to a controlled temperature program. Characteristic temperature transition, specific heat capacity, melting and crystallization temperature, heat of reaction, oxidative stability, melting and crystallization behavior, reaction kinetics and thermal stability can be studied through DSC analysis. If there is a phase transition, a peak in the scanning curve will be shown to indicate the heat capacity changed. As a rule, two successive scans were performed. The aim of the first scan is to eliminate the influence of the heat history. Results of the second scan were used to calculate the apparent partial heat capacity of specimen.

DSC thermograms were recorded using a PerkinElmer DSC 8000 differential scanning calorimeter (Waltham, Massachusetts, USA) followed temperature program below.

- 1) hold for 5.0 min at 0.00°C ;
- 2) heat from 0.00°C to 80.00°C at 10.00°C/min;
- 3) hold for 5.0 min at 80.00°C ;
- 4) cool from 80.00°C to 0.00°C at 10.00°C/min
- 5) hold for 5.0 min at 0.00°C ;
- 6) heat from 0.00°C to 80.00°C at 10.00°C/min;
- 7) hold for 5.0 min at 80.00°C ;

8) cool from 80.00°C to 0.00°C at 10.00°C/min.

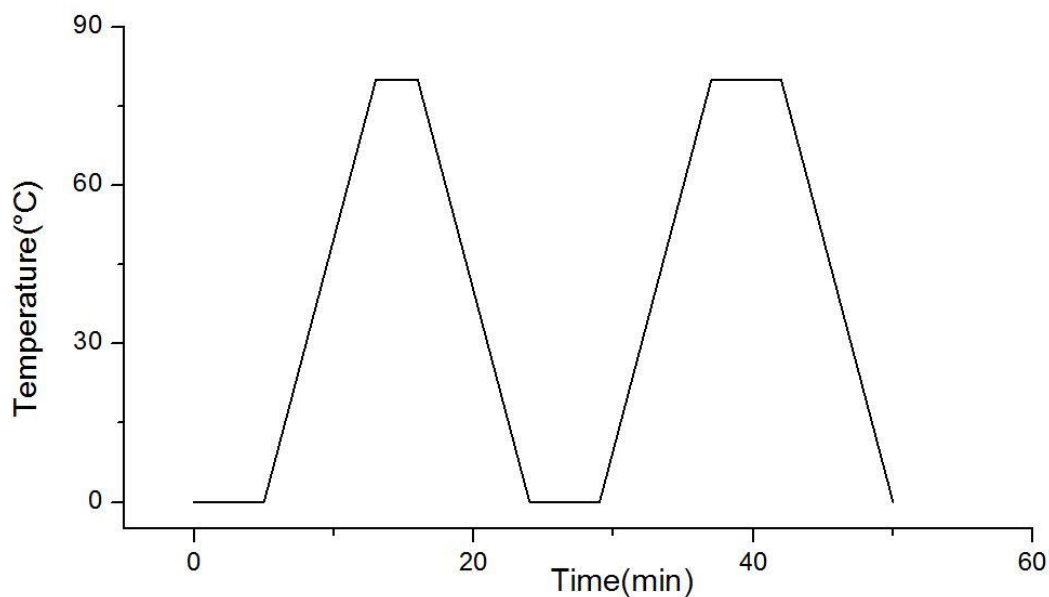


**Figure 3.3** Temperature program curve in DSC

### 3.4.3. Nuclear magnetic resonance (NMR)

NMR is used to analyse and determine unique structure of the testing compound. The carbon-hydrogen framework of the testing organic compound can be identified and confirmed by NMR analysis. There are main three spectrometers including H-NMR, C-NMR, and N-NMR. Hydrogen in H-NMR is the most common used in nuclear magnetic resonance spectroscopy.  $^1\text{H}$ -NMR spectrum of samples were acquired by dissolving prepared copolymers (10 mg) in  $\text{CDCl}_3$  using a Varian AS500 NMR spectrometer (Agilent Technologies, USA) at 298K with 32 scans to characterize chemical structure and composition. The number average molecular weight ( $M_n$ ) was also calculated by  $^1\text{H}$ -NMR.

A particularly useful feature of  $^1\text{H}$ -NMR in molecular weight determination is that the areas under the resonance peaks in the spectra are proportional to the molar concentration of the species in the sample being analyzed. The determination of  $M_n$  is therefore equivalent to dividing the total area or intensity

of the  $^1\text{H}$ -NMR peak of species by the total number of its constituent molecules. This establishes the relationship between the number-average molecular weight and the  $^1\text{H}$ -NMR resonance peaks of the detectable hydrogen atoms of a polymer.

#### **3.4.4. Gel permeation chromatography (GPC)**

GPC is a kind of separation technique based on the size of the polymer in solution. Polymer chains will open up to a certain relaxed conformation in solution, and the solvent chosen will determine the size of the polymer.

GPC separation is different from other techniques which depend upon chemical or physical interactions to separate analytes. The underlying principle of separation is based on polymer hydrodynamic volume. The separation occurs via the use of porous beads packed in a column. These smaller molecules spend more time in the column and therefore will elute last. Conversely, larger analytes spend little if any time in the pores and are eluted quickly. All columns have a range of molecular weights that can be separated. As can be inferred, there is a limited range of molecular weights that can be separated by each column and therefore the size of the pores for the packing should be chosen according to the range of molecular weight of analytes to be separated. For polymer separations the pore sizes should be on the order of the polymers being analyzed. If a sample has a broad molecular weight range it may be necessary to use several GPC columns in tandem with one another to fully resolve the sample.

Waters 1515 gel-permeation chromatography (GPC, Waters Co., Milford, USA) was used to determine the macromolecular weight and macromolecular weight distribution of the prepared copolymers. The samples were dissolved in freshly distilled tetrahydrofuran (THF) at a concentration of 1-2mg/mL. THF

was eluted at a rate of 1.0 mL/min through two Waters Styragel HT columns and a linear column (Waters Co., Milford, USA). The external and column temperature were kept at 27°C. The molecular weights of the specimens were calculated based on polystyrene standard samples with a known narrow molecular weight distribution. The Poly Dispersity Index (PDI) is calculated from GPC using the equation  $PDI = M_w/M_n$ , where  $M_w$  and  $M_n$  represent weight-average molar mass and number-average molar mass respectively. It is widely used to describe the degree of “non-uniformity” of a distribution of polymers.

#### **3.4.5. Freeze-drying**

Freeze-drying is a lyophilization technique applied widely for the fabrication of porous hydrogels for tissue engineering. This method uses rapid cooling to cause phase separation and produce thermodynamic instability within a system. The solvent is then removed by sublimation under vacuum leaving behind voids in the regions where it previously occupied. In this study, the temperature of freeze-drying is -50°C.

#### **3.4.6. Scanning electron microscopy (SEM)**

SEM (TM3000 Tabletop Microscope, Hitachi, Japan) was employed to investigate the microscopic morphologies of the as-formed hydrogel and nonwoven with hydrogels coating after pre-freezing in liquid nitrogen and then lyophilization treatment for 24 h. Before the SEM observation, a thin gold film was sputtered onto the lyophilized specimen surface. And the accelerating voltage is 15 kV.

### 3.4.7. Ultraviolet-visible spectroscopy (UV-Vis)

Ultraviolet-visible spectroscopy refers to reflectance spectroscopy or absorption spectroscopy in the ultraviolet-visible spectral region. This means the testing light is in the visible and adjacent (near-infrared (NIR) and near-UV) ranges. The reflectance or absorption in the visible range directly affects the perceived color of the chemicals involved.

UV-visible spectroscopy is the measurement of the wavelength and intensity of absorption of visible light and near ultraviolet by a sample. The UV-Visible spectra are very useful for quantitative measurements. The concentration of analyses in solution can be calculated and determined based on calibration curve showed in **Figure 3.4(a and b)**. In this study, the samples were analyzed by Lambda 18, Perkin Elmer UV-vis spectrophotometer (Waltham, Massachusetts, USA) and the typical absorptions at  $\lambda_{\max} = 291$  and 426 nm were used to monitor the release of the aloin and curcumin, respectively.

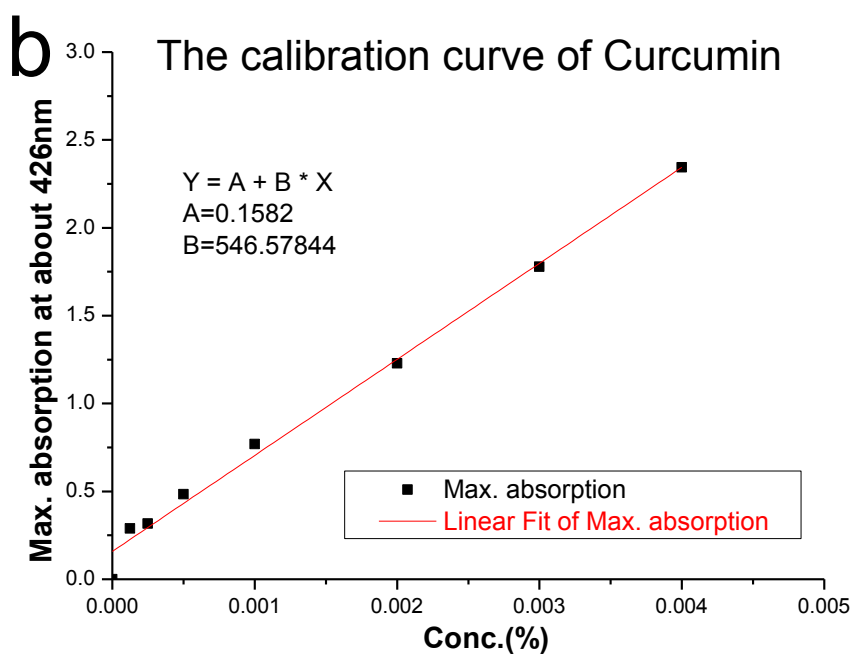
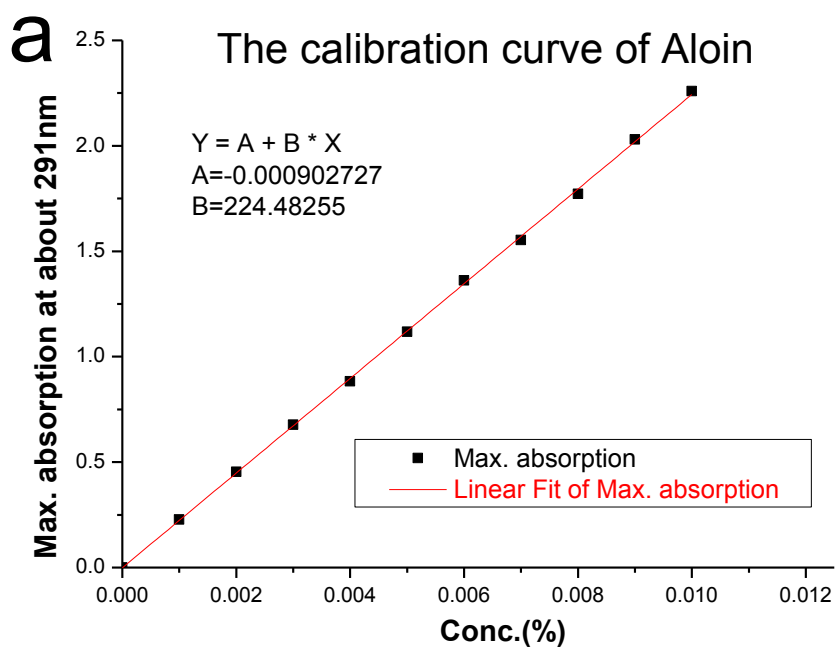


Figure 3.4 The calibration curve of aloin (a) and curcumin (b)

### 3.4.8. Sol-gel-sol transition behavior detection

The sol-gel transition of prepared hydrogel was verified visually by a test tube inversion method. The as-synthesized copolymer was solubilized in

deionized water and stored at 4°C to yield a water solution (25%). For the test tube inverting method, the tubes containing the polymer solutions were immersed in a water bath. The transition temperatures were determined by monitoring phase transition of flowing sol to no flowing gel criterion when the tube was inverted for 1°C rise in temperature. The accuracy of the temperature for sol-gel transition detection is  $\pm 2^\circ\text{C}$  [220-222].

### **3.4.9. Cytotoxicity test**

The cytotoxicity of the prepared PEG-PCL-PEG hydrosol was evaluated by investigating the skin keratinocytes inhibitory effect. Sulforhodamine B assay was used for cell viability evaluation. Human cells including HaCaT skin keratinocytes were removed from 75 ml sterile cell culture flasks by trypsin, and neutralized with fetal bovine serum. After washing with phosphate buffered saline and centrifugation, the skin cells were re-suspended in complete cell culture medium at a concentration of approximately  $1 \times 10^5$  cells  $\text{ml}^{-1}$  and counted manually using a haematocytometer under an inverted microscope. Human cells seeded in the 96 wells microtitre plates for 24 h were prepared for the screening of our hydrosol. The 0.002ml hydrosol (2mg prepared PEG-PCL-PEG copolymer dissolved in 1ml DI water) was added and incubated with cells for an additional period of 24 h. Afterwards, the evaluation of possible inhibitory potential was performed by the sulforhodamine B protein staining methods. Briefly, skin cells were fixed with trichloroacetic acid, washed with distilled water, and stained with sulforhodamine B. The cells were washed again with acetic acid, followed by dissolving in a 0.1 ml unbuffered Tris-base. The optical absorptions were then measured at 575 nm by a microplate reader (Victor

V form Perkin–Elmer, Life Sciences) [223].

### **3.4.10. In vitro skin toxicity test**

In vitro skin toxicity was measured to investigate the toxic effects of the hydrogel sample on skin. Different from previous cytotoxicity test, in vitro skin toxicity was determined by a tetrazolium-based colorimetric (MTT) and lactate dehydrogenase (LDH) assays, and 5% (w/v) of sodium dodecyl sulfonate (SDS, supplied by MatTek Co.) was used as the positive control, and the non-treated skin insert as the negative control.

#### **3.4.10.1. Epiderm culture**

A commercially available human epidermal equivalent, the epiderm (EPI-200, MatTek Corporation, Ashland, MA, USA) was used to mimic normal human epidermis. These epiderm cultures were composed of human-derived epidermal keratinocytes, which were cultured on standing cell culture inserts (Millipore, Billerica, MA, USA) at the air-liquid interface to form a multilayered, differentiated model of the human epidermis. The epiderm cultures were placed in 6 wells plates and were pre-conditioned overnight at 37°C and 5% CO<sub>2</sub>. Test samples were added to the skin inserts the next day and allowed to incubate for 1h. Afterwards, all skin inserts were transferred to a fresh medium for the cytokines release to the medium for 24 h. Medium were recovered and stored at -80°C for the LDH assay. All skin inserts were then transferred to fresh plates for the MTT assay.

#### **3.4.10.2. LDH assay–cell membrane integrity test**

The integrity of cell membrane (or cell damage) of the epiderm cultures was measured by a colorimetric LDH assay (LDH Cytotoxicity Detection Kit, Takara

Bio Inc., Otsu, Shiga, Japan). This assay measures the membrane integrity as a function of the amount of cytoplasmic LDH released into the medium. Briefly, an assay mixture was prepared by mixing one portion of the LDH assay catalyst with 45 portions of dye solutions. As for all cultures, the assay mixture was added to the medium in equal proportions. After incubation for 30 min at room temperature in the dark, the color reaction was stopped by 1 M HCl. A plain medium was used as blank in this assay. Absorbance and background correction were performed at 490 nm. The cell membrane integrity was expressed as the ratio of the amount of LDH released (per treatment) to the maximum amount of LDH released from the positive control.

#### **3.4.10.3. MTT assay-cell viability test**

Skin inserts were transferred to fresh plates with a pre-filled MTT solution (MTT was dissolved in phosphate buffered saline (PBS) at 5 mg/mL and filtered to sterilize and remove a small amount of insoluble residue present in some batches of MTT) and were allowed to incubate for 3 h at 37°C and 5% CO<sub>2</sub>. Upon completion of incubation, all MTT solutions were removed. Skin inserts were transferred to fresh plates and isopropanol was added to each insert for 2 h for the formazan extraction, before transferring to 96 wells plates for a spectrophotometric analysis at 550 nm. Cytotoxicity was expressed as the ratio of cell viability (per treatment) to the maximum cell viability from the negative control.

#### **3.4.11. In vitro drug release behavior test**

A given quantity of aloin (0.1% w/w%) or curcumin (0.1% w/w%)-loaded hydrogels was coated onto a glass sheet (the thickness of hydrogel on the glass is

about 4mm) after gel forming. Then, the coated glass sheet was immersed in a 20 ml phosphate solution PBS (pH 7.4 and 5.0) medium in tubes, and agitation of the incubator was then conducted at 50 rpm and  $35 \pm 2^\circ\text{C}$ . Aliquots were taken at specific time intervals (1, 2, 4, 8, 16, 24, 48, 72, 96, 120 h). The sample was drawn and filtered by a filter paper. The clear filtrate and residue after filtering were poured back into previous solution after testing [224]. The clear filtrate was analyzed by a UV-vis spectrophotometer (Lambda 18, Perkin Elmer) and the typical absorptions at  $\lambda_{\text{max}} = 291$  and 426 nm were used to monitor the release of the aloin and curcumin, respectively. The accumulated drug release was then calculated for integration and analysis. The results were presented in terms of cumulative release as a function of time:

$$\text{Accumulated release(\%)} = (M_t/M_0) \times 100\%$$

Where  $M_t$  is the amount of drug released from the hydrogel at the time  $t$  and  $M_0$  is the initial amount of drug loaded in the hydrogels. The experiment was performed in triplicate for each sample.

#### **3.4.12. Antibacterial test**

The antibacterial activity of hydrogels was tested quantitatively and qualitatively by viable cell count and inhibition zone methods respectively against two representative bacterias, namely *E. coli* (Gram-negative) and *S. aureus* (Gram-positive) with AATCC 147 and AATCC 100 test methods as reference. As for the qualitative analysis with the inhibition zone method, a 200  $\mu\text{L}$  of the inoculum solution was spread onto hard nutrient agar plates. The paper discs were pre-soaked by hydrogels and then placed on the bacterial lawn. The plates were incubated at  $37^\circ\text{C}$  for 2 days, and then the possible inhibition zones

around the samples were examined visually. Concerning the quantitative analysis using the viable cell count method, the suspensions containing approximately  $10^5$  CFU of the bacteria were treated with the 0.1g hydrogel sample overnight, followed by spreading the suspension onto nutrient agar plates. The colonies in the plates were counted after incubation at  $37^\circ\text{C}$  for 24 h. For comparison, negative and positive control samples were also considered according to the above evaluation procedures.

### **3.4.13. Transdermal drug delivery (TDD)**

Transdermal drug delivery was investigated by qualitative observations using freshly excised pig skin which was used to simulate human skin. Pig skin of 8x4cm was selected randomly in the market. Before starting the experiment, it should be cleaned with water and detergent. The pig skin was then soaked in the beaker of sodium phosphate buffer solution at pH 5.5 before it was ready to use. And two kinds of hydrogels respectively loaded with 0.1% w/w yellow water insoluble curcumin and 0.1% w/w red water soluble rhodamine B were prepared for use. Then coat the two kinds of colored hydrogels (1g) onto half piece of pig skin respectively, afterwards place the two samples into the thermostatically controlled incubator maintained at  $35 \pm 2^\circ\text{C}$  for 24h, then take out the samples, scrape off the hydrogel coating completely for following test and clean pig skin with detergent. By observing and comparing the status of color penetration into the pig skin to evaluate the transdermal drug delivery. Then test the residual amount of curcumin and rhodamine B in the scraped hydrogel. The transdermal drug delivery amount (TDDA) was calculated by using the following formula:

$$\text{TDDA} = (M_0 - M_1) / M_0 \times 100\%$$

Where  $M_0$  is the initial amount of curcumin and rhodamine B in the hydrogel

before testing and  $M_1$  is the residual amount of active ingredients in the scraped hydrogel after testing. The reported data were mean  $\pm$  standard deviation of five times tests.

#### **3.4.14. Water vapor transmission rate (WVTR)**

The WVTR test is important for wound dressing material, the liquid formed inside the wound layer are changes to vapor and transport to atmosphere. This moisture vapor transmission is helps to heal the wound; otherwise the wound dressing material is not allowing the moisture vapor to atmosphere will create wound infection [225]. The water vapor transmission rate (WVTR) across the hydrogel coated nonwoven fabric was determined as stipulated by ASTM standard E96-00. The nonwoven fabric with hydrogels coating was mounted on the mouth of glass vial (16mm diameter) containing 10 ml water, and placed in an oven at  $35^\circ\text{C} \pm 2^\circ\text{C}$ , with a constant relative humidity of  $35 \pm 1\%$  for 24 h. The WVTR was calculated by the following formula:

$$\text{WVTR} = (W_i - W_t) / A \times 10^6 \text{ g/m}^2 \text{ day}^{-1}$$

Where WVTR is expressed in  $\text{g/m}^2 \text{ h}$ , A is the area of bottle mouth ( $\text{mm}^2$ ),  $W_i$  and  $W_t$  are the weight of vial before and after placing in oven, respectively. The reported data were mean  $\pm$  standard deviation of five parallel runs.

#### **3.4.15. Air permeability (AP)**

According to standard test method for air permeability of textile fabrics ASTM D 737, a powerful, muffled vacuum pump draws air through an interchangeable test head with a circular opening. The specimen is clamped over the test head opening by pressing down the clamping arm which automatically starts the vacuum pump. In this study, air permeability of nonwoven fabric and

hydrogel coated nonwoven fabric was test at 100Pa. The AP was calculated by using the following formula:  $AP = (D/5.08) \times cc/s/cm^2$  at 100Pa, D is the test data (cc/s) of permeable air. The reported data were mean  $\pm$  standard deviation of five parallel runs.

#### **3.4.16. Moisture management test (MMT)**

The basic function of the wound care materials is to provide absorption of exudates and blood, protection against infection. More and more functional wound dressings are designed and developed using composite materials consisting of an absorbent layer placed between a flexible substrate material and a wound contact layer. The function of absorbent layer is to absorb blood or other exudate liquids and provide cushioning effect to protect a wound.

Moisture management test (MMT) is for the classification, evaluation and measurement of liquid moisture management properties of textile fabrics. It can be used to quantitatively measure liquid moisture transport in a fabric in multidirections in one step, where liquid moisture transports from one surface of the fabric to the opposite and spreads on both surfaces [226]. The unidirectional water transport was evaluated by moisture management tester according to AATCC 195-2011 liquid moisture management properties of textile fabrics.

# **Chapter 4 Thermoresponsive hydrogel system based on amphiphilic block copolymers: synthesis, characterization and application**

## **4.1. Introduction**

As a soft material, hydrogel is composed of a three-dimensional network, similar to the body tissue. It is an ideal drug delivery material for biomedical and personal care in skin applications, particularly for the amphiphilic block copolymers-based thermoresponsive hydrogels that have attracted a great deal of attention in recent years. This is because of their potential applications in biomedical fields, such as wound dressing, cell encapsulation, drug delivery, tissue repair, etc [36, 39, 42, 227-231]. To produce the thermoresponsive hydrogel for the application to human body, the biocompatible and biodegradable polymers are considered the best choice as the raw materials due to their completely harmlessness to humans and environmental friendliness. A major class of biodegradable copolymers with the thermoresponsive gelation behavior can be synthesized based on the reaction systems of poly(ethylene

glycol) (PEG) and aliphatic polyesters, especially the system of PEG and poly( $\epsilon$ -caprolactone) (PCL). PEG and PCL have been extensively used in the biomedical field because of their biocompatibility and biodegradability (approved by Food and Drug Administration (FDA)). These PCL-PEG block copolymers have attracted much attention since 1970s [53, 92, 232-235]. For instance, Hwang et al. reported the synthesis of PEG-PCL-PEG copolymer and investigation on the micelle behavior and the multiple transitions of the as-synthesized copolymer aqueous solution [85, 236]. An injectable thermosensitive acellular bone matrix (ABM)/PEG-PCL-PEG hydrogel composite was prepared and showed a promising potential in bone regeneration [237]. Additionally, a mannan-loaded biodegradable and injectable thermosensitive PCL-PEG-PCL hydrogel was investigated for vaccine delivery application [238].

In this study, thermoresponsive hydrogel system PEG-PCL-PEG was successfully synthesized using Hexamethylene diisocyanate (HMDI) as the coupling agent between PEG and PCL. The sol-gel transition was visually observed by the tube inverting method, which mainly depended on hydrophilic/hydrophobic balance in macromolecular structure under different temperature. The structure and surface morphology of the thermoresponsive hydrogel, sol-gel transition behavior, in vitro drug release behavior, and the cytotoxicity were investigated in detail.

## **4.2. Results and discussion**

### **4.2.1. Synthesis of PEG-PCL-PEG copolymers**

**Table 4.1** The PEG-PCL-PEG copolymers prepared in this work

No.	Copolymer	Total $M_n^a$ (Theoretical)	Total $M_n^b$ ( $^1\text{H-NMR}$ )	Total $M_n^c$ (GPC)	PDI <sup>d</sup> (GPC)	Gelation concentration at $35 \pm 2^\circ\text{C}$
1	550-530-550	1630	1826	2029	1.24	unavailable
2	550-1250-550	2350	2534	2648	1.20	45%
3	550-2000-550	3100	3246	3291	1.12	25%
4	750-530-750	2030	2112	2442	1.31	unavailable
5	750-1250-750	2750	3016	3116	1.28	50%
6	750-2000-750	3500	3683	3954	1.43	35%

a. Calculated from theoretical value.

b. Calculated from  $^1\text{H-NMR}$  results.

c. Calculated from GPC results.

d. Polydispersity, calculated by  $M_w/M_n$ .

A series of PEG-PCL-PEG triblock copolymers were synthesized by coupling mPEG and PCL using HMDI as a chemical linker. The synthesized triblock copolymers in this study were summarized in **Table 4.1**.  $^1\text{H-NMR}$  and GPC were used to evaluate molecular weight and to determine the chemical structure of prepared copolymers. Macromolecular weight and macromolecular weight distribution (polydispersity, PDI,  $M_w/M_n$ ) of prepared triblock copolymers were calculated by GPC in the range of 3000-5000 and 1.10-1.50,

respectively. According to **Table 4.1**, the macromolecular weight ( $M_n$ ) estimated from  $^1\text{H-NMR}$  spectrum and GPC were consistent with theoretical value. So, for simplicity, results of molecular weight from  $^1\text{H-NMR}$  and GPC indicated that the designed PEG-PCL-PEG triblock copolymer according to **Scheme 3.1** was successfully synthesized. Owing to the combination of hydrophobic PCL block and hydrophilic PEG block, the PEG-PCL-PEG is an amphiphilic block copolymer. Aqueous solutions of PEG-PCL-PEG copolymers have sol to gel transition behavior with increase in temperature, which seems to be driven by the micelle packing and aggregation. Because the hydrophobicity of PCL<sub>530</sub> is too weak to form gel, so the gelation concentrations of copolymers No.1,4 at  $35\pm 2^\circ\text{C}$  are unavailable. While the molecular weight of PEG block was kept at 550 or 750, gelation concentration decreased gradually with the length of PCL blocks increasing from 1250 to 2000. Among them, the aqueous solution of No.3 PEG<sub>550</sub>-PCL<sub>2000</sub>-PEG<sub>550</sub> has the lowest gelation concentration at  $35\pm 2^\circ\text{C}$  and is most thermosensitive hydrogel. PEG<sub>550</sub>-PCL<sub>2000</sub>-PEG<sub>550</sub> copolymer will be used in the following testing, characterization and application.

#### 4.2.2. Structure analysis of PEG-PCL-PEG triblock copolymer

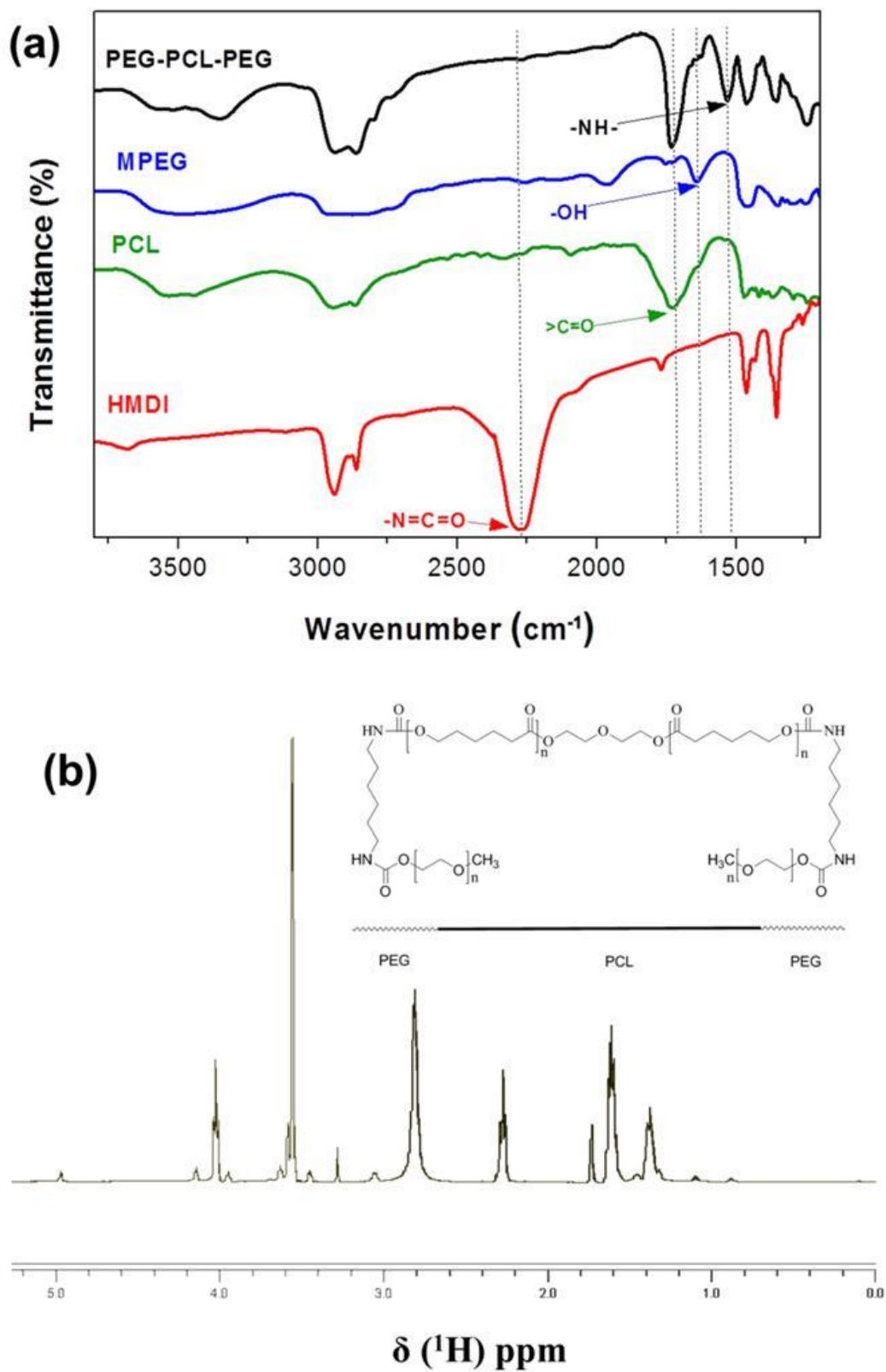


Figure 4.1 Chemical structure analysis of the PEG<sub>550</sub>-PCL<sub>2000</sub>-PEG<sub>550</sub> triblock

copolymer: (a) FTIR spectra of the raw materials and the as-prepared PEG-PCL-PEG triblock copolymer; (b)  $^1\text{H-NMR}$  spectrum of the PEG-PCL-PEG triblock copolymer. The inset of (b) shows the molecular structure of the PEG-PCL-PEG triblock copolymer that helps to analyze the spectra.

**Figure 4.1(a)** presents the typical FTIR spectra of PEG<sub>550</sub>-PCL<sub>2000</sub>-PEG<sub>550</sub> triblock copolymer. There is no absorption in the range of 2250–2270 $\text{cm}^{-1}$ , which indicates that the -NCO groups of hexamethylene diisocyanate disappear completely because of the effective coupling reaction of -NCO with the -OH group. The occurrence of absorption band around 1525 $\text{cm}^{-1}$  can be attributed to the N-H bending vibrations, which confirms the formation of triblock copolymers. Moreover, NMR spectroscopy was employed to further analyze the chemical structure of our prepared triblock copolymer, and the as-obtained  $^1\text{H-NMR}$  spectrum is shown in **Figure 4.1(b)**. The sharp peak at 3.58 and 3.28ppm can be attributed to methylene protons of -CH<sub>2</sub> CH<sub>2</sub>O- and -OCH<sub>3</sub> end groups in PEG block, respectively. The methylene protons of -(CH<sub>2</sub>)<sub>3</sub> -, -OCCH<sub>2</sub>-, and -CH<sub>2</sub> OOC- in PCL blocks can be indexed to the peaks centered at 1.37, 1.61, 2.27, and 4.13 ppm [239]. An interesting absorption peak located at 2.81 ppm can be assigned to the -N-CH<sub>2</sub>- protons [240], indicating the successful chemical linking of the PCL and PEG. In addition, the THF-d<sub>8</sub> solvent residual signal can be found at 1.73 ppm [241]. Based on the analysis of the FTIR and  $^1\text{H-NMR}$  spectra, the chemical structure of PEG-PCL-PEG triblock copolymer is well unraveled as the structure presented in the inset of **Figure 4.1(b)**.

### 4.2.3. Microscopic morphology of hydrogel by SEM

#### observations

The microscopic surface morphology and topology of the hydrogel are observed by SEM, with the obtained images shown in **Figure 4.2**. The specimens were prepared by being frozen in liquid nitrogen and then lyophilized for 24 h. From **Figure 4.2**, different shape and size of pores in the hydrogel interior can be observed clearly. The lyophilized hydrogel presented an interconnected porous 3-dimensional network structure, many irregular pores with size from 2 $\mu\text{m}$ -10 $\mu\text{m}$  could be found in the hydrogel composite. The pores formed due to sublimation of water inside the hydrogel, and they could help to form a high-water-content hydrogel composite. This porous structure also endows the hydrogel with good drug loading capacity and sustained drug release performance. But you can see they are all discontinuous fragments. This indicates the mechanical strength and flexibility of the prepared hydrogel is poor and need to be improved for practical application.

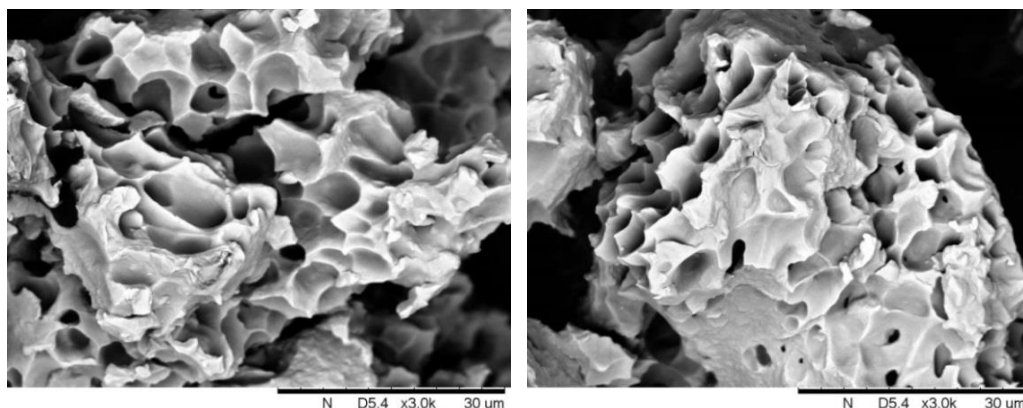


**Figure 4.2** SEM images of the lyophilized hydrogel PEG<sub>550</sub>-PCL<sub>2000</sub>-PEG<sub>550</sub>

### 4.2.4. Sol-gel phase transition behavior detection

The PEG-PCL-PEG triblock copolymers prepared in this study are

amphiphilic in nature due to combination of hydrophilic PEG block and hydrophobic PCL block. The temperature-dependent sol-gel transition behavior of these block copolymers primarily depends on the balance of hydrophobicity and hydrophilicity of the macromolecular structure. The as-prepared thermoresponsive hydrogel of a given concentration exhibits a sol-gel transition which is in a sol state at lower temperature, namely 10°C (**Figure 4.3(a-c)**) and then changes into a gel when increasing the temperature to about normal human skin temperature of approximately 35°C (**Figures 4.3(b-d)**). The gelation mechanism of this kind of hydrogels can be explained as following points: (i) the enhanced hydrophobic interactions at elevated temperatures; (ii) self-assembling into physical cross-linking networks. **Figure 4.3 (e)** shows the sol-gel-sol transition phase diagram of PEG-PCL-PEG triblock copolymers in aqueous solutions. This polymer aqueous solution has concentration-dependent critical gelation concentration (CGC), lower critical gelation temperature (LCGT), and upper critical gelation temperature (UCGT).

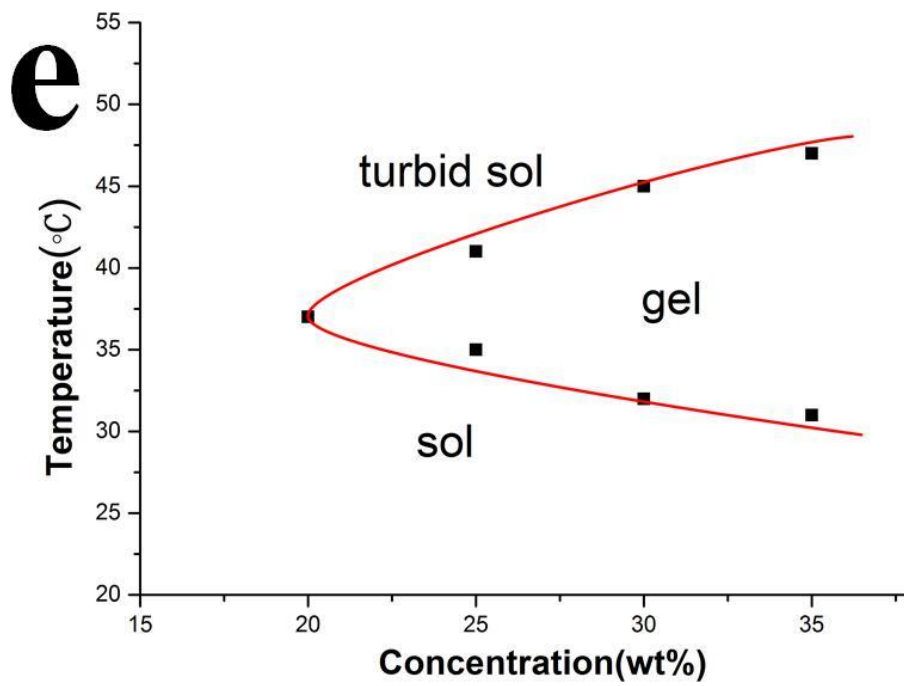
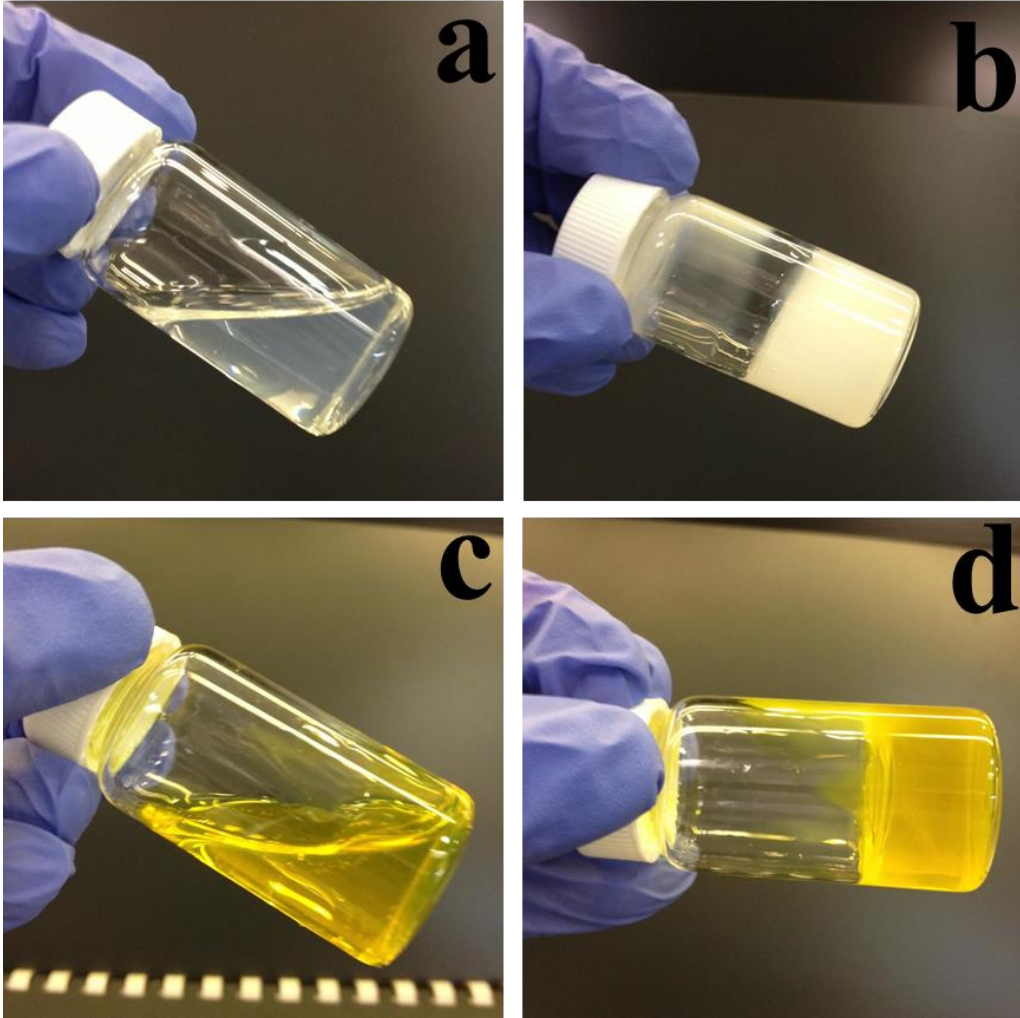


**Figure 4.3** Photographs of the prepared thermoresponsive hydrogel (a, b the hydrogel loaded with 0.1% aloin; c, d the hydrogel filled with 0.1% curcumin) at different temperatures: (a,c) 10°C and (b,d) 35°C; (e) Sol-gel-sol transition phase diagram of PEG<sub>550</sub>-PCL<sub>2000</sub>-PEG<sub>550</sub> hydrogel.

#### 4.2.5. Cytotoxicity study

Here, the cytotoxicity of the prepared PEG<sub>550</sub>-PCL<sub>2000</sub>-PEG<sub>550</sub> hydrogel was evaluated by testing the viability of skin keratinocytes. As revealed in **Figure 4.4**, both control (**Figure 4.4(a)**) and blank hydrogel (**Figure 4.4(b)**) exhibit a high integrity of cellular structure. The results thus demonstrate the non-cytotoxicity of our hydrogel for treatment of skin keratinocytes. Results are shown as mean  $\pm$  SD calculated from their mean values of these three independent experiments.

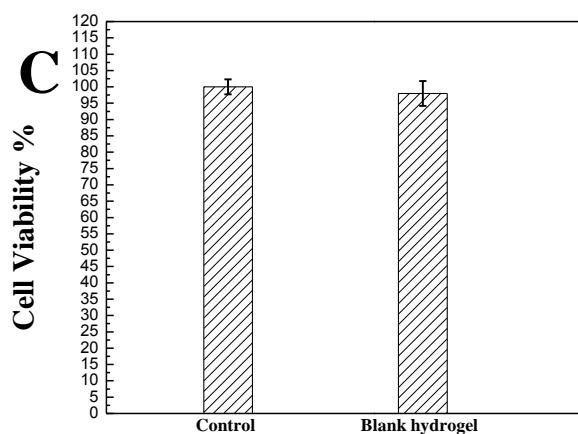
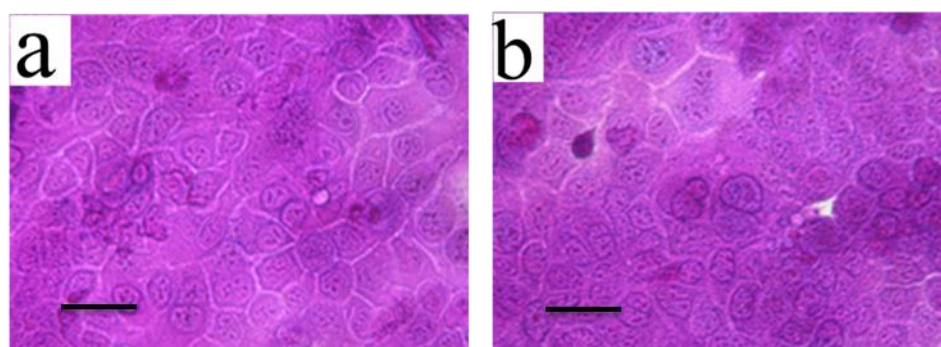


**Figure 4.4** Viability of skin keratinocytes: (a) control; (b) blank prepared hydrogel PEG<sub>550</sub>-PCL<sub>2000</sub>-PEG<sub>550</sub>; (c) percentage of cell viability. Scale bars in (a,b): 50mm

#### **4.2.6. In vitro drug release behavior study**

The in vitro cumulative drug release was monitored by UV-vis spectrophotometer, and calculated by the calibration curve of aloin and curcumin, showed in **Figure 3.4 (a) and (b)**. In vitro release model of 0.1% w/w% aloin-loaded hydrogels under different pH conditions (pH 5.0 and 7.4) at 35°C was investigated and monitored in PBS for a time period of 120 h (**Figure 4.5 (a)**). There is an initial drastic release of 18% aloin occurring in the first one hour, followed by release of 70% with a high rate in one day. The release rate is gradually decreased, and becomes very low after 24 h. The final releasing content of aloin is about 85% after 120h. Aloin released a little faster in pH5.0 than pH 7.4 from the hydrogel

The in vitro release of the curcumin (with 0.1% w/w% loading content) from the hydrogels in PBS (pH 5.0 and 7.4) is shown in **Figure 4.5 (b)**. Similar to that for aloin, note that the first 1h affords a significantly high release rate with 15% releasing content for the system and sustained drug release was also observed. But it was dependent on the pH of the release medium more than aloin release. After 24 h, approximately 30% and 38% curcumin are released from the hydrogels respectively in PH 7.4 and 5.0 PBS. The curcumin is further released gradually from the hydrogels, as shown in **Figure 4.5 (b)**, the cumulative release of curcumin reached to around 60% in pH 5.0 and 50% in pH 7.4 phosphate buffered solution after 120 h.

In summary, aloin and curcumin were encapsulated within hydrogels and

released from the hydrogels, faster in pH 5.0 than pH 7.4, showed rapid release at the initial stage and slow release later. The drug adsorbed on the surface of the hydrogels was separated from the carrier material into the aqueous phase, which contributed to the burst release stage. The initial fast release for about 12h was followed by a sustained released of drug from the hydrogels. The controlled release study demonstrates that PEG-PCL-PEG hydrogel provide a reliable and effective sustained drug release. We speculate that the higher release rate in the acidic buffer solution can be ascribed to the following two points: (i) the copolymers become more hydrolysable; (ii) the higher solubility of the drugs under acidic conditions.

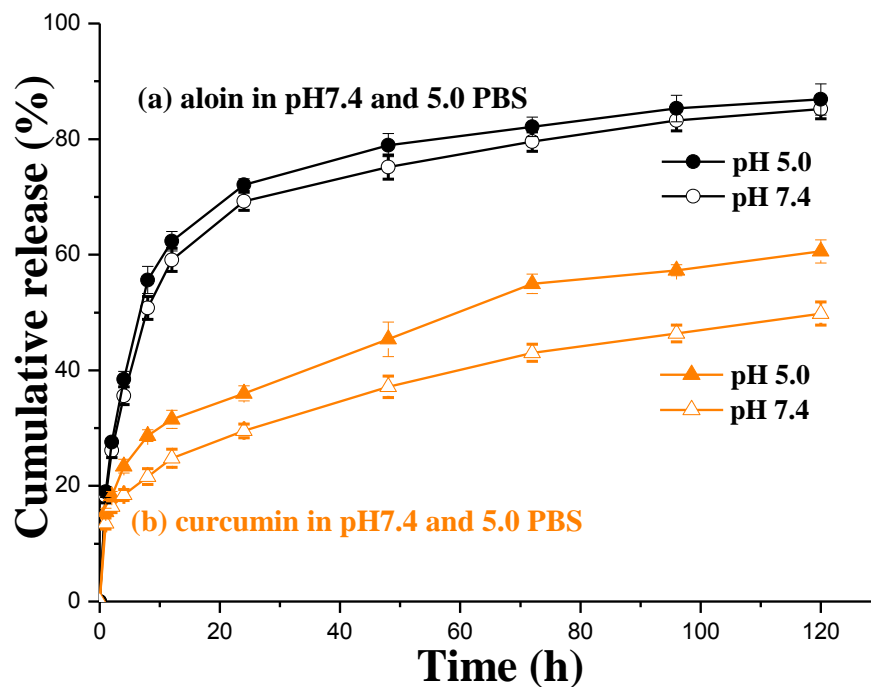


**Figure 4.5** In vitro drug release behavior of the thermoresponsive hydrogels PEG<sub>550</sub>-PCL<sub>2000</sub>-PEG<sub>550</sub>: in vitro cumulative release (a) loaded with aloin (0.1%) and (b) curcumin (0.1%) in PBS (pH 5.0 and 7.4).

#### 4.2.7. Transdermal drug delivery study

Transdermal drug delivery and permeation were investigated by qualitative observations using pig skin which was selected randomly in the market as a medium to simulate human skin. After 24h contact of hydrogels loaded with fluorescent materials on the pig skin, hydrogels were removed and pig skin was cleaned with detergent. From the photos under UV illumination in **Figure 4.6**, we can see that the fluorescent color was penetrated into the pig skin, demonstrate the two materials were transdermal delivered into the pig skin. And after calculation of transdermal drug delivery amount (TTDA) in the **Table 4.2**, it shows that approximately 7% curcumin and 13% rhodamine were transdermal delivered to the skin after 24 hours testing. This indicates the hydrophilic drugs released faster from the hydrogel than the hydrophobic drugs. According to the results, it can be stated that the drug loaded hydrogels offer drug transdermal delivery and control-release behavior.

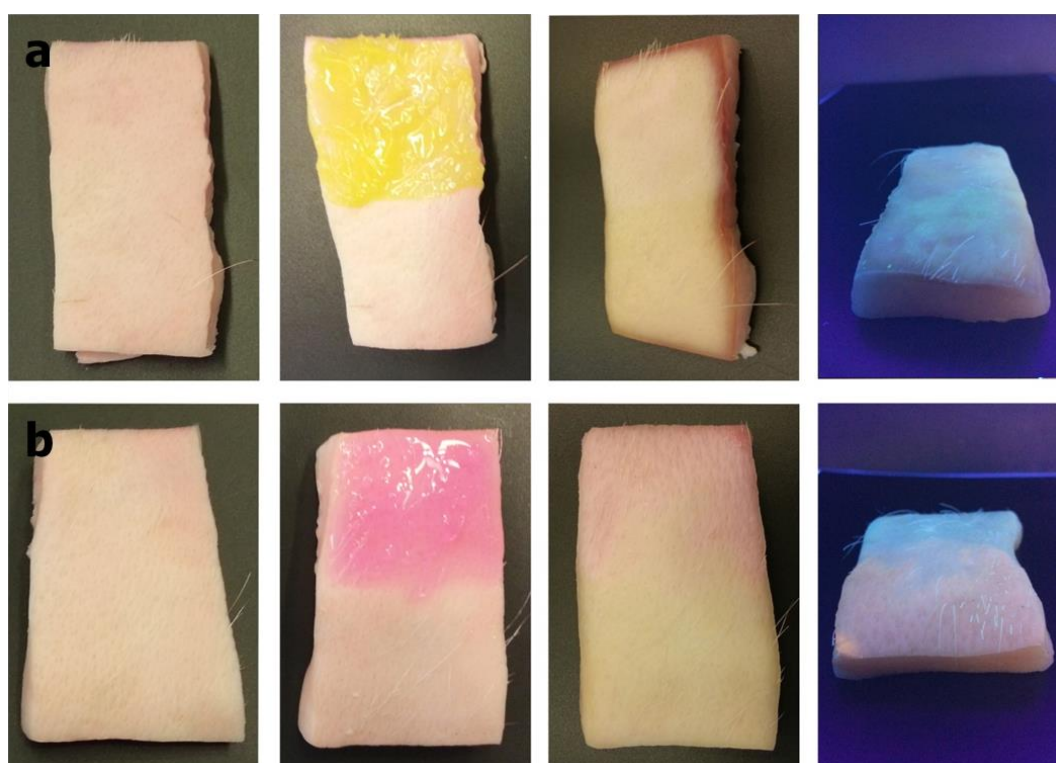


**Figure 4.6** Demonstration of transdermal drug delivery of hydrogels

PEG<sub>550</sub>-PCL<sub>2000</sub>-PEG<sub>550</sub> with pig skin at 35±2°C for 24h. (a) 1g 0.1% curcumin loaded hydrogel coated on the half of pig skin; (b) 1g 0.1% rhodamine loaded hydrogel coated on the half of pig skin.

**Table 4.2** Transdermal drug delivery amount (TTDA)

<b>Sample</b>	<b>Mean ± S.D. (n = 5)%</b>
hydrogel loaded with curcumin(0.1%)	7.75 ± 1.92
hydrogel loaded with rhodamine(0.1%)	13.83 ± 2.88

# **Chapter 5 Antibacterial modification of thermoresponsive hydrogel: synthesis, characterization and application**

## **5.1. Introduction**

With the development and civilization of human society, reliable, safe and intelligent materials become of growing importance for meeting with the increasing demand for health care worldwide, especially in biomedical fields [242-247]. As a soft material, polymer hydrogels can retain a large fraction of liquids within their three-dimensional networks [248-250]. They resemble natural living tissue more than any other class of synthetic biomaterials [251, 252], affording their potential applications in biomedical fields, such as tissue engineering, cell encapsulation, wound dressing and drug delivery [228, 229, 253, 254]. Polymer hydrogels generally fall into chemical and physical gels. Chemical gels have been well explored as potential drug delivery systems for *in vivo* and *in vitro* applications [255]. However, the network in chemical gels is constructed via covalent crosslinking, implying their inferior biodegradability and irreversible sol-gel transition in most cases, as compared to physical gels. This is because the high stability of the network structure is most likely to make chemical gels lack responsive properties towards external stimuli [256]. In this

regard, physical gels formed by means of non-covalent interactions show a greater potential as stimuli-responsive smart materials for various biomedical applications [257].

Block copolymer-based physical gels, such as the copolymers consisting of poly( $\epsilon$ -caprolactone) (PCL) and poly(ethylene glycol) (PEG) blocks, have been widely studied due to their biocompatibility, biodegradability, injectability, nontoxicity and thermosensitivity that promise their widespread applications [220, 237, 256, 258-261]. For instance, *in vivo* PEG-PCL-PEG gel formation and degradation behaviors were explored through subcutaneously injecting a PEG-PCL-PEG copolymer aqueous solution in a mice model [220]. Functioning as an anti-adhesion barrier with a controlled drug delivery system, a PEG-PCL-PEG hydrogel was used to prevent postsurgical adhesion [262]. A thermosensitive PEG-PCL-PEG hydrogel was also explored as an injectable bevacizumab carrier system for glaucoma filtration surgery [261]. As a result, due to the minimally invasive nature, the therapy based on injectable, non-toxic thermogels with PEG and PCL blocks holds a great promise for *in vivo* sustained drug release and cell grow applications [85]. More importantly, such a therapy can be easily administered by a simple syringe injection of a copolymer sol, loaded with pharmaceutical agents or cells, to a target site. With the body temperature-induced sol-gel transition, the injected sol quickly turns to be a gel depot for drug delivery, cell culture and tissue engineering applications, etc [263].

However, biocompatible and biodegradable materials can be easily infected with microorganisms such as bacteria [131]. World Health Organization statistics have revealed that more than 1.4 million people are suffering from infectious

complications that occur in hospital, most likely originated from the use of medical devices that frequently contact with susceptible biomaterials without immunity to microorganisms [255]. It is therefore highly desirable and significant to explore and develop a general route to the antibacterial modification of vulnerable biomaterials, which will enable better biomedical applications.

Herein, we employed biocompatible, biodegradable, non-toxic poly (ethylene glycol) methyl ether (mPEG)-PCL-mPEG block copolymer as a model biomaterial. In order to explore a simple and inexpensive way for achieving the antibacterial modification of the block copolymer, without sacrificing its fascinating intrinsic properties including the thermogelling ability, non-toxicity, and controlled drug release performance, inexpensive commercial bis(2-hydroxyethyl) methylammonium chloride (DMA) was used as an antibacterial unit. It could be easily grafted onto the mPEG-PCL-mPEG polymer chains to produce an intelligent thermogel with antibacterial performance. A mechanism of the sol-gel-sol transition of the resulting antibacterial modified block copolymer with increasing temperature was also discussed in this study, such as the micelle aggregation mechanism for the body temperature-induced gel formation at the lower transition temperature and micelle destruction mechanism for the turbid sol formation at the upper transition temperature. We also found that the crystallization degree of the PCL block can be somewhat increased with the enhancement of quaternization (i.e. increase of the initial reaction ratio of DMA), but further increasing the DMA ratio can largely depress the PCL block crystallization to a point even lower than that for the counterpart without quaternization treatment. Interestingly, such critically lowered crystallization

was found to be correlated strongly with the disappearance of the sol-gel-sol transition phenomenon. We thus suggest that the synthetic reactions involving too much DMA are mostly likely to disrupt the balance between hydrophilicity and hydrophobicity of the PEG and PCL blocks respectively, which disturbs the micelle structure and hence makes the micelle aggregation mechanism no longer work for the body temperature-induced gel formation. The positive charge and long alkyl chain of the DMA moiety might affect heavily the molecular arrangement, crystallinity and sol-gel-sol transition behavior of the antibacterial modified block copolymer PEG-PCL-DMA-PCL-PEG when the DMA ratio increases to a critical value at which the sol-gel-sol transition is lost. Nevertheless, an appropriate extent of quaternization can endow PEG-PCL-DMA-PCL-PEG with thermogelling properties, low toxicity and impressive antibacterial performance.

The present study, which offers a general route to the antibacterial modification of PEG-PCL-PEG block copolymers, will therefore provide an impetus to the fabrication of smart biomaterials with antibacterial performance, especially block copolymers based on DMA, PEG, PCL, poly(acrylic acid), polypropylene, poly-(D,L-lactide), poly-(D,L-lactide-co-glycolide) and/or others as building blocks, for many promising biomedical applications such as cancer theranostics [264], bone regeneration [237], bioactive reversible oxygen transfer [265] and tissue engineering [262]. This study is also expected to shed light on understanding the sol-gel-sol transition behaviors of multiblock copolymers.

## **5.2. Results and discussion**

### **5.2.1. Synthesis of antibacterial modified copolymer with QAS**

**Table 5.1** The reactant ratios for preparation of various block copolymers including PEG<sub>550</sub>-PCL<sub>2000</sub>-PEG<sub>550</sub> (N<sup>+</sup>0) and PEG<sub>550</sub>-PCL<sub>1000</sub>-DMA-PCL<sub>1000</sub>-PEG<sub>550</sub> (N<sup>+</sup>5, N<sup>+</sup>10, N<sup>+</sup>15, N<sup>+</sup>20, N<sup>+</sup>30, and N<sup>+</sup>50), along with the evaluation result of their phase transition behaviors

Sample Code	Molar ratio PEG-PCL-OH:HMDI:DMA	Phase transition evaluation
N <sup>+</sup> 0	100:50:0	✓ sol-gel-sol
N <sup>+</sup> 5	100:55:5	✓ sol-gel-sol
N <sup>+</sup> 10	100:60:10	✓ sol-gel-sol
N <sup>+</sup> 15	100:65:15	✓ sol-gel-sol
N <sup>+</sup> 20	100:70:20	× no transition
N <sup>+</sup> 30	100:70:30	× no transition
N <sup>+</sup> 50	100:100:50	× no transition

The schematic illustration (with molecular structures) of the synthesis of the antibacterial modified block copolymer PEG<sub>550</sub>-PCL<sub>1000</sub>-DMA-PCL<sub>1000</sub>-PEG<sub>550</sub> is presented in **Scheme 3.2**. The details of the sample codes for the prepared block copolymers are shown in **Table 5.1**. Three steps are involved in the synthesis, including coupling of DMA with HMDI, copolymerization of mPEG and  $\epsilon$ -CL, and a final coupling reaction.

### 5.2.2. Characterization of antibacterial modified copolymer

The successful synthesis of the antibacterial modified block copolymer PEG<sub>550</sub>-PCL<sub>1000</sub>-DMA-PCL<sub>1000</sub>-PEG<sub>550</sub> is confirmed by FTIR and <sup>1</sup>H-NMR characterization, as shown in **Figure 5.1** and **Figure 5.2** respectively.

### 5.2.2.1. FTIR analysis

Many sharp narrow FTIR peaks can be found for  $\epsilon$ -CL as a raw material, indicative of its small molecule nature [266]. An obvious FTIR absorption band around  $1730\text{ cm}^{-1}$  can be assigned to lactone group. After ring opening copolymerization and condensation reaction with mPEG, the sharp narrow peaks found for  $\epsilon$ -CL turns to be broadened, with a much lower number of peaks, revealing the success in the copolymerization. Concerning HMDI, we can clearly observe a distinct FTIR absorption peak at  $\sim 2250\text{ cm}^{-1}$ , which can be ascribed to the N=C=O group [267]. After the reaction with DMA and subsequent coupling with mPEG-PCL-OH, the FTIR absorption of the N=C=O group completely disappears, which can be an indication of the effective reaction of the N=C=O group and formation of the -NHCOO- group. The C-N moiety of the -NHCOO- group exhibits typical FTIR absorption bands at  $\sim 1530\text{ cm}^{-1}$  (C-N stretch) and  $\sim 1240\text{ cm}^{-1}$  (C-N deformation) [268-270], which can be well seen in the spectra of the final block copolymers. After the coupling reaction with the intermediate product mPEG-PCL-OH (leading to the formation of final copolymers), the reactive OH group is also found to be depleted, as evidenced by the loss of the broad absorption of mPEG-PCL-OH centered at  $\sim 3524\text{ cm}^{-1}$  [271-274].

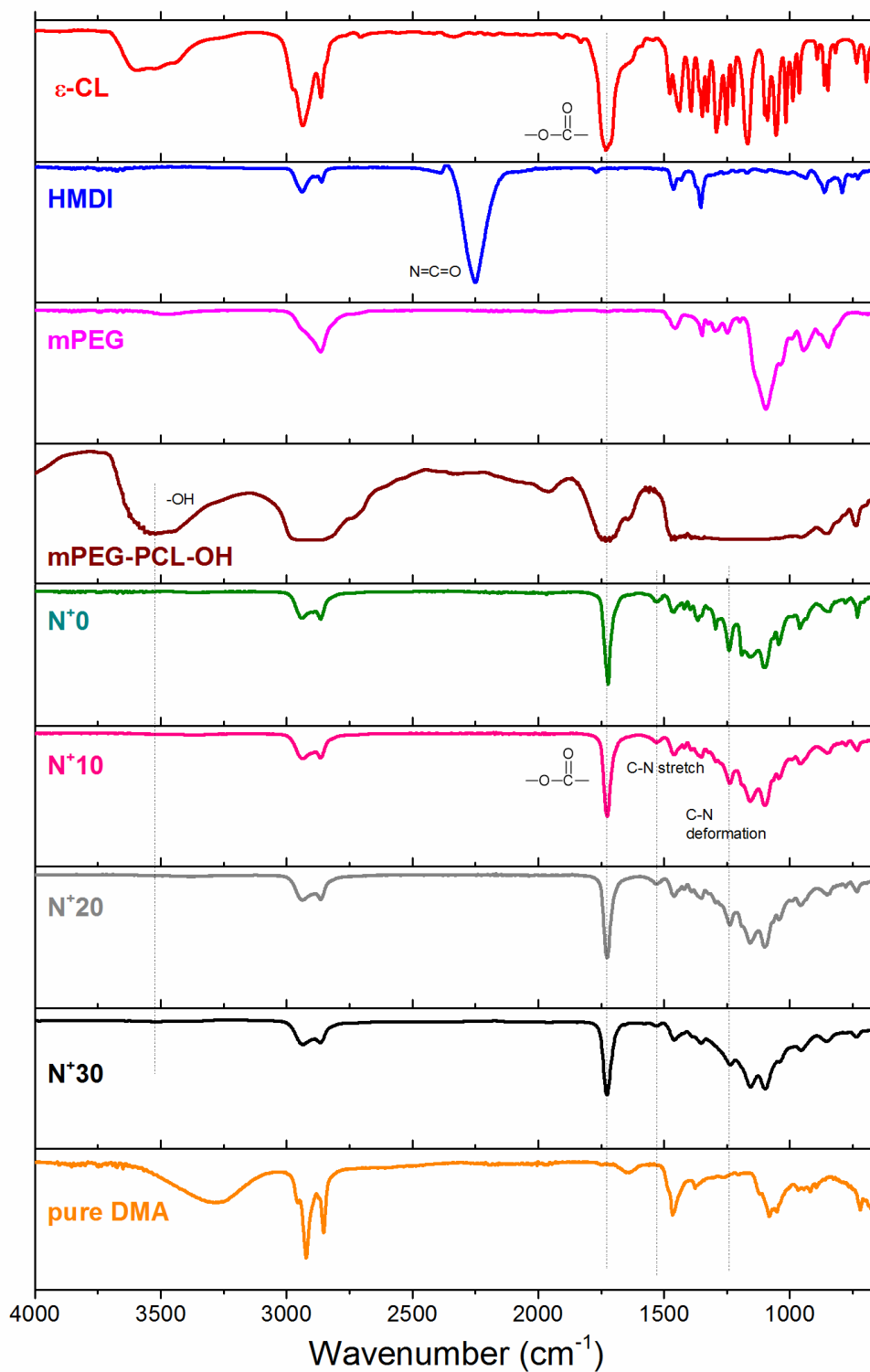


**Figure 5.1** FTIR spectra of various samples including raw materials adopted and block polymers synthesized

### 5.2.2.2. $^1\text{H-NMR}$ analysis

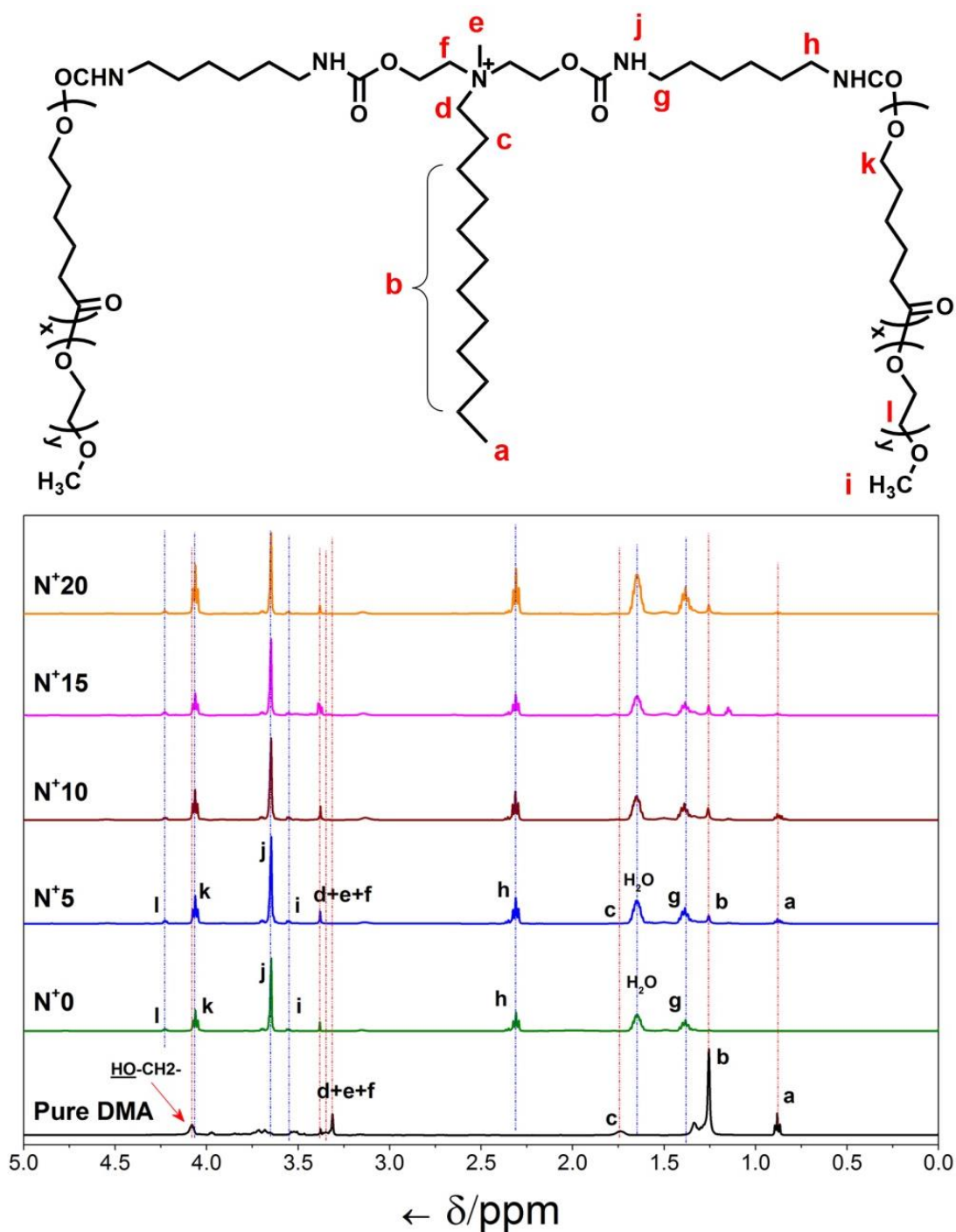


**Figure 5.2**  $^1\text{H-NMR}$  spectra of pure DMA and various as-synthesized block copolymers

To further verify the effective synthesis of the antibacterial modified block copolymers mPEG-PCL-DMA-PCL-mPEG,  $^1\text{H-NMR}$  spectra are provided in

**Figure 5.2**, together with the molecular structure shown on the top of the figure. The characteristic peaks of each building block were unequivocally detected and assigned. The signals of the DMA units ( $H^a$ ,  $H^b$ ) were observed in the  $^1H$ -NMR spectra of  $N^{+5}$ ,  $N^{+10}$ ,  $N^{+15}$  and  $N^{+20}$ , but cannot be found in that of  $N^{+0}$ . In addition, the peak (at  $\sim 4.1$  ppm) assignable to the OH moiety of DMA cannot be detected in the final block copolymers. These results thus suggest the effective grafting of DMA units on the backbone of mPEG-PCL-mPEG [255].

### 5.2.2.3.DSC and GPC analysis

DSC analysis was further employed to investigate the melting and crystallization behaviors of the block copolymer. More DSC data thus obtained are supplied in **Figure 5.3**. As for all the investigated copolymers, two melting peaks can be found on the DSC heating curves, while one exothermic crystallization peak can be seen on the DSC cooling traces (**Figure 5.3**). The two melting peaks observed are likely indexed to the initial melting of PCL segments and next melting of the re-crystallized PCL domains [220, 260]. The normalized DSC cooling thermograms are shown in **Figure 5.4**, together with the comparison plots of relative crystallinity and full width at half maximum (FWHM) among different copolymers. Of more interest is that the relative crystallinity is stepwise increased for the copolymer from  $N^{+0}$ ,  $N^{+5}$ ,  $N^{+10}$ , to  $N^{+15}$ , but becomes sharply lowered for  $N^{+20}$  to a value even less than that for  $N^{+0}$ . A similar tendency of the change in FWHM can also be observed.

On the contrary, the average molecular weight  $M_n$  of  $N^{+20}$  shows a steep increase as compared to the remaining samples (**Figure 5.4 (c)**), which thus consolidates that the crystallinity loss of  $N^{+20}$  can be ascribed to the restriction of close packing of PCL segments by the too large extent of quaternization with

DMA since the positive effect of the molecular weight increase on the crystallinity could be neglected. It can also be found that our synthesized copolymers exhibit a narrow molecular weight distribution as indicated by the polydispersity index (PDI) of GPC that is close to 1 (**Figure 5.4 (d)**).

Significantly, we note that the sol-gel-sol transition behavior can be detected for the copolymers N<sup>+</sup>0, N<sup>+</sup>5, N<sup>+</sup>10 and N<sup>+</sup>15, but is lost for the copolymers N<sup>+</sup>20 and N<sup>+</sup>50 (**Table 5.1**). The sharp decrease of the relative crystallinity of N<sup>+</sup>20 is thus strongly correlated with the loss of the sol-gel-sol transition. Since the crystallization peak on the DSC thermogram has a close relationship with the crystallization behavior of PCL blocks, the sharp decrease of the relative crystallinity of N<sup>+</sup>20 can be originated from the disturbance of the PCL block by DMA units. As for N<sup>+</sup>20, the positive charge and long alkyl chains of DMA units might be present in a too large quantity, which is most likely to impede the PCL chain from folding into a regular and closely packed crystalline structure, and thus lead to the large reduction of the relative crystallinity. Such a disturbance can also heavily disrupt the hydrophilic and hydrophobic balance between mPEG and PCL blocks, thereby causing a loss of the sol-gel-sol transition. As also found in **Figure 5.4**, N<sup>+</sup>20 becomes more readily to crystallize, as the starting point of the crystallization peak occurs earlier during the cooling process. A possible reason for this result is proposed as follows: a too high extent of quaternization with DMA that possesses positive charges and long alkyl chains may lead to the formation of a large number of crystal defects indexed to PCL blocks. A part of these defects could be easily restored during the cooling process.

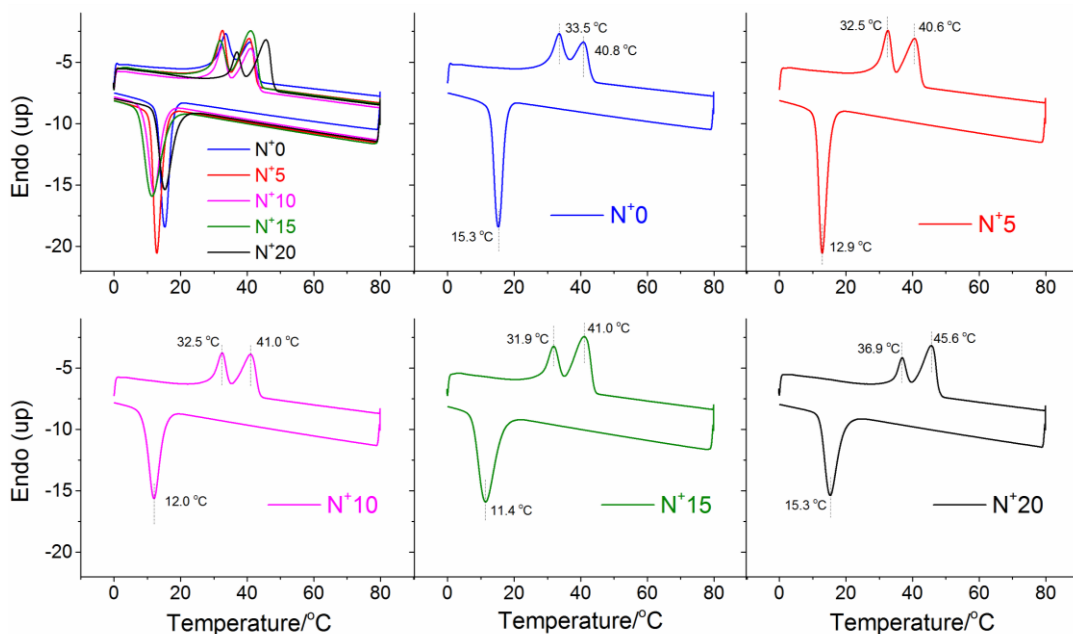


**Figure 5.3** DSC analysis of thermal melting and crystallization behaviors of different block copolymers during the heating and cooling processes respectively, including PEG<sub>550</sub>-PCL<sub>2000</sub>-PEG<sub>550</sub> without quaternization and PEG<sub>550</sub>-PCL<sub>1000</sub>-DMA-PCL<sub>1000</sub>-PEG<sub>550</sub> with different extents of quaternization.

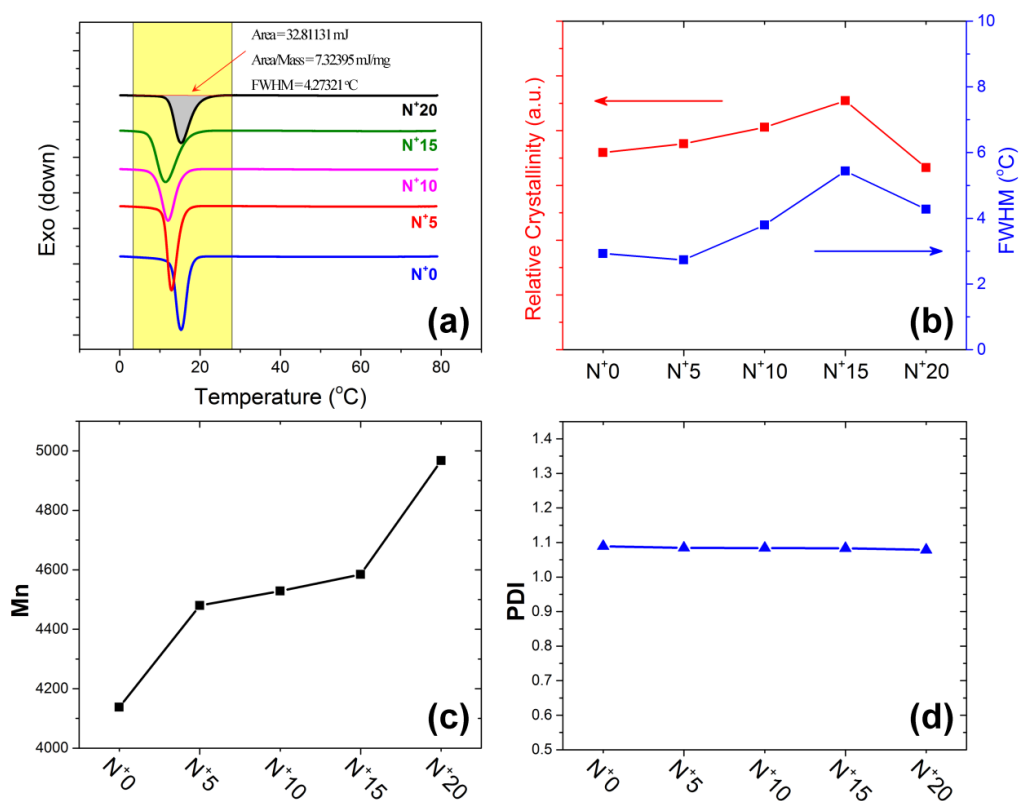


**Figure 5.4** DSC and GPC analysis of block copolymers with different extents of quaternization. (a) Normalized DSC cooling thermograms, with exothermic peaks that are clearly shown. (b) Comparison plots (in double y axis fashion) of relative crystallinity and FWHM among the block copolymers with different extents of quaternization, as calculated from the DSC cooling curves (the relative crystallinity is calculated by integrating the peak area and then normalizing with the mass of the specimen used in the DSC measurement). (c and d) Dependence of  $M_n$  (c) and polydispersity (d) on the extent of quaternization.

### **5.2.3. Study of the phase transition behavior of the modified hydrogel**

A schematic illustration of the phase transition of an aqueous solution of the typical copolymer N<sup>+</sup>5 with the 35 wt.% concentration is shown in **Figure 5.5**. A clear sol-gel-sol transition can be noted, with, actually, total four observable states (transparent sol, opaque sol, gel, and turbid sol with sediment). In the schematic illustration of the sol-gel-sol transition, at a low temperature (in this case 20°C), the amphiphilic block copolymers are aggregated into micelles via self-assembly. With increasing temperature to 25°C, the interactions between micelles become stronger and more micelles are likely to be formed, indicating the smaller interval between the micelles, which falls in the range of the wavelength of visible light. Thus, the transparent sol turns opaque. Further raising the temperature to 35°C, interactions between micelles are strong enough and amount is sufficient by self-assembly, and thus the sol-gel transition takes place. Finally, continue increasing the temperature to 55°C, leads to disruption of the hydrophobic and hydrophilic balance of the copolymer and the collapse of

the micelle structure, and thus turns to a turbid sol with precipitate. Phase diagrams of our typical copolymers N<sup>+</sup>0 and N<sup>+</sup>10 are also given in the bottom right corner. Three basic physical states, namely sol, gel, and turbid sol with precipitate, can be observed for both the samples. Nevertheless, the copolymer N<sup>+</sup>0 seems to be more sensitive to temperature since a much lower polymer concentration is needed to obtain a sol-gel transition, which thus reveals that the incorporation of DMA units can indeed make N<sup>+</sup>10 more insensitive to temperature resulting from the partial disruption the hydrophilic and hydrophobic balance between mPEG and PCL respectively. This result can also offer us an indication that a desirable balance should be struck between the antibacterial performance and thermosensitivity, in order to produce intelligent biomaterials being suitable for practical biomedical applications.

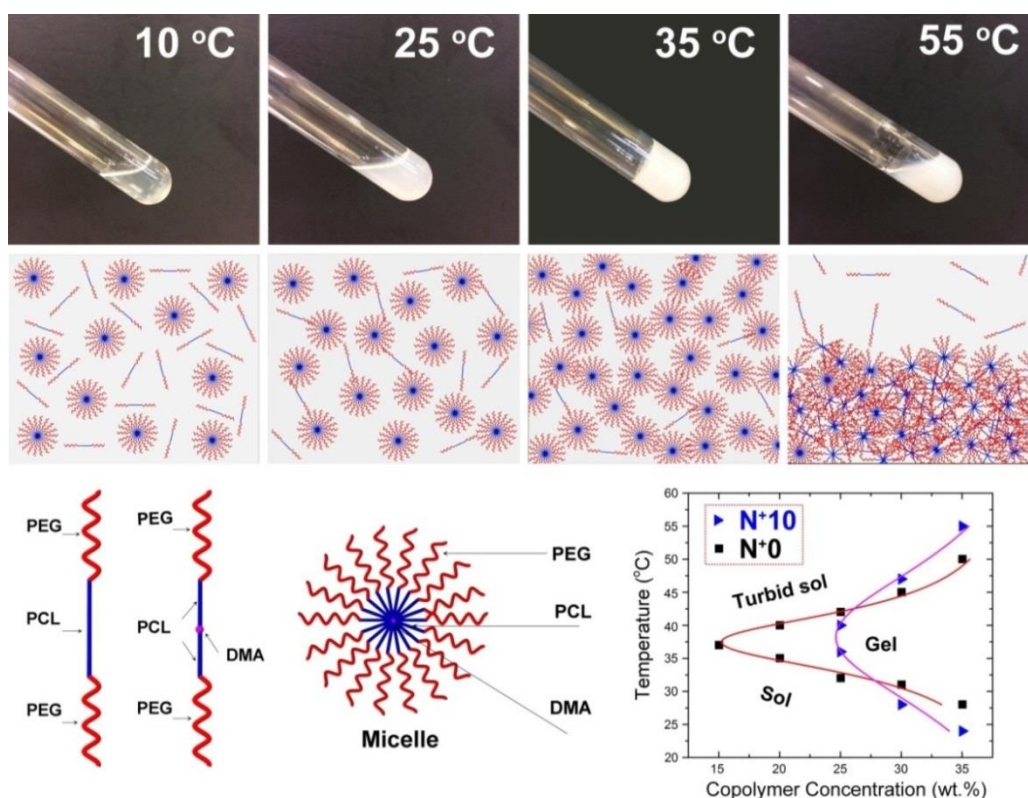


**Figure 5.5** Investigation of the sol-gel-sol transition behavior of the thermogel PEG<sub>550</sub>-PCL<sub>1000</sub>-DMA-PCL<sub>1000</sub>-PEG<sub>550</sub>. The photos in the top row display

sol-gel-sol transition of 35 wt.% N<sup>+</sup>5 copolymer water solution with the increase of temperature from 10 to 55°C. The schematic illustration of the sol-gel-sol transition is shown in the middle row. Phase diagrams of copolymers N<sup>+</sup>10 and N<sup>+</sup>0 are presented at the bottom right corner.

The polymer concentration-dependent sol-gel-sol transition is also validated by the observation of the phase transition behaviors of the typical N<sup>+</sup>5 solutions with different polymer contents, as shown in **Figure 5.6**. These photos show the thermosensitivity of N<sup>+</sup>5 with different concentration. You can see that no temperature-triggered sol-gel transition can be found for the 5% and 20 wt.% polymer solutions, whereas a clear sol-gel-sol transition can be observed for the 35 wt.% polymer solution. We also investigated the dependence of the sol state on the quaternization extent of the typical copolymers (**Figure 5.7**). These photos show the thermosensitivity of N<sup>+</sup>5 and N<sup>+</sup>15 with the same concentration. They are transparent sol at 10°C. Heating to 55°C, N<sup>+</sup>5 becomes white turbid sol, while N<sup>+</sup>15 has no obvious change. At the same 5 wt.% copolymer concentration, the higher extent of quaternization (in this case N<sup>+</sup>15) can lead to the formation of a more transparent sol at both 10 and 55°C, as compared to that for the lower extent of quaternization (namely N<sup>+</sup>5). This demonstrates N<sup>+</sup>5 is more thermosensitive than N<sup>+</sup>15. These results from **Figure 5.6 and 5.7** reveal that more DMA incorporation can make hydrogel more insensitive to temperature.

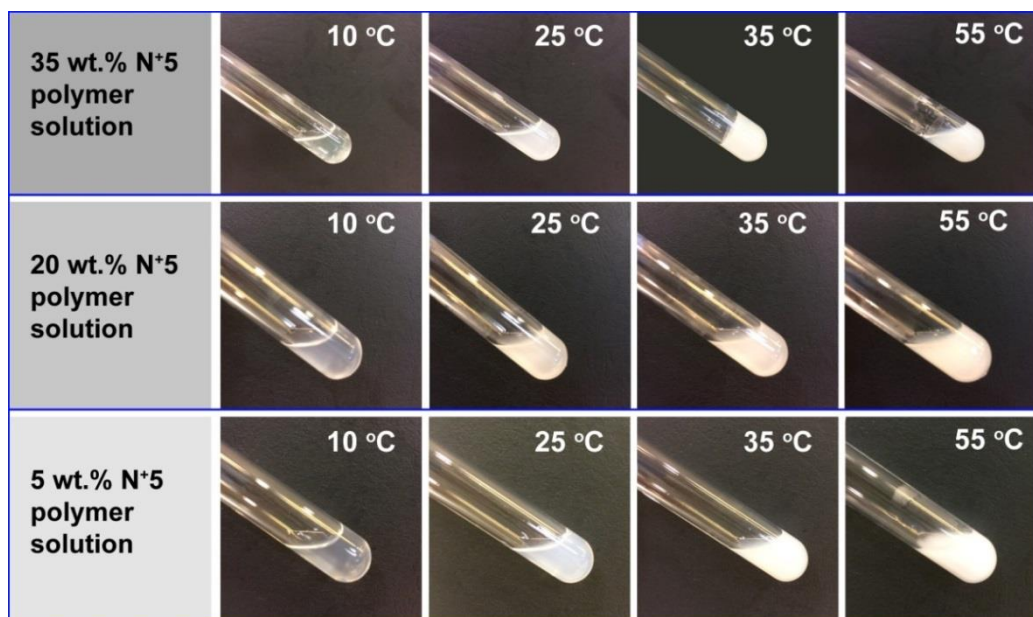


**Figure 5.6** Photos showing the temperature-responsive behaviors of the copolymer N<sup>+</sup>5 solutions at concentrations of 5 wt.% (bottom row), 20 wt.% (middle row) and 35 wt.% (top row).

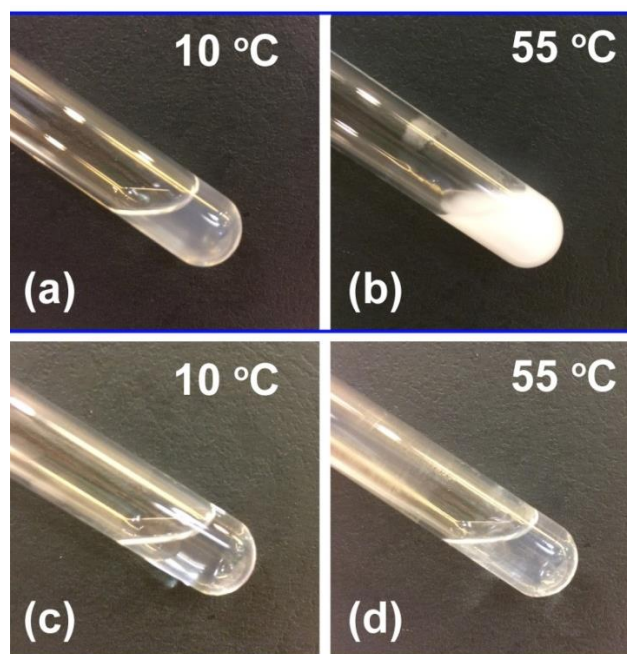


**Figure 5.7** Photos showing the temperature-responsive behaviors of aqueous solutions containing the 5 wt.% copolymer N<sup>+</sup>5 (a, b), and 5 wt.% copolymer N<sup>+</sup>15 (c, d).

#### 5.2.4. Study of in vitro skin toxicity

In this study, the antibacterial block copolymers modified with QAS show very low skin toxicity, as evaluated using MTT (**Figure 5.8(a)**) and LDH (**Figure 5.8(b)**) assays. Specifically, as revealed in **Figure 5.8(a)**, the positive control shows the lowest percentage of cell viability, while the negative control exhibits the highest percentage of cell viability. It is satisfying to find that the hydrogel samples N<sup>+</sup>0, N<sup>+</sup>5, N<sup>+</sup>10 and N<sup>+</sup>15 have a very low toxic effect on cells, rather close to the negative control. The modification with DMA only has a negligible influence on the skin toxicity as compared to the counterpart without antibacterial modification (N<sup>+</sup>0). With regard to the LDH assay (**Figure 5.8(b)**), a high LDH release implies the cell membrane damage. As expected, the positive control shows the highest LDH release, in good agreement with the MTT assay results. The other samples including negative control and a series of block copolymers (N<sup>+</sup>0, N<sup>+</sup>5, N<sup>+</sup>10 and N<sup>+</sup>15) show a very limited effect on the LDH release. Consequently, the results of the combined MTT and LDH assays demonstrate that our prepared copolymers are basically non-cytotoxic.

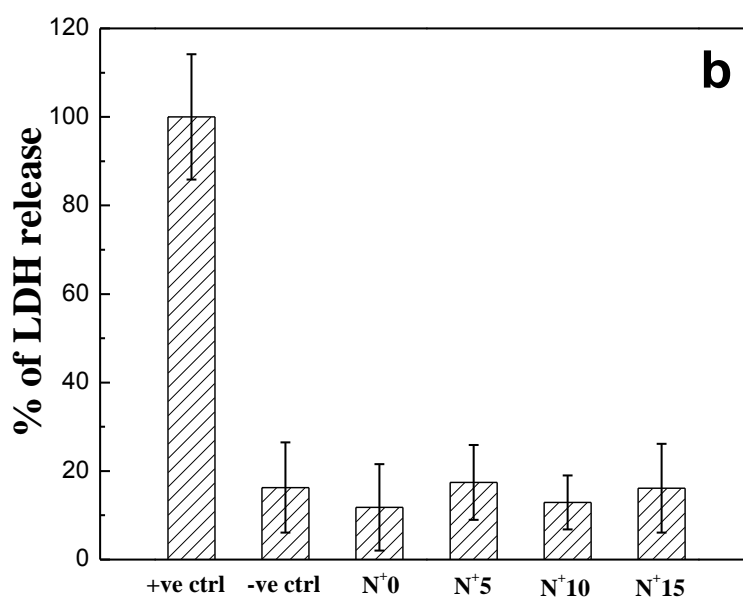
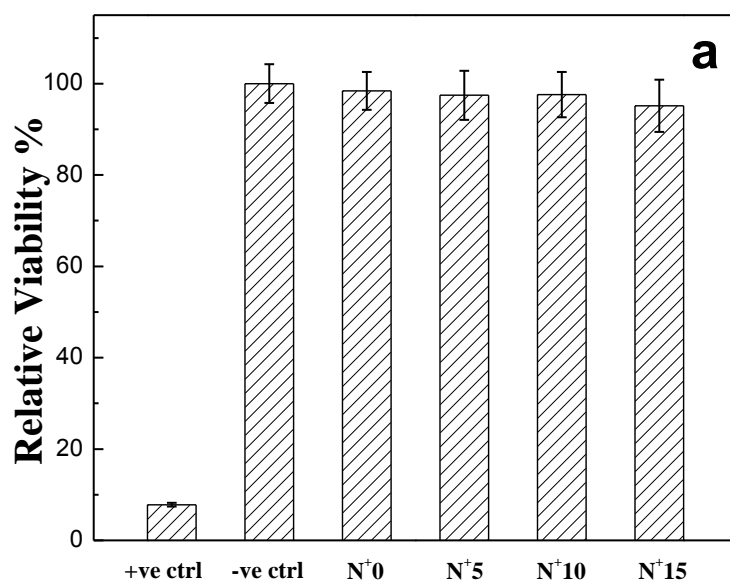


**Figure 5.8** In vitro skin toxicity: (a) The in vitro skin toxicity evaluation result through a cell viability measurement; (b) The in vitro skin toxicity evaluation result through a LDH release test.

### **5.2.5. Study on the antibacterial modified hydrogel**

From previous characterization of various synthesized copolymers and study of the phase transition behavior and in vitro skin toxicity, sample N<sup>+</sup>10 of the antibacterial modified copolymer PEG-PCL-DMA-PCL-PEG exhibits the optimal performance among the synthesized copolymers. The result of the microscopic morphology, thermoresponsive ability, controlled drug release and antibacterial performance of the prepared hydrogel N<sup>+</sup>10 will be presented in this study on the antibacterial modified hydrogel.

#### **5.2.5.1. Microscopic morphology of the modified hydrogel by SEM observations**

The microscopic morphology and topology of the modified PEG-PCL-DMA-PCL-PEG hydrogel was probed by SEM (**Figure 5.9**). The specimens were prepared by being frozen in liquid nitrogen and then lyophilized for 24 h. The lyophilized gel features a network structure with numerous micropores, which can be favorable for the drug loading and hence for the subsequent controlled drug release. But the structure is irregular and discontinuous. These show the disadvantages of the prepared antibacterial hydrogel, such as the weak mechanical strength and inflexibility which can be improved and modified by secondary substrate supporting.

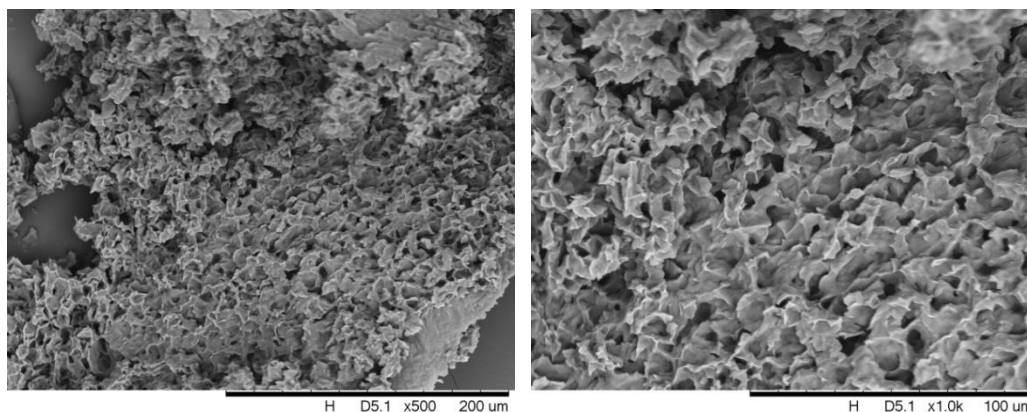


**Figure 5.9** SEM observation of the microstructure of the lyophilized hydrogel N<sup>+</sup>10 under different magnification scales

### 5.2.5.2. Sol-gel phase transition detection of modified hydrogel

It is worth pointing out that our lyophilized copolymer powder can be quickly dissolved to form a sol within 30 s, as shown in **Figure 5.10**. This is an advantage over some traditional thermogels that exhibit as a sticky paste state even after lyophilization treatment and need several hours to be dissolved to make an injectable aqueous solution [85]. Our block copolymer-based thermogel can thus be much easier to weigh and to transfer. It can be seen in **Figure 5.11 (a-c)** that the prepared sol at room temperature can be quickly transformed to a gel when placed on a human finger, which well demonstrates the body temperature-induced sol-gel transition. This result also elucidates that an appropriate extent of modification with DMA does not heavily affect the thermosensitive properties of the PEG-PCL-PEG copolymer, even though a too large DMA addition ratio can lead to a loss of the sol-gel-sol transition, e.g. as for the as-prepared copolymers N<sup>+</sup>20 and N<sup>+</sup>50 (**Table 5.1**). We also tested the FT-IR for the lyophilized gel and normal gel. From the results, both of them have the same FT-IR curve, except, there is another water peak in the normal gel sample around 3500cm<sup>-1</sup> region in broad peak. But for the lyophilized gel, there

is not this peak. It is because the water inside hydrogel was sublimated by freeze drying. In previous SEM observation, the porous microstructure in the lyophilized gel was also formed due to the sublimation.

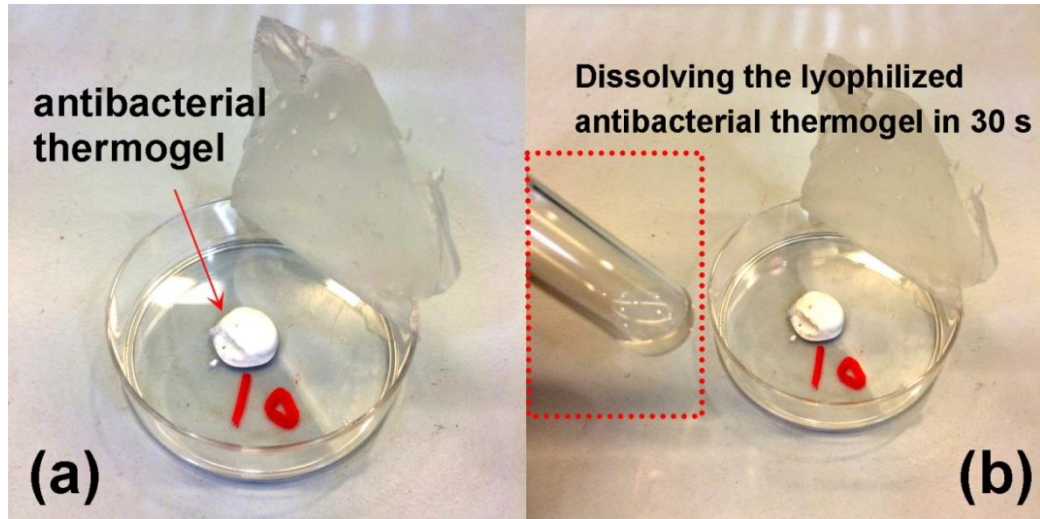


**Figure 5.10** Photoimages showing that our lyophilized antibacterial thermoresponsive hydrogel  $N^{+}10$  can be quickly dissolved in water to form a transparent sol (taking around 30 s). (a) The photoimage of lyophilized hydrogel. (b) The image of the resultant sol in a glass tube is highlighted in a dotted red rectangle. Dissolving the lyophilized hydrogel  $N^{+}10$  in water by stirring at 50-60°C and then quickly cooling to room temperature (25°C).

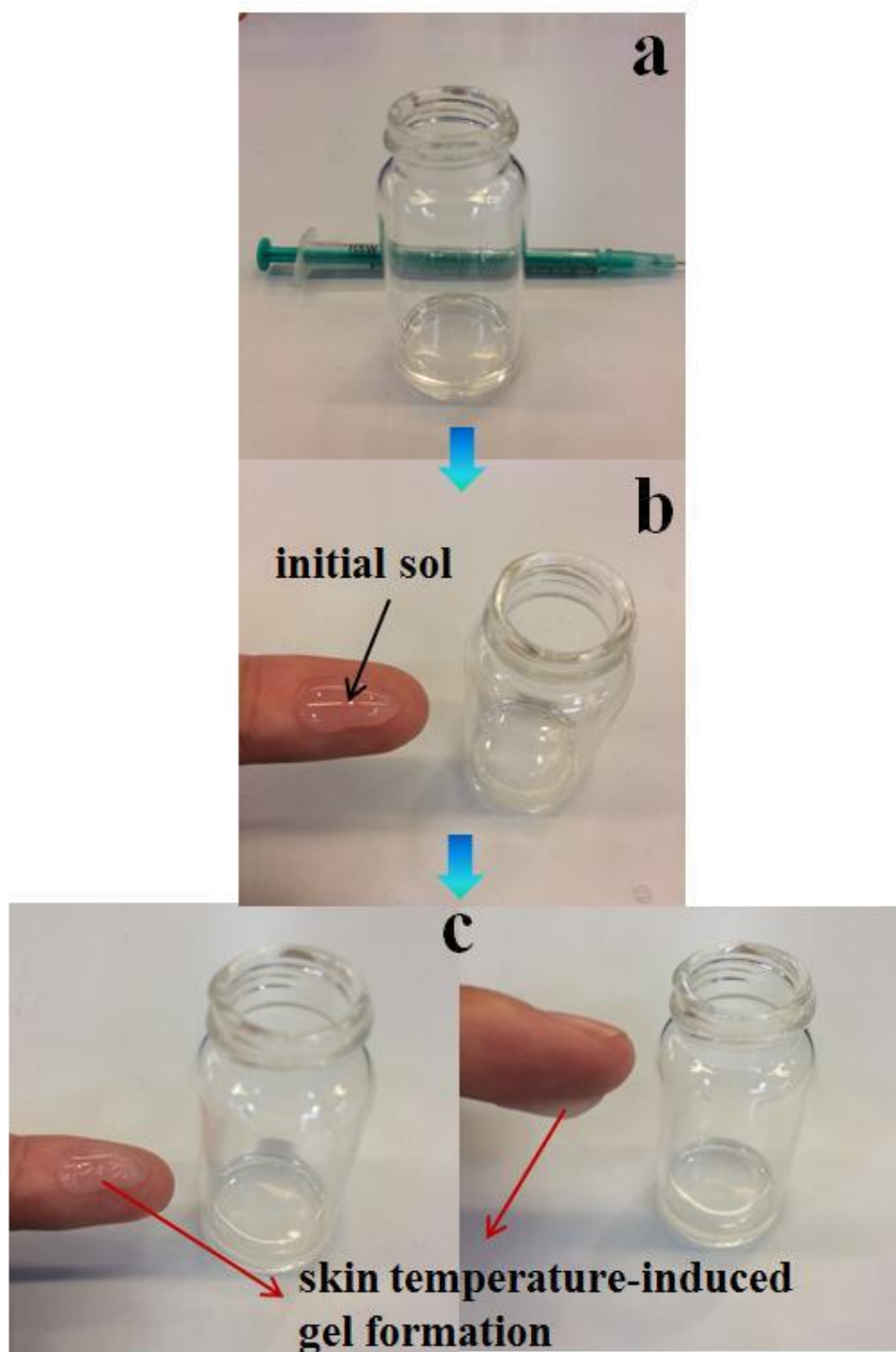


**Figure 5.11** Formation of the modified hydrogel N<sup>+</sup>10 at skin temperature: sol (a, b) to gel (c) transition at skin temperature.

### **5.2.5.3. In vitro drug release behavior of modified hydrogel**

The in vitro cumulative drug release of modified hydrogel was monitored by a UV-vis spectrophotometer. In vitro release model of 0.1% w/w% aloin and

curcumin-loaded hydrogels under different pH conditions (pH 5.0 and 7.4) at 35°C was investigated and monitored in PBS for a time period of 120 h in **Figure 5.12**. Compared with previous unmodified PEG-PCL-PEG hydrogel, there is no big difference for drug release. Similar to previous results, aloin and curcumin were released faster in pH 5.0 PBS than in pH 7.4 PBS, showed rapid release at the initial stage and slow release later.

The controlled release study also demonstrates that an appropriate extent of modification with DMA does not heavily affect the in vitro drug release properties and the modified hydrogel N<sup>+</sup>10 can provide a reliable and effective sustained drug release.

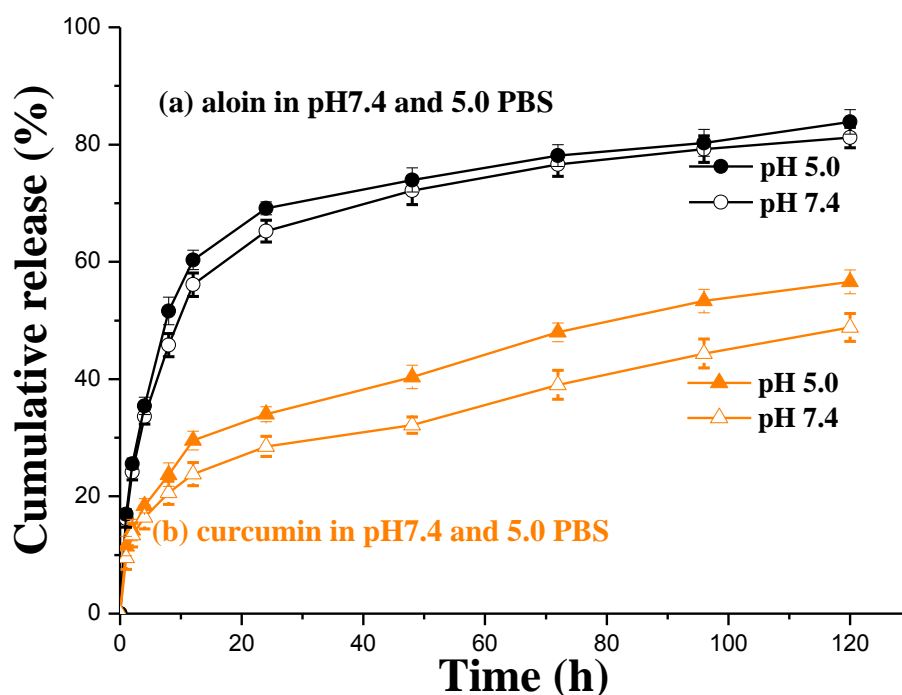


**Figure 5.12** In vitro drug release behavior of the modified antibacterial hydrogel N<sup>+</sup>10: in vitro cumulative release (a) loaded with aloin (0.1%) and (b) curcumin (0.1%) in PBS (pH 5.0 and 7.4).

#### 5.2.5.4. Investigation of the antibacterial performance of the QAS modified hydrogel

The main target of this part study is to achieve the antibacterial treatment of the mPEG-PCL-mPEG copolymer, and the result of the antibacterial performance evaluation is shown in **Figure 5.13**. The antibacterial activity of as-prepared hydrogels mPEG-PCL-DMA-PCL-mPEG was tested in both qualitative and quantitative manners according to the inhibition zone method and viable cell count method respectively. The microorganisms adopted were two representative clinically relevant bacterial strains, namely *S. aureus* (Gram-positive) and *E. coli* (Gram-negative). As for the qualitative analysis (**Figure 5.13(a)**), inhibition zones can be clearly observed around the hydrogel samples N<sup>+</sup>5, N<sup>+</sup>10, N<sup>+</sup>15 and N<sup>+</sup>20, and N<sup>+</sup>50 against the Gram-positive *S. aureus*, and are gradually enlarged for the samples with involving a larger DMA reaction ratio, indicating that the antibacterial performance of the block copolymers can indeed be improved with more DMA building units. In contrast, no inhibition zone can be found around the hydrogel N<sup>+</sup>0 without DMA units, which is good consistence with a previous report on a PEG-PCL-PEG based thermoresponsive hydrogel [249]. As a consequence, the antibacterial performance of our copolymers can be medicated easily through adjusting the extent of modification with DMA.

The result of quantitative analysis is shown in **Figure 5.13(b-d)**. A 99% reduction of *E. coli* bacteria can be noted for the hydrogel N<sup>+</sup>10 (**Figure 5.13(d)**). The antibacterial activity of DMA mainly lies in the positive charge density and hydrophobic long alkyl substituents by means of electrostatic and hydrophobic interactions with bacteria respectively. Specifically, the hydrophobic long alkyl

chains can have strong hydrophobic/binding interactions with the hydrophobic inner part of the bacterial cell wall and membrane, in addition to the electrostatic interactions between the positive antibacterial copolymers and negative bacteria, thereby enhancing the propensity of the copolymer chains to penetrate the hydrophobic bacterial membrane and eventually causing bacteria lysis [132]. Therefore, we effectively demonstrate that the as-prepared copolymers with DMA units exhibit an impressive antibacterial activity against both Gram-positive and Gram-negative bacteria.

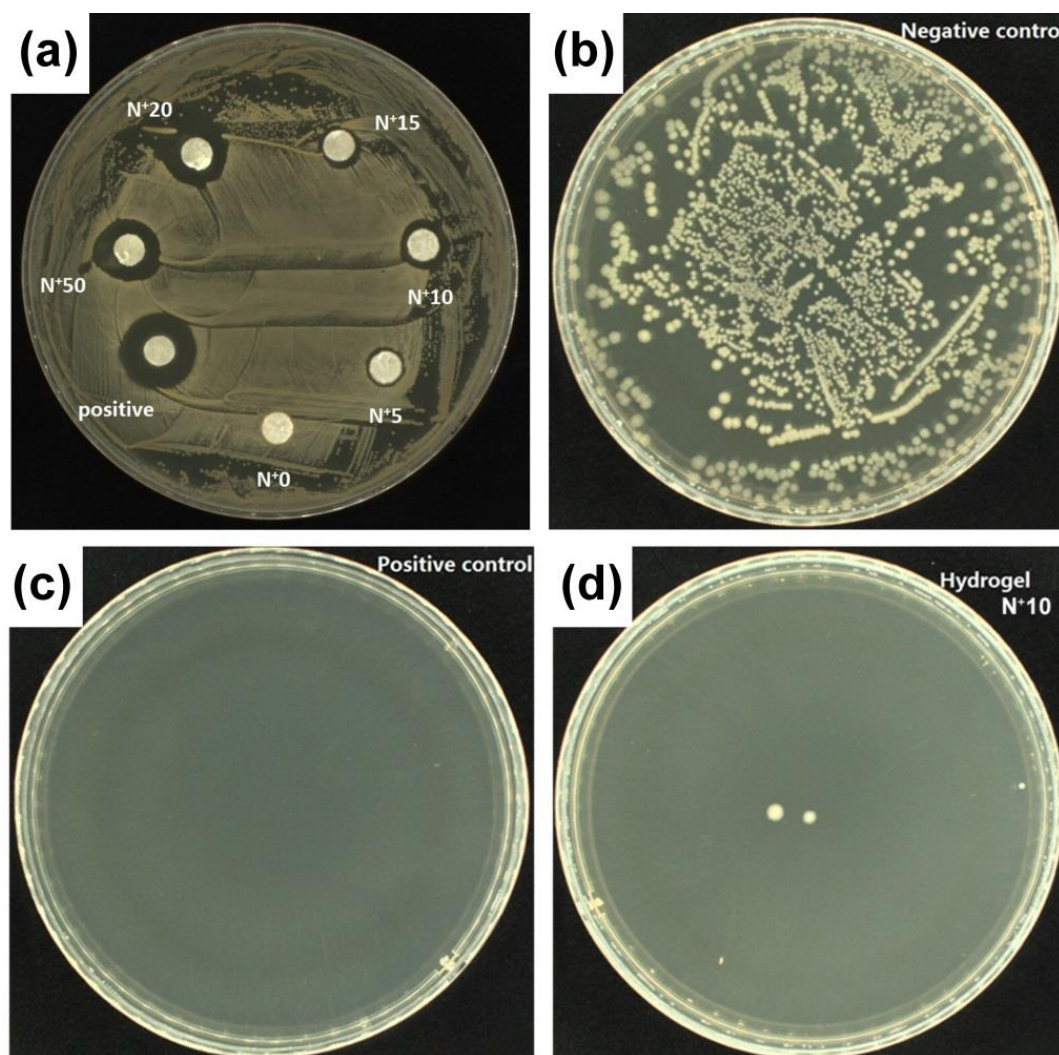


**Figure 5.13** Study on the antibacterial properties of the prepared block copolymers. (a) The qualitative antibacterial property analysis by the inhibition zone method using *S. aureus* as the testing microorganism; (b)-(d) The

quantitative antibacterial performance analysis of hydrogel N<sup>+</sup>10 by the viable cell count method using E. coli as the testing microorganism.

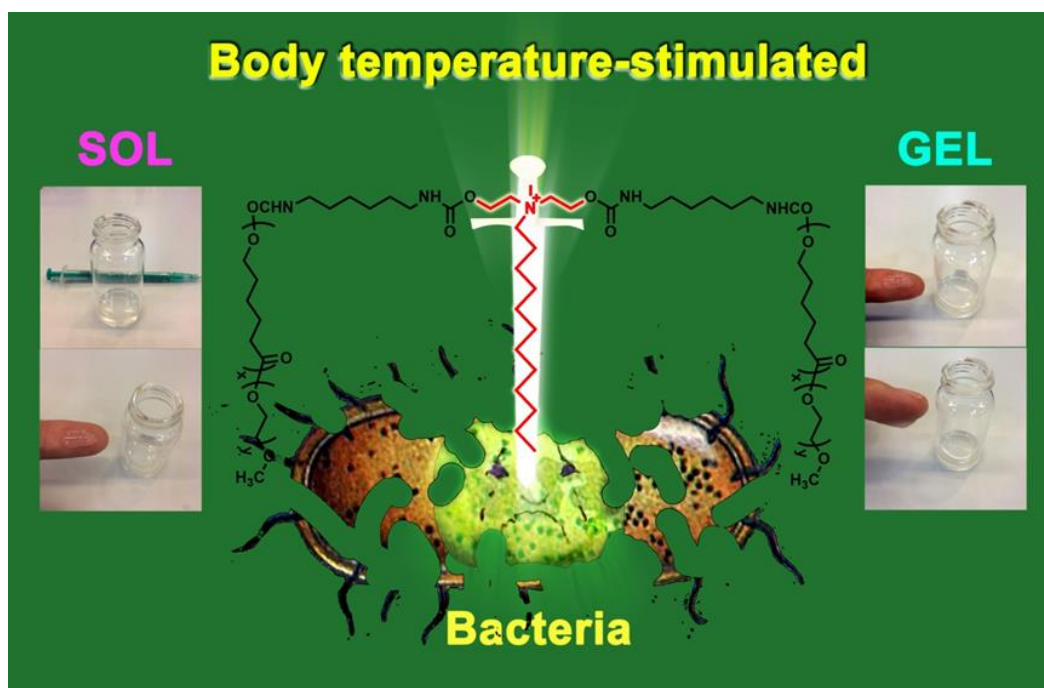


**Figure 5.14** Schematic diagram of the antibacterial thermo-responsive hydrogel with sol-gel transition behavior

# Chapter 6 Smart hydrogel coated textile materials for skin and wound care

## 6.1. Introduction

Along with the enhancement of people's living standard, functional textiles used in medical and related healthcare and hygiene sectors are an important and rapidly growing segment of the textile field especially in recent years [275, 276]. In order to add more properties and better performance onto traditional dressings for better skin and wound care, such as protecting against infections, keeping moist environment, absorbing body liquid and exudate, providing gas exchange, creating a protective barrier and avoiding the secondary trauma, surface modification with functional polymers is an indispensable process for traditional nonwoven dressing without a loss of its original properties. With the development of biomedical technologies, more and more modern dressings have been developed as an improvement upon the traditional wound dressings. The novel functionalities can be delivered to textiles through integrating stimuli-responsive hydrogels [277]. Some smart hydrogels have already been applied in textiles to improve or achieve novel and smart functionalities. These hydrogel-integrated textiles with novel functionalities can considerably improve the performance for a wide variety of applications and for meeting consumers' demands of comfort, easy care, health and hygiene.

Considering the high potential of hydrogel in biomedical applications and the extensive utilization of medical disposable nonwoven fabrics in skin and wound care products, the trend of the development of medical textile products, functional thermoresponsive hydrogels, and complex dressings prepared by coating the developed hydrogels onto the nonwoven fabric for skin and wound care are designed and synthesized/fabricated in this study. This study aims to study the smart textile materials for skin and wound care through combining stimuli-responsive hydrogels with the textile materials. Benefiting from the advantages of textile materials and thermoresponsive hydrogels, a complex dressing with novel functions for skin and wound care is developed using a physical doctor blading method. This kind of smart textile dressing equipped with biocompatible, thermoresponsive hydrogel coating and the multi-layer structure of nonwoven fabric should significantly improve the performances and potentially bring high added value to biomedical textiles.

## **6.2. Results and discussion**

### **6.2.1. Morphology of hydrogel coated nonwoven fabric**

Morphology of hydrogel coated nonwoven was investigated by SEM. The samples were frozen in liquid nitrogen and lyophilized for 24 h before the test. According to **Figure 6.1**, you can see the hydrogel coating was partly on the surface of fabric and partly inside the textile structure between fiber and fiber. And with the fibre supporting, the structure of the hydrogel coating becomes more regular and continuous. And there are no fragments in the hydrogel on the fabric surface. These results demonstrate that the weak mechanical strength and inflexibility of the prepared hydrogel were improved and modified by nonwoven

fabric supporting. Figuratively, the structure of prepared hydrogel just like "tofu dreg construction" is reinforced with fibre like steel after coating on the nonwoven fabric. Not only the structure of prepared hydrogel are reinforces, also other unique functions are achieved from this complex system.

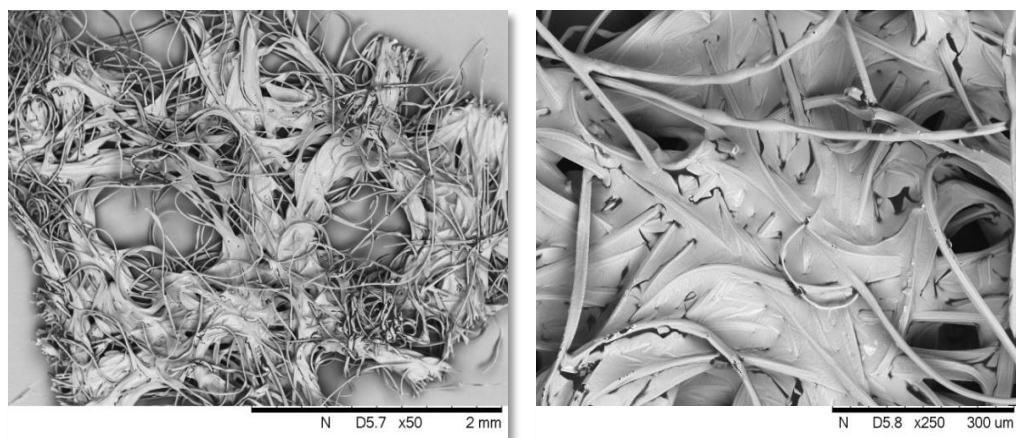
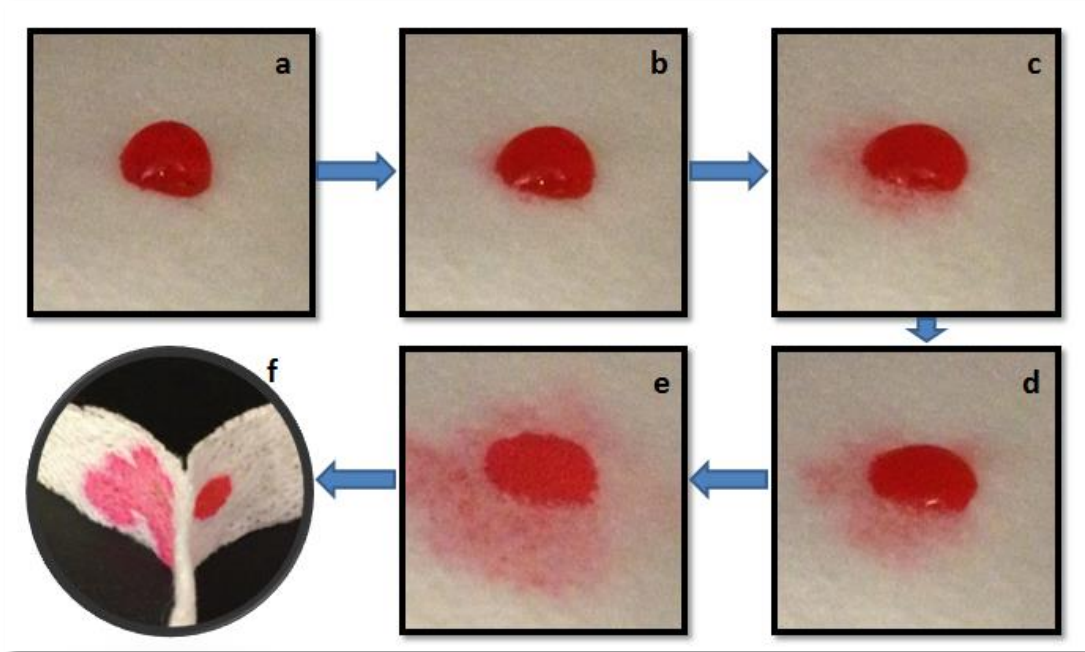


**Figure 6.1** SEM photograph of antibacterial modified hydrogel coated nonwoven fabric

### 6.2.2. Unidirectional water transport test

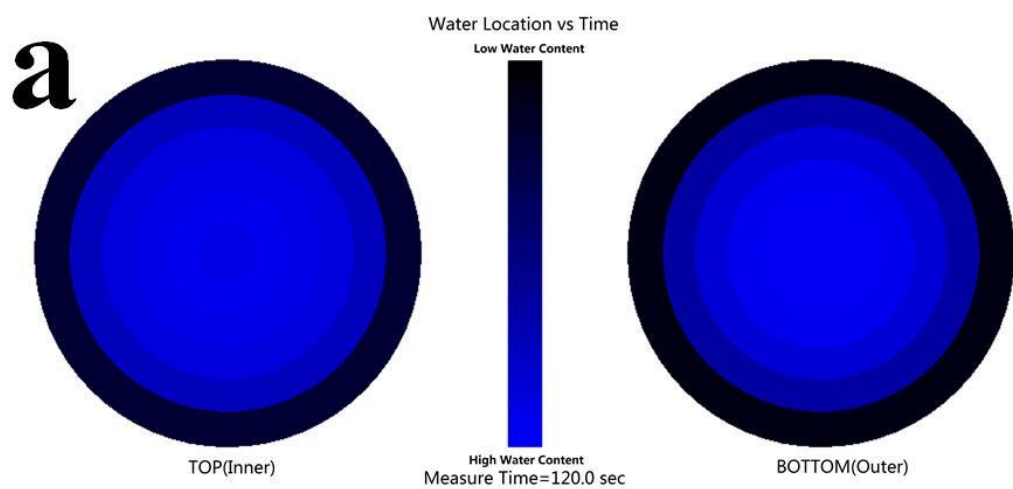
In this study, the prepared hydrogels were coated on one side of nonwoven fabric for the unidirectional water transport test. The surface wettability of the fabrics and unidirectional water transport were studied. The photos were taken after the water droplet dropping onto the hydrogel coating surface. **Figure 6.2 (a-e)** captured the process of unidirectional transportation of coloured water droplet from the hydrophobic side (hydrogel coating side) to the hydrophilic side (the other non-woven fabric side without hydrogel). We observed that the water drop on the hydrogel coated hydrophobic side firstly formed a spherical bead and stayed on the surface for a little while and then gradually was transported to the hydrophilic side. The whole process from **Figure 6.2 (a) to (e)** lasted about 5 seconds. **Figure 6.2 (f)** showed that when the water droplet transported to the

hydrophilic side there was one red dot left on the hydrogel coating side, indicating that the surface maintained hydrophobic property. And that the hydrophilic side (nonwoven fabric side) was stained a large area by red color.



**Figure 6.2** The process of unidirectional transportation of coloured water droplet

### 6.2.3. Moisture management analysis



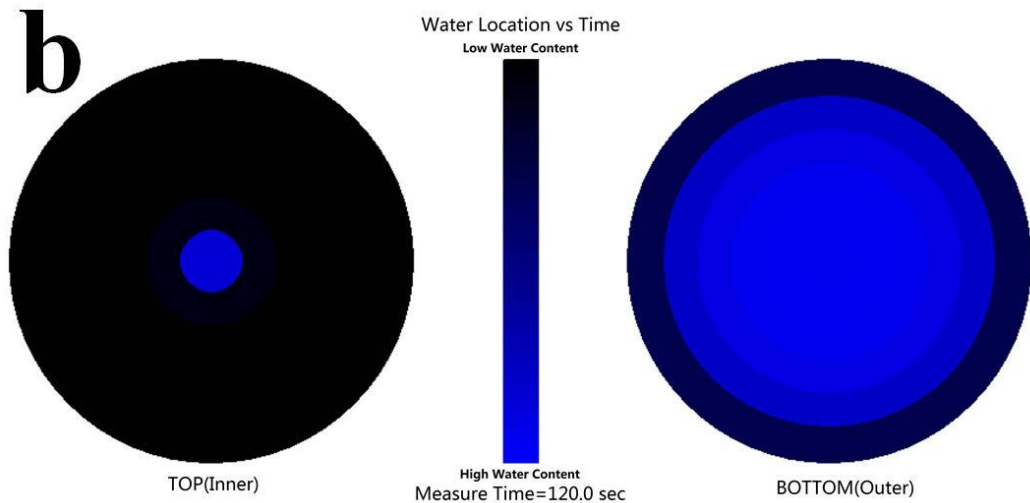


**Figure 6.3** Diagram of water location versus measure time (120s): (a) Untreated nonwoven fabric; (b) Nonwoven fabric with one side of hydrogel coating. Blue represents water.

**Table 6.1** Moisture management indexes

Mean $\pm$ S.D. (n = 3)	Untreated nonwoven	Nonwoven with one side of hydrogel coating
Wetting Time Top(sec)	2.516 $\pm$ 0.03	13.97 $\pm$ 0.09
Wetting Time Bottom(sec)	2.203 $\pm$ 0.03	4.52 $\pm$ 0.04
Top Max Wetted Radius(mm)	25 $\pm$ 0	5 $\pm$ 0
Bottom Max Wetted Radius(mm)	20 $\pm$ 0	20 $\pm$ 0
Top Spreading Speed(mm/sec)	5.8881 $\pm$ 0.04	0.35 $\pm$ 0.01
Bottom Spreading	3.6561 $\pm$ 0.05	3.56 $\pm$ 0.09

Speed(mm/sec)		
Accumulative one-way transport index(%)	$175.187 \pm 5.56$	$612.8 \pm 7.18$
Overall Liquid Moisture Management Capability (OMMC)	$0.5336 \pm 0.18$	$0.79 \pm 0.01$

---

MMT can be used to evaluate fabric liquid moisture spreading and transporting properties on both surfaces of the nonwoven fabric and transferring from one surface to the opposite. The measure time of the whole testing process is 120 s. The water location on the top and bottom surfaces is shown in **Figure 6.3**, which demonstrates that the water location of the top surface is the same as that of the bottom surface (**Figure 6.3 (a)**). The water location of the top surface is much lower than that of the bottom surface, as presented in **Figure 6.3 (b)**. This indicates that most of the liquid is introduced onto the top surface of the fabric, and then transfers quickly to the bottom surface. In the **Table 6.1**, a set of indexes are provided for evaluating the moisture management properties of the hydrogel coated-nonwoven fabric. According to the AATCC 195–2011, the result shows an excellent accumulative one-way transport index (grade 5). The overall moisture management capability (OMMC), an index to indicate the overall capability of the fabric to manage the transport of liquid moisture, is also quite good (grade 4.5). As a result, the highly satisfactory liquid moisture spreading and transporting properties of the hydrogel-coated nonwoven fabric are well demonstrated.

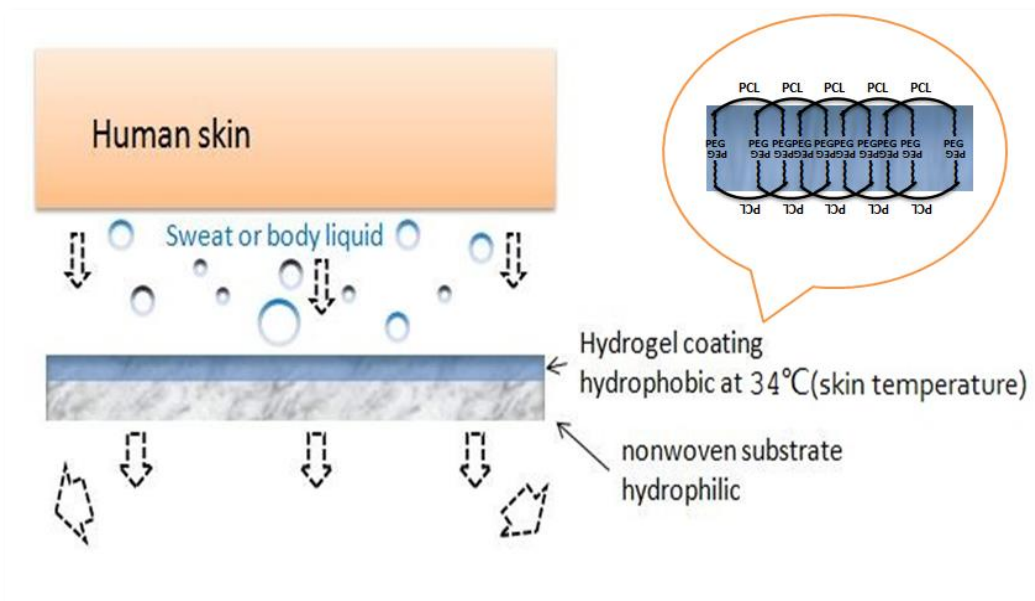


**Figure 6.4** Suggested schematic diagram of hydrogel coated nonwoven fabric with moisture management property

**Figure 6.4** shows the schematic diagram of hydrogel coated nonwoven fabric being capable of management of moisture and exudates. In this study, the nonwoven fabric is used as the support substrate for the smart hydrogel coating with absorption for exudates and drug control releasing properties. In the process of gelation caused by temperature change and thus forming a temperature-responsive hydrogel coating (the sol-gel transition point is around skin temperature), the hydrophobic interactions are enhanced and the self-assembly of the amphiphilic polymer occurs. The hydrophobic PCL segments stretch towards the outside of the hydrogel, while the hydrophilic PEG segments lie in the inside of hydrogel (see **Figure 6.4**). The hydrogel coating turns to be hydrophobic when the temperature is around the skin temperature, thus revealing the controllable transition between hydrophilicity and hydrophobicity of the hydrogel. The porous hydrophobic hydrogel, as well as the nonwoven fabric substrate with a micro-porous, macro-porous network,

contributes to the formation of a hierarchical multi-porous system that can serve as capillary channels for water transport [278]. This mechanistic explanation of the moisture management can thus be considered as the result of the contributions from the three-dimensional macro-capillary effect of the textile substrate and the hydrogel coating. The absorbent nonwoven fabric can be used as a beneficial substrate to support and protect the hydrogel from adhering to and staining the clothing when the users scratch the skin or move their body. More importantly, the substrate provides a number of channels for draining the liquids out of skin, including sweat, blood, and other body fluids. The synergistic effect of the smart hydrogel and textile material for contribution to the functionalized textile-based composite is therefore well demonstrated. These results also indicate that the topical skin area can be kept clean, breathable and comfortable during skin care and wound treatment using our fabric composite materials, which thereby shows a great potential and significance for practical applications.

#### **6.2.4. Water vapor transmission rate (WVTR) analysis**

The wound dressing is well known to prevent the loss of the body liquid. A controlling absorption and transmission can be imparted to the wound dressing to accelerate the granule formation and epithelialization. In addition, to maintain a high humidity in the wound area is a skillful strategy. On the other hand, the low WVTR causes the accumulation of exudates, which possibly results in the deceleration of healing process and even being more easily subjected to the risk of bacterial growth [279]. Lamke et al [280] reported that the WVTRs for normal skin, first degree burns and granulating wounds are  $204 \pm 12$ ,  $279 \pm 26$ , and  $5138 \pm 202$  g/m<sup>2</sup>/day, respectively. It was further recommended by Wong [281] that wound dressings with WVTRs in the range of 2000–2500 g/m<sup>2</sup>/day, with a

half the loss of granulating wounds, would be sufficient to give adequate moisture and prevent exudates accumulation. As shown in **Table 6.2**, the WVTR of samples covers the ideal range to maintain a proper fluid balance on the wound bed, which can thus promote epithelialization and cellular migration. The WVTR of nonwoven fabric coated with hydrogels is smaller than the value of nonwoven fabric because the hydrogel coating may block a small part of water vapor to transmit outside. This result indicates that hydrogels can reduce the loss of body liquid and maintain the proper humidity in the wound area.

**Table 6.2** Water vapor transmission rate (WVTR)

<b>Sample</b>	<b>Mean <math>\pm</math> S.D. (n=5)g/m<sup>2</sup>/day</b>
Nonwoven fabric	2353 $\pm$ 88
Nonwoven fabric coated with hydrogels	2209 $\pm$ 54

### **6.2.5. Air permeability (AP) analysis**

Air permeability is a very important property of textile fabric to allow passage of air through it. It is defined as the volume of air passing through a defined area under a specified pressure. It is closely related to the comfort of textile based wound dressing. The AP was calculated by using the following formula:  $AP = D/5.08 \times \text{cc/s/cm}^2$  at 100 Pa, D is the test data (cc/s) of permeable air.

**Table 6.3** Air permeability (AP)

Sample	Mean $\pm$ S.D. (n=5) cc/s/cm <sup>2</sup> at 100Pa.
Nonwoven fabric	320 $\pm$ 14
Nonwoven fabric coated with hydrogels	171 $\pm$ 8

As shown in **Table 6.3**, the AP of nonwoven fabric coated with hydrogels is almost half of the value of nonwoven fabric because the hydrogel coating may prevent part of air through the fabric and reduce the air permeability.

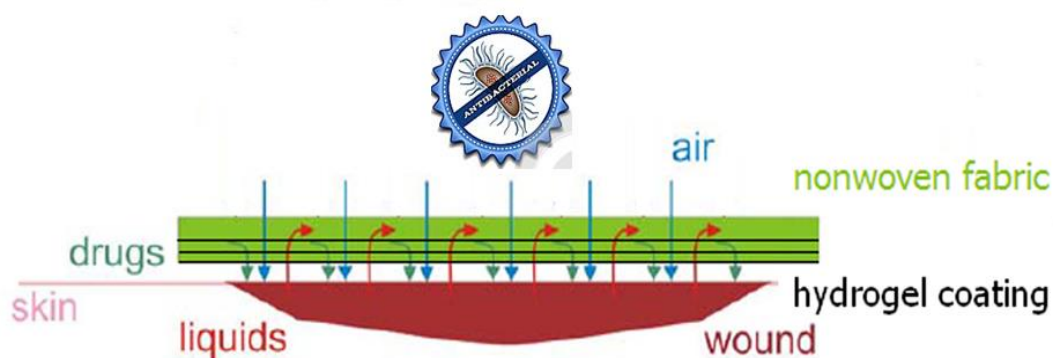


**Figure 6.5** The functionalities of smart hydrogel coated complex dressing

# Chapter 7 Conclusion

A thermo-responsive hydrogel material of the PEG-PCL-PEG block copolymer has been synthesized by a simple yet effective method in Chapter 4. The thermoresponsive hydrogel was synthesized easily through coupling of poly (ethylene glycol) (PEG) and poly ( $\epsilon$ -caprolactone) (PCL) with hexamethylene diisocyanate (HMDI) as a chemical linker. The structure and microscopic surface morphology of the thermoresponsive hydrogel, cytotoxicity, sol-gel phase transition behavior and in vitro drug release behavior were investigated and detected in detail. The hydrogel showed a temperature-triggered sol-gel transition behavior and high potential for use as drug controlled release.

Biomaterials are being extensively used in various biomedical fields; however, biomaterials are readily infected with microorganisms, thus posing a serious threat to the human health care. To address this problem, we herein presented a general route to antibacterial modification based on as-prepared PEG-PCL-PEG system with inexpensive, commercial bis(2-hydroxyethyl) methylammonium chloride (DMA) as an antibacterial modification agent in Chapter 5 - antibacterial modification of thermoresponsive hydrogel: synthesis, characterization and application. The effective synthesis of the resulting antibacterial copolymer mPEG-PCL-DMA-PCL-mPEG has been confirmed by FTIR and  $^1\text{H-NMR}$  spectra. The synthesized antibacterial hydrogel showed in **Figure 5.14** has been well demonstrated to be basically non-cytotoxic and to have a high thermosensitivity, with a clear sol-gel-sol transition, which thus reveals its injectability. Triggered by the body temperature, the copolymer sol can be quickly transformed to a gel with a network structure and high porosity,

facilitating its controlled drug release properties. We have also presented a probable mechanism for the sol-gel-sol transition behaviors of the copolymers, and discussed the relationship between the quaternization with DMA and the sol-gel-sol transition behaviors. It has been found that an appropriate extent of quaternization can lead to excellent antibacterial performance but does not sacrifice the other fascinating intrinsic properties including the non-cytotoxicity, thermosensitivity and controlled drug release ability. The work presented here will open up an avenue towards synthesis of various antibacterial copolymers with different kinds of blocks other than PEG and PCL using DMA or its analogue as a functional building block. Insights might also be shed on understanding the sol-gel-sol transition of multiblock copolymers.

In response to the recent increasing interest in dressing materials for skin care and wound treatment, a functionalized complex dressing system of nonwoven fabric modified with as-prepared hydrogel will be introduced in Chapter 6 - Functionalized thermoresponsive hydrogel coated textile materials for skin and wound care. This prepared smart hydrogel-nonwoven system is a combination of fabric structure with drug loaded thermoresponsive hydrogel coating. It is not only a drug control-release system, but also a moisture and exudate management system. The liquid like sweat, blood and body fluid out of skin can be transported unidirectionally from inside to outside. It will be very helpful to keep topical skin area like wound bed in a moist environment and breathable and comfortable in long term treatment. From the testing and evaluation, this complex dressing seems to be an excellent dressing material for skin care and wound treatment because of its special properties like biocompatibility, antibacterial activity, drug control-release, breathability and

moisture management showed in **Figure 6.5**. It is believed this multi-functional complex dressing is one kind of versatile candidates in the area of skin care and wound treatment.

# Chapter 8 Future work and potential application

Based on the experimental results, a general conclusion can be drawn: the amphiphilic block copolymers-based thermoresponsive hydrogel can be synthesized and quaternized easily through coupling of hydrophilic block (PEG), hydrophobic block (PCL) and antibacterial group (DMA) with the chemical linker (HMDI). Thermosensitivity can be controlled and adjusted by the hydrophobic/hydrophilic balance of amphiphilic block copolymer, e.g., by tuning of molecular weight and polymer concentration. For quaternization modification, it has been found that an appropriate extent of quaternization can lead to excellent antibacterial performance but does not scarify the other fascinating intrinsic properties of the thermoresponsive hydrogel including the non-cytotoxicity, thermosensitivity and controlled drug release ability.

After modification of traditional nonwoven dressing with the prepared drug-loaded thermoresponsive hydrogel, it's worth mentioning that this advanced dressing is not only a drug control-release system, but also a moisture and exudate management system. The liquid like sweat, blood and body fluid out of skin can be transported unidirectionally from inside to outside. It will be very helpful to keep topical skin area breathable and comfortable, like wound bed in a moist environment, in long-term treatment. From the testing and evaluation, it seems to be an excellent dressing material for skin care and wound treatment applications because of its excellent properties like biocompatibility, drug control-release, breathability and moisture management. It is believed that this

advanced complex dressing is a versatile and competitive candidate for skin and wound care applications.

### **8.1. Future work**

This study develops a kind of smart hydrogel-modified nonwoven fabric which can be used as a complex dressing with drug controlled release ability and moisture management functions. Some examples are demonstrated and shown to have potential applications for skin and wound care. Based on this research, it is believed that this multi-functional complex dressing is a versatile and competitive candidate for cosmetics and medical applications. Further, this kind of smart textile has a wide range of future opportunities for new lines of research and applications which may be used in scientific and commercial settings. Nevertheless, the further demonstration of the feasibility of the present developed materials for real-life applications is needed before the clinical trial in the future, e.g., using animal testing.

Animal testing is another important aspect to test and verify the biocompatibility of the developed dressing. The animal testing can minimize the side-effect of the final product before the clinical trial. The following parts show a feasible animal testing method.

#### (1) In vitro animal testing method

According to the grade of the dermal irritation reaction in hygienic standard for cosmetics 2007, whether the testing sample has irritation to rabbits' skins will be determined. Four healthy young adult New Zealand white albino rabbits are selected as test animals. Firstly, fur is removed by closely clipping the dorsal area approximately 24h before testing to avoid abrading the skin. After that, two dorsal areas (each area approximately 3×3cm) are prepared. One side is for

treated sample, and the other side serves as a control. Then, the prepared nonwoven gauze patch is applied to the test area (2.5 cm×2.5cm). The gauze patch is loosely held in place with a non-irritating tape. The other blank gauze patch is applied to the other site as a control .After 4h of exposure, the patches are removed and the test area is cleaned using warm water. The signs of erythema and edema are then examined on the basis of designated values in “Dermal Irritation Reaction Score” at 1, 24, 48 and 72h after residual test substance removal, accompanied by scoring the responses at each observation period. Only the 24, 48 and 72h scores are used to evaluate the irritation grade according to “Grade of Skin Irritation”.

## (2) In vivo animal testing method

Six-month-old male rabbits, weighting about 2~3 kg, can be used for in vivo experiments. The rabbits will be anaesthetized, with the hair of the dorsal area removed. The skin will be sterilized with a baticone alcoholic solution. Five or six circular full thickness skin wounds (diameter=0.8 cm, area=0.50cm<sup>2</sup>) will be created by using a sterile punch. For one group of rabbits, nothing will be applied to the wound cut (as a control). The wounds of the other group will be covered with gentamicin sulphate carried hydrogels grafted fabrics. Every other day, the rabbits will be checked and the length and width of the lesions will be measured for evaluating the healing effect. Skin samples containing the whole wound area will be considered for the evaluation of the healing effect.

Following the animal testing, an exploratory clinical study can be designed to investigate the safety and efficacy of this smart hydrogel coated functional dressing.

## **8.2. Potential application of the research**

Smart functional textiles used for medical and related healthcare and hygiene sectors are an important and rapidly growing segment of the textile field especially in recent years. In this study, the thermoresponsive A-B-A type block copolymer hydrogel, hydrogel modified with quaternary ammonium salt and hydrogel based smart textile dressing were investigated comprehensively.

To fabricate medical materials, especially for skin and wound care applications, the antibacterial activity, controlled/sustained drug delivery property and moisture management function are essential aspects to be considered. These requirements can be met based on our research. This smart hydrogel coated nonwoven system can serve as both a drug control-release system, and a moisture and exudate management system. The liquid like sweat, blood and body fluid out of skin can be transported unidirectionally from inside to outside. It will be very helpful to keep topical skin area breathable and comfortable, like wound bed in a moist environment, for wound treatment.

For personal care products, facial mask is widely used for face skin care, as well as for making up purpose. The attributes including moisturizing, hygiene, non-toxicity and no side effects can be realized by loading various nutrients into our smart hydrogel coated nonwoven system.

From the research results, a kind of smart hydrogel-nonwoven system with special properties and functions such as biocompatibility, controlled drug release, antibacterial activity, breathability and moisture management is established. This smart textile has a great potential for cosmetic and medical applications.

# References

1. Lazarus, G.S., et al., Definitions and guidelines for assessment of wounds and evaluation of healing. *Wound Repair and Regeneration*, 1994. 2(3): 165-170.
2. Scarborough, J., Guido Majno. *The Healing Hand: Man and Wound in the Ancient World*. Cambridge, Mass.: Harvard University Press. 1975. Pp. xxiii, 571. *The American Historical Review*, 1977. 82(1): 66-67.
3. Rajendran, S., *Advanced textiles for wound care*. Elsevier. 2009.
4. Winter, G.D., Formation of the scab and the rate of epithelization of superficial wounds in the skin of the young domestic pig. *Journal of wound care*, 1962: 293-294.
5. Caló E. and V.V. Khutoryanskiy, Biomedical applications of hydrogels: A review of patents and commercial products. *European Polymer Journal*, 2015. 65: 252-267.
6. SHINGADE, G., Review on: recent trend on transdermal drug delivery system. *Journal of Drug Delivery and Therapeutics*, 2012. 2(1):66-75.
7. Sood, A., M.S. Granick, and N.L. Tomaselli, Wound dressings and comparative effectiveness data. *Advances in wound care*, 2014. 3(8): 511-529.
8. Wichterle, O. and D. Lim, Hydrophilic gels for biological use. *Nature*, 1960. 185: 117-118.
9. Baker, R., M. Tuttle, and R. Helwing, Novel erodible polymers for the delivery of macromolecules. *Pharm. Technol*, 1984. 8: 26-28.

10. Ulbrich, K., et al., Synthesis of novel hydrolytically degradable hydrogels for controlled drug release. *Journal of controlled release*, 1995. 34(2): 155-165.
11. Khutoryanskiy, V.V., Hydrogen-bonded interpolymer complexes as materials for pharmaceutical applications. *International journal of pharmaceutics*, 2007. 334(1): 15-26.
12. Kashyap, N., N. Kumar, and M.R. Kumar, Hydrogels for pharmaceutical and biomedical applications. *Critical Reviews™ in Therapeutic Drug Carrier Systems*, 2005. 22(2).
13. Hoffman, A.S., Hydrogels for biomedical applications. *Advanced drug delivery reviews*, 2012. 64: 18-23.
14. Venkatesh, S., et al., Applications of biomimetic systems in drug delivery. *Expert Opin. Drug Deliv.* , 2005. 2(6): 1085-1096.
15. Gulrez, S.K., G.O. Phillips, and S. Al-Assaf, Hydrogels: methods of preparation, characterisation and applications. INTECH Open Access Publisher. 2011.
16. Rubinstein, M. and R.H. Colby, *Polymer physics*. OUP Oxford. 2003.
17. Jiang, H., S. Kelch, and A. Lendlein, Polymers move in response to light. *Advanced Materials*, 2006. 18(11): 1471-1475.
18. Feil, H., et al., Mutual influence of pH and temperature on the swelling of ionizable and thermosensitive hydrogels. *Macromolecules*, 1992. 25(20): 5528-5530.
19. Hu, J., *Shape memory polymers and textiles*. Elsevier. 2007.

20. Asaka, K. and K. Oguro, Bending of polyelectrolyte membrane platinum composites by electric stimuli: Part II. Response kinetics. *Journal of Electroanalytical Chemistry*, 2000. 480(1): 186-198.
21. Xulu, P.M., G. Filipcsei, and M. Zrinyi, Preparation and responsive properties of magnetically soft poly (N-isopropylacrylamide) gels. *Macromolecules*, 2000. 33(5): 1716-1719.
22. Yang, B., et al., Effects of moisture on the thermomechanical properties of a polyurethane shape memory polymer. *Polymer*, 2006. 47(4): 1348-1356.
23. Siegel, R.A. and B.A. Firestone, pH-dependent equilibrium swelling properties of hydrophobic polyelectrolyte copolymer gels. *Macromolecules*, 1988. 21(11): 3254-3259.
24. Han, I.S., et al., Constant-volume hydrogel osmometer: a new device concept for miniature biosensors. *Biomacromolecules*, 2002. 3(6): 1271-1275.
25. Sawai, T., Y. Ikariyama, and M. Aizawa. Electrically modulated/flocculation of ultra fine microgels. in *Proceedings of the International Conference on Intelligent Materials*. 1993.
26. Peppas, N., et al., Hydrogels in pharmaceutical formulations. *European journal of pharmaceutics and biopharmaceutics*, 2000. 50(1): 27-46.
27. Kiser, P.F., G. Wilson, and D. Needham, Lipid-coated microgels for the triggered release of doxorubicin. *Journal of controlled release*, 2000. 68(1): 9-22.

28. Drulis-Kawa, Z. and A. Dorotkiewicz-Jach, Liposomes as delivery systems for antibiotics. *International journal of pharmaceutics*, 2010. 387(1): 187-198.
29. Hoffman, A.S., et al., Really smart bioconjugates of smart polymers and receptor proteins. *Journal of Biomedical Materials Research*, 2000. 52(4): 577-586.
30. Galaev, I.Y. and B. Mattiasson, 'Smart' polymers and what they could do in biotechnology and medicine. *Trends in biotechnology*, 1999. 17(8): 335-340.
31. Ebara, M., et al., Copolymerization of 2-carboxyisopropylacrylamide with N-isopropylacrylamide accelerates cell detachment from grafted surfaces by reducing temperature. *Biomacromolecules*, 2003. 4(2): 344-349.
32. Ruel-Gariepy, E. and J.-C. Leroux, In situ-forming hydrogels-review of temperature-sensitive systems. *European Journal of Pharmaceutics and Biopharmaceutics*, 2004. 58(2): 409-426.
33. Park, K., W. Shalaby, and H. Park, Physical gels. *Biodegradable Hydrogels for Drug Delivery*, 1993: 99-140.
34. Kumar, N., M.N. Ravikumar, and A. Domb, Biodegradable block copolymers. *Advanced drug delivery reviews*, 2001. 53(1): 23-44.
35. Li, X., et al., Thermosensitive N-isopropylacrylamide-N-propylacrylamide-vinyl pyrrolidone terpolymers: Synthesis, characterization and preliminary application as embolic agents. *Biomaterials*, 2005. 26(34): 7002-7011.

36. Lee, J.W., F.-j. Hua, and D.S. Lee, Thermoreversible gelation of biodegradable poly ( $\epsilon$ -caprolactone) and poly (ethylene glycol) multiblock copolymers in aqueous solutions. *Journal of Controlled Release*, 2001. 73(2): 315-327.
37. Kissel, T., Y. Li, and F. Unger, ABA-triblock copolymers from biodegradable polyester A-blocks and hydrophilic poly (ethylene oxide) B-blocks as a candidate for in situ forming hydrogel delivery systems for proteins. *Advanced drug delivery reviews*, 2002. 54(1): 99-134.
38. Bae, Y.H., et al., Biodegradable amphiphilic multiblock copolymers and their implications for biomedical applications. *Journal of controlled release*, 2000. 64(1): 3-13.
39. Jeong, B., et al., Biodegradable block copolymers as injectable drug-delivery systems. *Nature*, 1997. 388(6645): 860-862.
40. Jeong, B., Y.H. Bae, and S.W. Kim, Thermoreversible gelation of PEG-PLGA-PEG triblock copolymer aqueous solutions. *Macromolecules*, 1999. 32(21): 7064-7069.
41. Zhong, Z., et al., Synthesis and aqueous phase behavior of thermoresponsive biodegradable poly (D, L-3-methylglycolide)-block-poly (ethylene glycol)-block-poly (D, L-3-methylglycolide) triblock copolymers. *Macromolecular Chemistry and Physics*, 2002. 203(12): 1797-1803.
42. Jeong, B., S.W. Kim, and Y.H. Bae, Thermosensitive sol-gel reversible hydrogels. *Advanced drug delivery reviews*, 2002. 54(1): 37-51.

43. Stevens, K.R., et al., In vivo biocompatibility of gelatin-based hydrogels and interpenetrating networks. *Journal of Biomaterials Science, Polymer Edition*, 2002. 13(12): 1353-1366.
44. Peretti, G.M., et al., Review of injectable cartilage engineering using fibrin gel in mice and swine models. *Tissue engineering*, 2006. 12(5): 1151-1168.
45. Wallace, D.G. and J. Rosenblatt, Collagen gel systems for sustained delivery and tissue engineering. *Advanced drug delivery reviews*, 2003. 55(12): 1631-1649.
46. Tønnesen, H.H. and J. Karlsen, Alginate in drug delivery systems. *Drug development and industrial pharmacy*, 2002. 28(6): 621-630.
47. Van Tomme, S.R. and W.E. Hennink, Biodegradable dextran hydrogels for protein delivery applications. *Expert Review of Medical Devices*, 2007. 4(2): 147-164.
48. Suh, J.-K.F. and H.W. Matthew, Application of chitosan-based polysaccharide biomaterials in cartilage tissue engineering: a review. *Biomaterials*, 2000. 21(24): 2589-2598.
49. Oh, E.J., et al., Target specific and long-acting delivery of protein, peptide, and nucleotide therapeutics using hyaluronic acid derivatives. *Journal of Controlled Release*, 2010. 141(1): 2-12.
50. Jin, R., et al., Synthesis and characterization of hyaluronic acid–poly (ethylene glycol) hydrogels via Michael addition: An injectable biomaterial for cartilage repair. *Acta Biomaterialia*, 2010. 6(6): 1968-1977.

51. Lee, C.H., A. Singla, and Y. Lee, Biomedical applications of collagen. *International journal of pharmaceutics*, 2001. 221(1): 1-22.
52. Dijkhuizen-Radersma, R., Biodegradable multiblock copolymers for drug delivery applications. University of Twente. 2004.
53. Zhou, S., X. Deng, and H. Yang, Biodegradable poly ( $\epsilon$ -caprolactone)-poly (ethylene glycol) block copolymers: characterization and their use as drug carriers for a controlled delivery system. *Biomaterials*, 2003. 24(20): 3563-3570.
54. Zhu, K., L. Xiangzhou, and Y. Shilin, Preparation, characterization, and properties of polylactide (PLA)-poly (ethylene glycol)(PEG) copolymers: a potential drug carrier. *Journal of applied polymer science*, 1990. 39(1): 1-9.
55. Bezemer, J., et al., A controlled release system for proteins based on poly (ether ester) block-copolymers: polymer network characterization. *Journal of controlled release*, 1999. 62(3): 393-405.
56. Bezemer, J., et al., Zero-order release of lysozyme from poly (ethylene glycol)/poly (butylene terephthalate) matrices. *Journal of Controlled Release*, 2000. 64(1): 179-192.
57. Deschamps, A.A., D.W. Grijpma, and J. Feijen, Poly (ethylene oxide)/poly (butylene terephthalate) segmented block copolymers: the effect of copolymer composition on physical properties and degradation behavior. *Polymer*, 2001. 42(23): 9335-9345.
58. van Blitterswijk, C., The Effect of PEO Ratio on Degradation, Calcification and Bone Bonding of PEO/PBT Copolymer(Polyactive). *Cells and Materials(USA)*, 1993. 3(1): 23-36.

59. Beumer, G., C. Van Blitterswijk, and M. Ponec, Degradative behaviour of polymeric matrices in (sub) dermal and muscle tissue of the rat: a quantitative study. *Biomaterials*, 1994. 15(7): 551-559.
60. Nagata, M., et al., Hydrolytic degradation of aliphatic polyesters copolymerized with poly (ethylene glycol) s. *Polymer international*, 1997. 42(1): 33-38.
61. Mallardé D., et al., PLGA–PEG microspheres of teverelix: influence of polymer type on microsphere characteristics and on teverelix in vitro release. *International journal of pharmaceutics*, 2003. 261(1): 69-80.
62. Penco, M., et al., Multiblock copolymers based on segments of poly (D, L-lactic-glycolic acid) and poly (ethylene glycol) or poly (ε-caprolactone): A comparison of their thermal properties and degradation behavior. *Journal of applied polymer science*, 2000. 78(10): 1721-1728.
63. Cohn, D. and H. Younes, Biodegradable PEO/PLA block copolymers. *Journal of biomedical materials research*, 1988. 22(11): 993-1009.
64. Panoyan, A., R. Quesnel, and P. Hildgen, Injectable nanospheres from a novel multiblock copolymer: cytocompatibility, degradation and in vitro release studies. *Journal of microencapsulation*, 2003. 20(6): 745-758.
65. Ferruti, P., et al., Synthesis and properties of novel block copolymers containing poly (lactic-glycolic acid) and poly (ethyleneglycol) segments. *Biomaterials*, 1995. 16(18): 1423-1428.
66. Penco, M., et al., Degradation behaviour of block copolymers containing poly (lactic-glycolic acid) and poly (ethylene glycol) segments. *Biomaterials*, 1996. 17(16): 1583-1590.

67. Luo, W., et al., Dependence of morphology on composition of poly (L-lactide)-poly (ethylene glycol) multiblock copolymers. *Polymers for Advanced Technologies*, 2002. 13(3-4): 233-238.
68. Huh, K.M. and Y.H. Bae, Synthesis and characterization of poly (ethylene glycol)/poly (L-lactic acid) alternating multiblock copolymers. *Polymer*, 1999. 40(22): 6147-6155.
69. Barbato, F., et al., Biodegradable microspheres of novel segmented poly (ether-ester-amide) s based on poly ( $\epsilon$ -caprolactone) for the delivery of bioactive compounds. *Biomaterials*, 2001. 22(11): 1371-1378.
70. Lee, S., et al., Synthesis and characterization of amphiphilic poly (2-ethyl-2-oxazoline)/poly ( $\epsilon$ -caprolactone) alternating multiblock copolymers. *Polymer*, 2000. 41(19): 7091-7097.
71. Li, S., et al., Hydrolytic degradation of poly (oxyethylene)-poly-( $\epsilon$ -caprolactone) multiblock copolymers. *Journal of applied polymer science*, 1998. 68(6): 989-998.
72. Velthoen, I.W., Thermo-responsive hydrogels based on branched block copolymers. University of Twente. 2008.
73. Ferry, J.D. and H.S. Myers, Viscoelastic properties of polymers. *Journal of The Electrochemical Society*, 1961. 108(7): 142-143.
74. Shim, M.S., et al., Poly (D, L - lactic acid-co-glycolic acid)-b-poly (ethylene glycol)-b-poly (D, L-lactic acid-co-glycolic acid) triblock copolymer and thermoreversible phase transition in water. *Journal of biomedical materials research*, 2002. 61(2): 188-196.

75. Lee, D.S., et al., Novel thermoreversible gelation of biodegradable PLGA-block-PEO-block-PLGA triblock copolymers in aqueous solution. *Macromolecular rapid communications*, 2001. 22(8): 587-592.
76. Hyon, S.-H., K. Jamshidi, and Y. Ikada, Synthesis of polylactides with different molecular weights. *Biomaterials*, 1997. 18(22): 1503-1508.
77. Lee, J., et al., Thermogelling aqueous solutions of alternating multiblock copolymers of poly (L-lactic acid) and poly (ethylene glycol). *Biomacromolecules*, 2006. 7(6): 1729-1734.
78. Joo, M.K., Y.S. Sohn, and B. Jeong, Stereoisomeric effect on reverse thermal gelation of poly (ethylene glycol)/poly (lactide) multiblock copolymer. *Macromolecules*, 2007. 40(14): 5111-5115.
79. Fujiwara, T., et al., Novel Thermo-Responsive Formation of a Hydrogel by Stereo-Complexation between PLLA-PEG-PLLA and PDLA-PEG-PDLA Block Copolymers. *Macromolecular Bioscience*, 2001. 1(5): 204-208.
80. Mukose, T., et al., Hydrogel Formation between Enantiomeric B-A-B Type Block Copolymers of Polylactides (PLLA or PDLA: A) and Polyoxyethylene (PEG: B); PEG-PLLA-PEG and PEG-PDLA-PEG. *Macromolecular bioscience*, 2004. 4(3): 361-367.
81. Peppas, N.A., et al., *Biomedical applications of hydrogels handbook*. Springer Science & Business Media. 2010.
82. Park, M.J. and K. Char, Gelation of PEO-PLGA-PEO triblock copolymers induced by macroscopic phase separation. *Langmuir*, 2004. 20(6): 2456-2465.

83. Mohan, N. and P.D. Nair, Polyvinyl alcohol-poly (caprolactone) Semi IPN scaffold with implication for cartilage tissue engineering. *Journal of Biomedical Materials Research Part B: Applied Biomaterials*, 2008. 84(2): 584-594.
84. Rohner, D., et al., In vivo efficacy of bone-marrow-coated polycaprolactone scaffolds for the reconstruction of orbital defects in the pig. *Journal of Biomedical Materials Research Part B: Applied Biomaterials*, 2003. 66(2): 574-580.
85. Hwang, M.J., et al., Caprolactonic Poloxamer Analog: PEG-PCL-PEG. *Biomacromolecules*, 2005. 6(2): 885-890.
86. Yenice, İ., et al., Hyaluronic acid coated poly- $\epsilon$ -caprolactone nanospheres deliver high concentrations of cyclosporine A into the cornea. *Experimental eye research*, 2008. 87(3): 162-167.
87. Huynh, D.P., et al., Functionalized injectable hydrogels for controlled insulin delivery. *Biomaterials*, 2008. 29(16): 2527-2534.
88. Jiang, Z., et al., Biodegradable and thermoreversible hydrogels of poly (ethylene glycol)-poly ( $\epsilon$ -caprolactone-co-glycolide)-poly (ethylene glycol) aqueous solutions. *Journal of Biomedical Materials Research Part A*, 2008. 87(1): 45-51.
89. Jones, D.S., et al., Physicochemical characterisation and biological evaluation of hydrogel-poly ( $\epsilon$ -caprolactone) interpenetrating polymer networks as novel urinary biomaterials. *Biomaterials*, 2005. 26(14): 1761-1770.
90. Zhao, S., et al., Synthesis and characterization of thermo-sensitive semi-IPN hydrogels based on poly (ethylene glycol)-co-poly

- ( $\epsilon$ -caprolactone) macromer, N-isopropylacrylamide, and sodium alginate. Carbohydrate research, 2010. 345(3): 425-431.
91. Gong, C.Y., et al., Biodegradable in situ gel - forming controlled drug delivery system based on thermosensitive PCL-PEG-PCL hydrogel: Part 1-synthesis, characterization, and acute toxicity evaluation. Journal of pharmaceutical sciences, 2009. 98(12): 4684-4694.
  92. Bae, S.J., et al., Thermogelling poly (caprolactone-b-ethylene glycol-b-caprolactone) aqueous solutions. Macromolecules, 2005. 38(12): 5260-5265.
  93. Heller, J., Polymers for controlled parenteral delivery of peptides and proteins. Advanced drug delivery reviews, 1993. 10(2): 163-204.
  94. Baker, R.W., Controlled release of biologically active agents. John Wiley & Sons. 1987.
  95. Kim, S.W., Y.H. Bae, and T. Okano, Hydrogels: swelling, drug loading, and release. Pharmaceutical research, 1992. 9(3): 283-290.
  96. Packhaeuser, C., et al., In situ forming parenteral drug delivery systems: an overview. European Journal of Pharmaceutics and Biopharmaceutics, 2004. 58(2): 445-455.
  97. Jeong, B., et al., New biodegradable polymers for injectable drug delivery systems. Journal of Controlled Release, 1999. 62(1): 109-114.
  98. Jeong, B., Y.H. Bae, and S.W. Kim, Drug release from biodegradable injectable thermosensitive hydrogel of PEG-PLGA-PEG triblock copolymers. Journal of controlled release, 2000. 63(1): 155-163.

99. Zentner, G.M., et al., Biodegradable block copolymers for delivery of proteins and water-insoluble drugs. *Journal of Controlled Release*, 2001. 72(1): 203-215.
100. Chen, S., et al., Triblock copolymers: synthesis, characterization, and delivery of a model protein. *International journal of pharmaceutics*, 2005. 288(2): 207-218.
101. Qiao, M., et al., Injectable biodegradable temperature-responsive PLGA–PEG–PLGA copolymers: synthesis and effect of copolymer composition on the drug release from the copolymer-based hydrogels. *International Journal of Pharmaceutics*, 2005. 294(1): 103-112.
102. Pratoomsot, C., et al., A thermoreversible hydrogel as a biosynthetic bandage for corneal wound repair. *Biomaterials*, 2008. 29(3): 272-281.
103. Beeley, N.R., et al., Fabrication, implantation, elution, and retrieval of a steroid - loaded polycaprolactone subretinal implant. *Journal of Biomedical Materials Research Part A*, 2005. 73(4): 437-444.
104. STAMM, W.E., Infections related to medical devices. *Annals of Internal Medicine*, 1978. 89(5\_Part\_2): 764-769.
105. von Eiff, C., et al., Infections associated with medical devices. *Drugs*, 2005. 65(2): 179-214.
106. Guggenbichler, J.P., et al., Incidence and clinical implication of nosocomial infections associated with implantable biomaterials–catheters, ventilator-associated pneumonia, urinary tract infections. *GMS Krankenhaushygiene interdisziplin är*, 2011. 6(1):1-19.
107. Rosenthal, V.D., et al., International Nosocomial Infection Control Consortium: Device-associated nosocomial infections in 55 intensive

- care units of 8 developing countries. *Ann Intern Med*, 2006. 145(8): 582-591.
108. Gould, I., A review of the role of antibiotic policies in the control of antibiotic resistance. *Journal of Antimicrobial Chemotherapy*, 1999. 43(4): 459-465.
109. Stone, A., Microbicides: a new approach to preventing HIV and other sexually transmitted infections. *Nature Reviews Drug Discovery*, 2002. 1(12): 977-985.
110. Boucher, H.W., et al., Bad bugs, no drugs: no ESKAPE! An update from the Infectious Diseases Society of America. *Clinical Infectious Diseases*, 2009. 48(1): 1-12.
111. Álvarez-Paino, M., et al., Effect of glyconunits on the antimicrobial properties and toxicity behavior of polymers based on quaternized DMAEMA. *Biomacromolecules*, 2014. 16(1): 295-303.
112. Burman, W.J., Rip Van Winkle wakes up: development of tuberculosis treatment in the 21st century. *Clinical Infectious Diseases*, 2010. 50(Supplement 3): 165-172.
113. Christian, K.A., et al., What we are watching-five top global infectious disease threats, 2012: a perspective from CDC's Global Disease Detection Operations Center. *Emerging health threats journal*, 2013. 6:20632.
114. Fuchs, A.D. and J.C. Tiller, Contact-Active Antimicrobial Coatings Derived from Aqueous Suspensions. *Angewandte Chemie International Edition*, 2006. 45(40): 6759-6762.

115. Thomassin, J.-M., et al., Grafting of poly [2-(tert-butylamino) ethyl methacrylate] onto polypropylene by reactive blending and antibacterial activity of the copolymer. *Biomacromolecules*, 2007. 8(4): 1171-1177.
116. Ilker, M.F., et al., Tuning the hemolytic and antibacterial activities of amphiphilic polynorbornene derivatives. *Journal of the American Chemical Society*, 2004. 126(48): 15870-15875.
117. Dong, C., et al., Antibacterial modification of cellulose fibers by grafting  $\beta$ -cyclodextrin and inclusion with ciprofloxacin. *Cellulose*, 2014. 21(3): 1921-1932.
118. Majumdar, P., et al., Synthesis and antimicrobial activity of quaternary ammonium-functionalized POSS (Q-POSS) and polysiloxane coatings containing Q-POSS. *Polymer*, 2009. 50(5): 1124-1133.
119. Malmsten, M., Antimicrobial and antiviral hydrogels. *Soft Matter*, 2011. 7(19): 8725-8736.
120. Zheng, A., et al., Synthesis and characterization of antimicrobial polyvinyl pyrrolidone hydrogel as wound dressing. *Soft Materials*, 2014. 12(3): 179-187.
121. Domagk, G., A new class of disinfectants. *Dtsch. Med. Wochenscher*, 1935. 61: 829-832.
122. Fu, E., K. McCue, and D. Boesenberg, Chemical disinfection of hard surfaces-Household, industrial and Institutional Settings. *Handbook of Cleaning/Decontamination of Surfaces*, 2007: 573-592.
123. Tezel, U. and S.G. Pavlostathis, Role of quaternary ammonium compounds on antimicrobial resistance in the environment. *Antimicrobial Resistance in the Environment*, 2011: 349-387.

124. Kourai, H., et al., Syntheses and antimicrobial activities of a series of new bis-quaternary ammonium compounds. *European journal of medicinal chemistry*, 2006. 41(4): 437-444.
125. Zhang, Y., et al., Synthesis and antibacterial characterization of gemini surfactant monomers and copolymers. *Polymer Chemistry*, 2012. 3(4): 907-913.
126. Tan, H. and H. Xiao, Synthesis and antimicrobial characterization of novel l-lysine gemini surfactants pended with reactive groups. *Tetrahedron Letters*, 2008. 49(11): 1759-1761.
127. Arciola, C.R., et al., Biofilm formation in Staphylococcus implant infections. A review of molecular mechanisms and implications for biofilm-resistant materials. *Biomaterials*, 2012. 33(26): 5967-5982.
128. Buffet-Bataillon, S., et al., Emergence of resistance to antibacterial agents: the role of quaternary ammonium compounds-a critical review. *International journal of antimicrobial agents*, 2012. 39(5): 381-389.
129. Carmona-Ribeiro, A.M. and L.D. de Melo Carrasco, Cationic antimicrobial polymers and their assemblies. *International journal of molecular sciences*, 2013. 14(5): 9906-9946.
130. Yue, J., et al., Reduction-responsive shell-crosslinked micelles prepared from Y-shaped amphiphilic block copolymers as a drug carrier. *Soft Matter*, 2012. 8(28): 7426-7435.
131. Liu, X., et al., Preparation of quaternized organic-inorganic hybrid brush polyphosphazene-co-poly [2-(dimethylamino) ethyl methacrylate] electrospun fibers and their antibacterial properties. *Polymer Chemistry*, 2012. 3(8): 2082-2091.

132. Li, F., M. Weir, and H. Xu, Effects of quaternary ammonium chain length on antibacterial bonding agents. *Journal of dental research*, 2013. 92(10): 932-938.
133. Parent, J.S., et al., Synthesis and characterization of isobutylene-based ammonium and phosphonium bromide ionomers. *Macromolecules*, 2004. 37(20): 7477-7483.
134. Eren, T., et al., Antibacterial and hemolytic activities of quaternary pyridinium functionalized polynorbornenes. *Macromolecular Chemistry and Physics*, 2008. 209(5): 516-524.
135. Abel, T., et al., Preparation and investigation of antibacterial carbohydrate-based surfaces. *Carbohydrate research*, 2002. 337(24): 2495-2499.
136. Dizman, B., M.O. Elasri, and L.J. Mathias, Synthesis and antimicrobial activities of new water-soluble bis-quaternary ammonium methacrylate polymers. *Journal of applied polymer science*, 2004. 94(2): 635-642.
137. Ng, V.W.L., et al., Antimicrobial polycarbonates: Investigating the impact of nitrogen-containing heterocycles as quaternizing agents. *Macromolecules*, 2014. 47(4): 1285-1291.
138. Lenoir, S., et al., New antibacterial cationic surfactants prepared by atom transfer radical polymerization. *Journal of Polymer Science Part A: Polymer Chemistry*, 2006. 44(3): 1214-1224.
139. Riva, R., et al., Contribution of "click chemistry" to the synthesis of antimicrobial aliphatic copolyester. *Polymer*, 2008. 49(8): 2023-2028.
140. Sellenet, P.H., et al., Synergistic activity of hydrophilic modification in antibiotic polymers. *Biomacromolecules*, 2007. 8(1): 19-23.

141. Antonucci, J.M., et al., Synthesis and characterization of dimethacrylates containing quaternary ammonium functionalities for dental applications. *Dental Materials*, 2012. 28(2): 219-228.
142. Marini, M., et al., Preparation and antibacterial activity of hybrid materials containing quaternary ammonium salts via sol-gel process. *European polymer journal*, 2007. 43(8): 3621-3628.
143. Codling, C.E., J.-Y. Maillard, and A.D. Russell, Aspects of the antimicrobial mechanisms of action of a polyquaternium and an amidoamine. *Journal of Antimicrobial Chemotherapy*, 2003. 51(5): 1153-1158.
144. Guan, Y., L. Qian, and H. Xiao, Novel Anti - Microbial Host - Guest Complexes Based on Cationic  $\beta$  -Cyclodextrin Polymers and Triclosan/Butylparaben. *Macromolecular Rapid Communications*, 2007. 28(23): 2244-2248.
145. Haldar, J., P. Kondaiah, and S. Bhattacharya, Synthesis and antibacterial properties of novel hydrolyzable cationic amphiphiles. Incorporation of multiple head groups leads to impressive antibacterial activity. *Journal of medicinal chemistry*, 2005. 48(11): 3823-3831.
146. Rawlinson, L.-A.B., et al., Antibacterial effects of poly (2-(dimethylamino ethyl) methacrylate) against selected gram-positive and gram-negative bacteria. *Biomacromolecules*, 2009. 11(2): 443-453.
147. Lu, G., D. Wu, and R. Fu, Studies on the synthesis and antibacterial activities of polymeric quaternary ammonium salts from dimethylaminoethyl methacrylate. *Reactive and Functional Polymers*, 2007. 67(4): 355-366.

148. Campoccia, D., L. Montanaro, and C.R. Arciola, A review of the biomaterials technologies for infection-resistant surfaces. *Biomaterials*, 2013. 34(34): 8533-8554.
149. Fantner, G.E., et al., Kinetics of antimicrobial peptide activity measured on individual bacterial cells using high-speed atomic force microscopy. *Nature nanotechnology*, 2010. 5(4): 280-285.
150. Qian, L., et al., Synthesis of modified guanidine-based polymers and their antimicrobial activities revealed by AFM and CLSM. *ACS applied materials & interfaces*, 2011. 3(6): 1895-1901.
151. Gabriel, G.J., et al., Synthetic mimic of antimicrobial peptide with nonmembrane-disrupting antibacterial properties. *Biomacromolecules*, 2008. 9(11): 2980-2983.
152. Fadida, T., et al., Air-ozonolysis to generate contact active antimicrobial surfaces: Activation of polyethylene and polystyrene followed by covalent graft of quaternary ammonium salts. *Colloids and Surfaces B: Biointerfaces*, 2014. 122: 294-300.
153. Kenawy, E.R. and Y.A.G. Mahmoud, Biologically active polymers, 6. *Macromolecular Bioscience*, 2003. 3(2): 107-116.
154. Naoto, O., et al., The fusogenic effect of synthetic polycations on negatively charged lipid bilayers. *Journal of biochemistry*, 1986. 100(4): 935-944.
155. Yaroslavov, A., et al., Reversibility of structural rearrangements in the negative vesicular membrane upon electrostatic adsorption/desorption of the polycation. *Biochimica et Biophysica Acta (BBA)-Biomembranes*, 2002. 1560(1): 14-24.

156. Yaroslavov, A.A., N.S. Melik-Nubarov, and F.M. Menger, Polymer-induced flip-flop in biomembranes. *Accounts of chemical research*, 2006. 39(10): 702-710.
157. Timofeeva, L. and N. Kleshcheva, Antimicrobial polymers: mechanism of action, factors of activity, and applications. *Applied microbiology and biotechnology*, 2011. 89(3): 475-492.
158. Tamami, M., et al., Structure-Property Relationships of Water-Soluble Ammonium-Ionene Copolymers. *Macromolecular Chemistry and Physics*, 2012. 213(9): 965-972.
159. Rodič, P., et al., Influence of the hydrophobic groups and the nature of counterions on ion-binding in aliphatic ionene solutions. *Colloids and Surfaces A: Physicochemical and Engineering Aspects*, 2013. 424: 18-25.
160. Williams, S.R. and T.E. Long, Recent advances in the synthesis and structure-property relationships of ammonium ionenes. *Progress in Polymer Science*, 2009. 34(8): 762-782.
161. Laschewsky, A., Recent trends in the synthesis of polyelectrolytes. *Current Opinion in Colloid & Interface Science*, 2012. 17(2): 56-63.
162. Bachl, J., et al., Synergistic Computational-Experimental Approach to Improve Ionene Polymer-Based Functional Hydrogels. *Advanced Functional Materials*, 2014. 24(31): 4893-4904.
163. Cakmak, I., et al., Synthesis and characterization of novel antimicrobial cationic polyelectrolytes. *European Polymer Journal*, 2004. 40(10): 2373-2379.

164. Zheng, A., et al., Preparation of antistatic and antimicrobial polyethylene by incorporating of comb-like ionenes. *Journal of Materials Science*, 2012. 47(20): 7201-7209.
165. Xu, X., et al., Novel comb-like ionenes with aliphatic side chains: synthesis and antimicrobial properties. *Journal of Materials Science*, 2013. 48(3): 1162-1171.
166. Beyth, N., et al., Antibacterial activity of dental composites containing quaternary ammonium polyethylenimine nanoparticles against *Streptococcus mutans*. *Biomaterials*, 2006. 27(21): 3995-4002.
167. Yudovin-Farber, I., et al., Surface characterization and biocompatibility of restorative resin containing nanoparticles. *Biomacromolecules*, 2008. 9(11): 3044-3050.
168. Beyth, N., et al., Surface antimicrobial activity and biocompatibility of incorporated polyethylenimine nanoparticles. *Biomaterials*, 2008. 29(31): 4157-4163.
169. Rembaum, A., Biological activity of ionene polymers. *Polymeric materials for unusual service conditions*, 1973: 299-317.
170. Rembaum, A., A. Senyei, and R. Rajaraman, Interaction of living cells with polyionenes and polyionene-coated surfaces. *Journal of biomedical materials research*, 1977. 11(1): 101-110.
171. Ikeda, T., H. Yamaguchi, and S. Tazuke, Phase separation in phospholipid bilayers induced by biologically active polycations. *Biochimica et Biophysica Acta (BBA)-Biomembranes*, 1990. 1026(1): 105-112.

172. Narita, T., et al., Effects of charge density and hydrophobicity of ionene polymer on cell binding and viability. *Colloid and Polymer Science*, 2000. 278(9): 884-887.
173. Narita, T., et al., Kinetic study of cell disruption by ionic polymers with varied charge density. *Colloid and Polymer Science*, 2001. 279(2): 178-183.
174. Mattheis, C., M. Zheng, and S. Agarwal, Closing One of the Last Gaps in Polyionene Compositions: Alkyloxyethylammonium Ionenes as Fast-Acting Biocides. *Macromolecular bioscience*, 2012. 12(3): 341-349.
175. WILLIAMS, J.F. and S.D. WORLEY, Infection-resistant nonleachable materials for urologic devices. *Journal of endourology*, 2000. 14(5): 395-400.
176. Hugues, C., et al., Complexation of an acrylic resin by tertiary amines: synthesis and characterisation of new binders for antifouling paints. *European polymer journal*, 2003. 39(2): 319-326.
177. Ho, C.H., et al., Nanoseparated polymeric networks with multiple antimicrobial properties. *Advanced materials*, 2004. 16(12): 957-961.
178. Tiller, J., C. Sprich, and L. Hartmann, Amphiphilic conetworks as regenerative controlled releasing antimicrobial coatings. *Journal of Controlled Release*, 2005. 103(2): 355-367.
179. Sambhy, V., et al., Silver bromide nanoparticle/polymer composites: dual action tunable antimicrobial materials. *Journal of the American Chemical Society*, 2006. 128(30): 9798-9808.
180. Zeiger, D.N., et al., Effects of sample preparation on bacterial colonization of polymers. *Langmuir*, 2009. 26(4): 2659-2664.

181. Bazaka, K., et al., Efficient surface modification of biomaterial to prevent biofilm formation and the attachment of microorganisms. *Applied microbiology and biotechnology*, 2012. 95(2): 299-311.
182. Sang, Y. and H. Xiao, Preparation and application of cationic cellulose fibers modified by in situ grafting of cationic PVA. *Colloids and Surfaces A: Physicochemical and Engineering Aspects*, 2009. 335(1): 121-127.
183. Zhang, D. and H. Xiao, Dual-functional beeswaxes on enhancing antimicrobial activity and water vapor barrier property of paper. *ACS applied materials & interfaces*, 2013. 5(8): 3464-3468.
184. Roy, D., et al., Antibacterial cellulose fiber via RAFT surface graft polymerization. *Biomacromolecules*, 2007. 9(1): 91-99.
185. Charnley, M., M. Textor, and C. Acikgoz, Designed polymer structures with antifouling–antimicrobial properties. *Reactive and Functional Polymers*, 2011. 71(3): 329-334.
186. Tiller, J.C., et al., Designing surfaces that kill bacteria on contact. *Proceedings of the National Academy of Sciences*, 2001. 98(11): 5981-5985.
187. Lin, J., et al., Mechanism of bactericidal and fungicidal activities of textiles covalently modified with alkylated polyethylenimine. *Biotechnology and Bioengineering*, 2003. 83(2): 168-172.
188. Waschinski, C.J., et al., Design of Contact-Active Antimicrobial Acrylate - Based Materials Using Biocidal Macromers. *Advanced Materials*, 2008. 20(1): 104-108.

189. Cen, L., K. Neoh, and E. Kang, Surface functionalization technique for conferring antibacterial properties to polymeric and cellulosic surfaces. *Langmuir*, 2003. 19(24): 10295-10303.
190. Jampala, S.N., et al., Plasma-enhanced synthesis of bactericidal quaternary ammonium thin layers on stainless steel and cellulose surfaces. *Langmuir*, 2008. 24(16): 8583-8591.
191. Han, H., et al., Immobilization of amphiphilic polycations by catechol functionality for antimicrobial coatings. *Langmuir*, 2011. 27(7): 4010-4019.
192. Sever, M.J., et al., Metal - Mediated Cross - Linking in the Generation of a Marine-Mussel Adhesive. *Angewandte Chemie*, 2004. 116(4): 454-456.
193. Zürcher, S., et al., Biomimetic surface modifications based on the cyanobacterial iron chelator anachelin. *Journal of the American Chemical Society*, 2006. 128(4): 1064-1065.
194. Lee, H., et al., Mussel-inspired surface chemistry for multifunctional coatings. *science*, 2007. 318(5849): 426-430.
195. Shi, Z., K. Neoh, and E. Kang, Surface-grafted viologen for precipitation of silver nanoparticles and their combined bactericidal activities. *Langmuir*, 2004. 20(16): 6847-6852.
196. Podsiadlo, P., et al., Layer-by-layer assembly of nacre-like nanostructured composites with antimicrobial properties. *Langmuir*, 2005. 21(25): 11915-11921.
197. Grunlan, J.C., J.K. Choi, and A. Lin, Antimicrobial behavior of polyelectrolyte multilayer films containing cetrimide and silver. *Biomacromolecules*, 2005. 6(2): 1149-1153.

198. Li, Z., et al., Two-level antibacterial coating with both release-killing and contact-killing capabilities. *Langmuir*, 2006. 22(24): 9820-9823.
199. Lin, J., et al., Bactericidal properties of flat surfaces and nanoparticles derivatized with alkylated polyethylenimines. *Biotechnology progress*, 2002. 18(5): 1082-1086.
200. Cao, Z., et al., Reversibly switching the function of a surface between attacking and defending against bacteria. *Angewandte Chemie International Edition*, 2012. 51(11): 2602-2605.
201. Nigmatullin, R. and F. Gao, Onium-functionalised Polymers in the Design of Non-leaching Antimicrobial Surfaces. *Macromolecular Materials and Engineering*, 2012. 297(11): 1038-1074.
202. Lewis, K. and A.M. Klibanov, Surpassing nature: rational design of sterile-surface materials. *TRENDS in Biotechnology*, 2005. 23(7): 343-348.
203. Murata, H., et al., Permanent, non-leaching antibacterial surfaces-2: How high density cationic surfaces kill bacterial cells. *Biomaterials*, 2007. 28(32): 4870-4879.
204. Siedenbiedel, F. and J.C. Tiller, Antimicrobial polymers in solution and on surfaces: overview and functional principles. *Polymers*, 2012. 4(1): 46-71.
205. Larson, A.M. and A.M. Klibanov, Biocidal packaging for pharmaceuticals, foods, and other perishables. *Annual review of chemical and biomolecular engineering*, 2013. 4: 171-186.

206. Lee, S.B., et al., Permanent, nonleaching antibacterial surfaces. 1. Synthesis by atom transfer radical polymerization. *Biomacromolecules*, 2004. 5(3): 877-882.
207. Huang, J., et al., Nonleaching antibacterial glass surfaces via “grafting onto”: the effect of the number of quaternary ammonium groups on biocidal activity. *Langmuir*, 2008. 24(13): 6785-6795.
208. Noble, W.C., *The skin microflora and microbial skin disease*. Cambridge University Press. 2004.
209. Horrocks, A.R. and S.C. Anand, *Handbook of technical textiles*. Elsevier. 2000.
210. Huang, S. and X. Fu, Naturally derived materials-based cell and drug delivery systems in skin regeneration. *Journal of Controlled Release*, 2010. 142(2): 149-159.
211. Goossens, A. and M.-B. Cleenewerck, New wound dressings: classification, tolerance. *European Journal of Dermatology*, 2010. 20(1): 24-26.
212. Rigby, A. and S. Anand, Nonwovens in medical and healthcare products Part 1: fabric formation, *Tech. Textiles Intern*, 1996.5: 22-27.
213. Fonder, M.A., et al., Treating the chronic wound: A practical approach to the care of nonhealing wounds and wound care dressings. *Journal of the American Academy of Dermatology*, 2008. 58(2): 185-206.
214. Boateng, J.S., et al., Wound healing dressings and drug delivery systems: a review. *Journal of pharmaceutical sciences*, 2008. 97(8): 2892-2923.
215. Chen, J.C., J.T. Yeh, and C.C. Chen, Crosslinking of cotton cellulose in the presence of alkyl diallyl ammonium salts. I. Physical properties and

- agent distribution. *Journal of applied polymer science*, 2003. 90(6): 1662-1669.
216. Seong, H.S., H.S. Whang, and S.W. Ko, Synthesis of a quaternary ammonium derivative of chito-oligosaccharide as antimicrobial agent for cellulosic fibers. *Journal of Applied Polymer Science*, 2000. 76(14): 2009-2015.
217. Kenawy, E.R., et al., Biologically active polymers. V. Synthesis and antimicrobial activity of modified poly (glycidyl methacrylate-co-2-hydroxyethyl methacrylate) derivatives with quaternary ammonium and phosphonium salts. *Journal of Polymer Science Part A: Polymer Chemistry*, 2002. 40(14): 2384-2393.
218. Kim, J.Y., et al., Synthesis of chitoooligosaccharide derivative with quaternary ammonium group and its antimicrobial activity against *Streptococcus mutans*. *International journal of biological macromolecules*, 2003. 32(1): 23-27.
219. Thorsteinsson, T., et al., Soft antimicrobial agents: synthesis and activity of labile environmentally friendly long chain quaternary ammonium compounds. *Journal of medicinal chemistry*, 2003. 46(19): 4173-4181.
220. Gong, C., et al., Synthesis and characterization of PEG-PCL-PEG thermosensitive hydrogel. *International Journal of Pharmaceutics*, 2009. 365(1): 89-99.
221. Jeong, B., et al., Phase transition of the PLGA-g-PEG copolymer aqueous solutions. *The Journal of Physical Chemistry B*, 2003. 107(37): 10032-10039.

222. Jeong, B., et al., Thermogelling biodegradable polymers with hydrophilic backbones: PEG-g-PLGA. *Macromolecules*, 2000. 33(22): 8317-8322.
223. Lam, P.-L., et al., Development of hydrocortisone succinic acid/and 5-fluorouracil/chitosan microcapsules for oral and topical drug deliveries. *Bioorganic & medicinal chemistry letters*, 2012. 22(9): 3213-3218.
224. Lam, P.-L., et al., Development of phyllanthin containing microcapsules and their improved biological activity towards skin cells and *Staphylococcus aureus*. *Bioorganic & medicinal chemistry letters*, 2012. 22(1): 468-471.
225. Chellamani, K., R. Vignesh Balaji, and J. Sathis, Spunlace wound dressing using bamboo fibres. *Asian Textile J*, 2013. 22(3): 69-79.
226. Hu, J., et al., Moisture management tester: A method to characterize fabric liquid moisture management properties. *Textile Research Journal*, 2005. 75(1): 57-62.
227. Song, M., et al., Thermosensitive sol-gel transition behaviors of poly (ethylene oxide)/aliphatic polyester/poly (ethylene oxide) aqueous solutions. *Journal of Polymer Science Part A: Polymer Chemistry*, 2004. 42(3): 772-784.
228. Alexander, A., et al., Poly (ethylene glycol)-poly (lactic-co-glycolic acid) based thermosensitive injectable hydrogels for biomedical applications. *Journal of Controlled Release*, 2013. 172(3): 715-729.
229. Vercelino, R., et al., Skin vasodilation and analgesic effect of a topical nitric oxide-releasing hydrogel. *Journal of Materials Science: Materials in Medicine*, 2013. 24(9): 2157-2169.

230. Zhang, Q., et al., Genipin-cross-linked thermosensitive silk sericin/poly (N-isopropylacrylamide) hydrogels for cell proliferation and rapid detachment. *Journal of Biomedical Materials Research Part A*, 2014. 102(1): 76-83.
231. Liang, X., et al., Thermosensitive multilayer hydrogels of poly (N-vinylcaprolactam) as nanothin films and shaped capsules. *Chemistry of Materials*, 2012. 24(19): 3707-3719.
232. An, J., et al., Thermal behaviour of poly ( $\epsilon$ -caprolactone)-poly (ethylene glycol)-poly ( $\epsilon$ -caprolactone) tri-block copolymers. *Journal of materials science*, 2001. 36(3): 715-722.
233. Li, J., et al., Self-assembled supramolecular hydrogels formed by biodegradable PEO-PHB-PEO triblock copolymers and  $\alpha$ -cyclodextrin for controlled drug delivery. *Biomaterials*, 2006. 27(22): 4132-4140.
234. Khoee, S. and K. Hemati, Synthesis of magnetite/polyamino-ester dendrimer based on PCL/PEG amphiphilic copolymers via convergent approach for targeted diagnosis and therapy. *Polymer*, 2013. 54(21): 5574-5585.
235. Jiang, C.-P., et al., Solid freeform fabrication and in-vitro response of osteoblast cells of mPEG-PCL-mPEG bone scaffolds. *Biomedical microdevices*, 2013. 15(2): 369-379.
236. Hwang, M.J., et al., Multiple Sol - Gel Transitions of PEG-PCL-PEG Triblock Copolymer Aqueous Solution. *Macromolecular rapid communications*, 2010. 31(23): 2064-2069.

237. Ni, P., et al., Injectable thermosensitive PEG-PCL-PEG hydrogel/acellular bone matrix composite for bone regeneration in cranial defects. *Biomaterials*, 2014. 35(1): 236-248.
238. Wu, Q., et al., Mannan loaded biodegradable and injectable thermosensitive PCL-PEG-PCL hydrogel for vaccine delivery. *Soft Materials*, 2012. 10(4): 472-486.
239. Gong, C.Y., et al., Thermosensitive PEG-PCL-PEG hydrogel controlled drug delivery system: sol–gel–sol transition and in vitro drug release study. *Journal of pharmaceutical sciences*, 2009. 98(10): 3707-3717.
240. Seven, P., M. Coşkun, and K. Demirelli, Synthesis and characterization of two-armed graft copolymers prepared with acrylate and methacrylate using atom transfer radical polymerization. *Reactive and Functional Polymers*, 2008. 68(5): 922-930.
241. Fulmer, G.R., et al., NMR chemical shifts of trace impurities: common laboratory solvents, organics, and gases in deuterated solvents relevant to the organometallic chemist. *Organometallics*, 2010. 29(9): 2176-2179.
242. Tang, Z., et al., Surface immobilization of a protease through an inhibitor-derived affinity ligand: a bioactive surface with defensive properties against an inhibitor. *Chemical Communications*, 2015. 51(75): 14263-14266.
243. Tang, Z., et al., Conjugation of polymers to proteins through an inhibitor-derived peptide: taking up the inhibitor “berth”. *Chemical Communications*. 2015.

244. Ramimoghadam, D., S. Bagheri, and S.B.A. Hamid, Stable Monodisperse Nanomagnetic Colloidal Suspensions: An overview. *Colloids and Surfaces B: Biointerfaces*. 2015.
245. Gou, Q., et al., Polymeric nanoassemblies entrapping curcumin overcome multidrug resistance in ovarian cancer. *Colloids and Surfaces B: Biointerfaces*, 2015. 126: 26-34.
246. Cui, C., et al., Reduction-sensitive micelles with sheddable PEG shells self-assembled from a Y-shaped amphiphilic polymer for intracellular doxorubicine release. *Colloids and Surfaces B: Biointerfaces*, 2015. 129: 137-145.
247. Cai, M., et al., Synthesis of amphiphilic copolymers containing zwitterionic sulfobetaine as pH and redox responsive drug carriers. *Colloids and Surfaces B: Biointerfaces*, 2015. 126: 1-9.
248. Chen, L., et al., Effects of Molecular Weight and Its Distribution of PEG Block on Micellization and Thermogellability of PLGA-PEG-PLGA Copolymer Aqueous Solutions. *Macromolecules*. 2015.
249. Wang, X., et al., Smart hydrogel-functionalized textile system with moisture management property for skin application. *Smart Materials and Structures*, 2014. 23(12): 125027.
250. Chen, L., et al., Effects of Molecular Weight Distribution of Amphiphilic Block Copolymers on Their Solubility, Micellization, and Temperature-Induced Sol-Gel Transition in Water. *Macromolecules*, 2014. 47(17): 5895-5903.
251. Vermonden, T., R. Censi, and W.E. Hennink, Hydrogels for protein delivery. *Chemical Reviews*, 2012. 112(5): 2853-2888.

252. Seliktar, D., Designing cell-compatible hydrogels for biomedical applications. *Science*, 2012. 336(6085): 1124-1128.
253. Hu, Y., et al., Magnetically responsive photonic films with high tunability and stability. *Nano Research*, 2015. 8(2): 611-620.
254. Smeets, N.M., et al., Injectable and tunable poly (ethylene glycol) analogue hydrogels based on poly (oligoethylene glycol methacrylate). *Chemical Communications*, 2014. 50(25): 3306-3309.
255. Du, H., et al., Fully biodegradable antibacterial hydrogels via thiol-ene “click” chemistry. *Polymer Chemistry*, 2014. 5(13): 4002-4008.
256. Yim, S.-L., H.-F. Chow, and M.-C. Chan, Transition from low molecular weight non-gelating oligo (amide-triazole)s to a restorable, halide-responsive poly (amide-triazole) supramolecular gel. *Chemical Communications*, 2014. 50(23): 3064-3066.
257. Sun, Y., et al., Multi-responsive and tough hydrogels based on triblock copolymer micelles as multi-functional macro-crosslinkers. *Chemical Communications*, 2015. 51(40): 8512-8515.
258. Khodaverdi, E., et al., Injectable Supramolecular Hydrogel from Insulin-Loaded Triblock PCL-PEG-PCL Copolymer and  $\gamma$ -Cyclodextrin with Sustained-Release Property. *AAPS PharmSciTech*, 2015. 16(1): 140-149.
259. Gong, C.Y., et al., Prevention of postsurgical cauterization-induced peritoneal adhesions by biodegradable and thermosensitive micelles. *Journal of biomedical nanotechnology*, 2013. 9(12): 1984-1995.
260. Ferruti, P., et al., Polycaprolactone-poly (ethylene glycol) multiblock copolymers as potential substitutes for di (ethylhexyl) phthalate in

- flexible poly (vinyl chloride) formulations. *Biomacromolecules*, 2003. 4(1): 181-188.
261. Han, Q., et al., Effects of bevacizumab loaded PEG-PCL-PEG hydrogel intracameral application on intraocular pressure after glaucoma filtration surgery. *Journal of Materials Science: Materials in Medicine*, 2015. 26(8): 1-9.
262. Wu, Q., et al., Thermosensitive hydrogel containing dexamethasone micelles for preventing postsurgical adhesion in a repeated-injury model. *Scientific reports*, 2015. 5:13553.
263. Liu, S., K.T. Dicker, and X. Jia, Modular and orthogonal synthesis of hybrid polymers and networks. *Chemical Communications*, 2015. 51(25): 5218-5237.
264. Li, Y.-L., N. Van Cuong, and M.-F. Hsieh, Endocytosis pathways of the folate tethered star-shaped PEG-PCL micelles in cancer cell lines. *Polymers*, 2014. 6(3): 634-650.
265. Shen, L., et al., Complex micelles with the bioactive function of reversible oxygen transfer. *Nano Research*, 2015. 8(2): 491-501.
266. Hu, H., et al., Structural and mechanistic understanding of an active and durable graphene carbocatalyst for reduction of 4-nitrophenol at room temperature. *Nano Research*, 2015. 8(12): 3992-4006.
267. Xiao, L., et al., Novel triple-shape PCU/PPDO interpenetrating polymer networks constructed by self-complementary quadruple hydrogen bonding and covalent bonding. *Polymer Chemistry*, 2014. 5(7): 2231-2241.

268. Ott, C., et al., Applying “click” chemistry to polyurethanes: a straightforward approach for glycopolymer synthesis. *Polymer Chemistry*, 2011. 2(12): 2782-2784.
269. Hu, H., J.H. Xin, and H. Hu, PAM/graphene/Ag ternary hydrogel: Synthesis, characterization and catalytic application. *Journal of Materials Chemistry A*, 2014. 2(29): 11319-11333.
270. Hu, H., et al., Multifunctional organically modified graphene with super-hydrophobicity. *Nano Research*, 2014. 7(3): 418-433.
271. Hu, H., et al., A pH-mediated enhancement of the graphene carbocatalyst activity for the reduction of 4-nitrophenol. *Chemical Communications*, 2015. 51(93): 16699-16702.
272. Hu, H., et al., Glutaraldehyde–chitosan and poly (vinyl alcohol) blends, and fluorescence of their nano-silica composite films. *Carbohydrate polymers*, 2013. 91(1): 305-313.
273. Hu, H.W., J.H. Xin, and H. Hu, Highly Efficient Graphene - Based Ternary Composite Catalyst with Polydopamine Layer and Copper Nanoparticles. *ChemPlusChem*, 2013. 78(12): 1483-1490.
274. Wang, X., et al., Visible light-active sub-5nm anatase TiO<sub>2</sub> for photocatalytic organic pollutant degradation in water and air, and for bacterial disinfection. *Catalysis Communications*, 2015. 72: 81-85.
275. Wang, C. and S.L. Chen, Aromachology and its application in the textile field. *Fibres & Textiles in Eastern Europe*, 2005.6 (54): 41-44.
276. Fisher, G., Medical and hygiene textiles—continuing in good health. *Tech Textil Int*, 2002. 11: 10-16.

277. Hu, J., et al., A review of stimuli-responsive polymers for smart textile applications. *Smart Materials and Structures*, 2012. 21(5): 053001.
278. Kong, Y., Y. Liu, and J.H. Xin, Fabrics with self-adaptive wettability controlled by “light-and-dark”. *Journal of Materials Chemistry*, 2011. 21(44): 17978-17987.
279. Kim, I., et al., Evaluation of semi-interpenetrating polymer networks composed of chitosan and poloxamer for wound dressing application. *International journal of pharmaceutics*, 2007. 341(1): 35-43.
280. Lamke, L.-O., G. Nilsson, and H. Reithner, The evaporative water loss from burns and the water-vapour permeability of grafts and artificial membranes used in the treatment of burns. *Burns*, 1977. 3(3): 159-165.
281. Wong, P., Physical evaluation of hydrogel as a burn wound dressing. University of Strathclyde. 1980.